中央大学博士論文

High Frequency Scattering Analysis by Dielectric Edged Objects via Surface Equivalence Theorem

QUANG NGOC HIEU

博士 (工学)

中央大学大学院 理工学研究科 情報セキュリティ科学専攻

Information Security Science Course

Graduate School of Science and Engineering

Chuo University

March 2019

Contents

List of Figures

Chapter 1

Introduction

1.1 Research Background

Electromagnetic scattering describes and explains the field behavior in the object when an incident electromagnetic wave illuminates an object. The electromagnetic scattering can be found from the solutions of Maxwell's equations, however the exact solutions of Maxwell's equations only exist for a limited number of canonical shapes. In which, electromagnetic scattering by edged objects is one of the important problems, and these analyses can be applied for the propagation and diffraction estimation.

There are some exact solutions available to estimate the scattering field [1]–[5]. Although these methods are only possible for a simply shaped object composed of a simple material constitution, they are important for electromagnetic scattering estimation. The solutions of some idealized objects are used for calibration of measurement facilities, like metal sphere. Also, exact solutions can be used for validation of numerical solutions or evaluated approximately or asymptotically to give a simple analytic expressions for the scattering fields.

Electromagnetic scattering solutions can sometimes be very complex even for simple geometries when exact solutions are available. Therefore, some numerical methods are developed to estimated the scattering by the objects of small size compared with wavelength [6]–[13]. However, these numerical methods may have a problem to apply for the scattering by electrically large objects because of unrealistic execution time and heavy memory requirement. Additionally, the numerical solutions cannot provide a qualitative, physical insight into the basic mechanisms of scattering and diffraction.

Hence, an approximate approach, that can provide the fast and acceptably accurate scattering by a large object, is necessary. Several asymptotic techniques can be efficiently used for high frequency scattering problems as long as the object is made of conducting materials, such as the geometrical optics (GO), the geometrical theory of diffraction (GTD), the physical optics (PO), the physical theory of diffraction (PTD).

GO is a classical ray-based technique for describing the scattering by an object illuminated by an electromagnetic wave [14]–[17]. The basic tenet of GO consists in assuming that an incident ray is reflected by the scattering objects as if the latter's surface were plane at the reflection point. The GO fields can be calculated by using the laws of their propagation and reflection at material interfaces. In GO, the fields in the shadowed regions of the scattering bodies are not described.

GTD is an extension of the classical GO, which is designed to account for the penetration of the GO field in the shadow region, by adding the diffracted field which are generated at edges, conical points and shadow boundaries on the scattering surface [18]–[22]. Then, the scattering fields by a objects can be expressed as the sum of two parts: the GO field and the diffracted field.

PO is a current-based approach which can be efficiently used for high frequency scattering problems as long as the object is made of non-penetrable metal materials [23]–[27]. Here, the scattering field by an object is considered as the radiation from the equivalent currents induced by the magnetic incident wave on the illuminated surfaces. Since PO formulation involves the information of the incident wave and the scattering object's surface, it is easy to construct the equivalent currents for scattering field. When the observation point is located far from the body, the kernel of the integral can be simplified, known as the radiation integral which is widely used in a great many of applications, such as antenna design, wave propagation, scattering estimation. When an exact solution is available, the PO method provides accurate estimations of scattering fields.

PTD is a high frequency asymptotic technique which the diffracted field is considered as the radiation of the scattering sources. The basic idea of PTD is that the scattering sources are separated into uniform and nonuniform components. While the uniform component is defined as sources induced on the infinite plane tangent to the object at the source point, the nonuniform component is caused by any deviation of the scattering surface from the tangent plane. Then PTD is an extension of PO method and takes into account

the additional field generated by the nonuniform component [28]–[31].

So far, these methods are clear for the scattering by metal objects. However, when scattering objects are composed of dielectric materials, the problem becomes difficult to solve, since there is no reliable solution available for estimating the diffraction by dielectric/magnetic objects [32]–[36]. This question is just a motivation of our present study, in which equivalent electric and magnetic currents to the scattering problems have been discussed.

In this thesis, equivalent current method which is based on the surface equivalence theorem [37] has been used to solve the scattering by conducting edged objects. According to the surface equivalence theorem, the scattering field from a conducting body may be formulated as the corresponding radiation from equivalent currents on a postulated surface enclosing the scattering body. When the equivalent electric and magnetic currents on the surface of the scattering object are obtained from the reflected/incident GO waves, and the radiation integrals due to these equivalent currents are evaluated asymptotically, the results are found to coincide with those by the PO formulation. Since our formulation matches with PO for the impenetrable conducting case, and can be extended to the cases when the scattering objects are penetrable, this method may be called as *extended PO* method, in which the equivalent currents are obtained from the reflected/transmitted and incident GO waves.

Since the incident wave impinges on the dielectric body, it excites the reflected and transmitted waves. Then the transmitted wave excites the internal reflected and transmitted waves due to the multiple bouncing effects, and they radiate again from the body. The effect of these internal bouncing waves can also be considered in our formulation. While equivalent current formulation in terms of reflected fields from the dielectric objects has already been utilized to obtain the specular reflected field for estimating their dielectric constants [38], the accuracy of the scattering field in non-specular reflection direction has not been discussed fully yet. The numerical results by the dielectric rectangular cylinders are calculated and compared with those HFSS simulation. A good agreement has been observed to confirm the validity of this method.

1.2 Thesis Contents

This thesis consists of five chapters.

In Chapter 2, surface equivalence theorem is explained. This method is based on the assumption that scattering far field is generated by the equivalent electric and magnetic currents flow on a virtual surface enclosed the scattering object. This equivalent currents may be approximated from the reflected and minus incident waves for the conducting objects, and from the reflected/transmitted GO waves for the dielectric objects.

In Chapter 3, the PO approximation are applied to estimate electromagnetic scattering from the conducting wedge and rectangular cylinder. According to the PO approximation, if the scattering objects are large compared with the wavelength, the PO currents are approximated from the magnetic incident field and flow on the physically illuminated surfaces. Then, the scattering field from this object may be derived by integrating these PO currents with the free-space Green's function. This chapter starts by applying the PO method to derive diffraction field from a conducting wedge in Section 3.1. Here, the scattering field is obtained from only one PO current flowing on the illuminated surface. The results include the edge diffracted field and the GO field which gives a reflected field in the illuminated region or a field to cancel the incident field in the shadow region. In Section 3.2, the conducting rectangular cylinder has been considered. In this case, the incident wave impinges on the cylinder at two surfaces and excites two PO currents on these illuminated surfaces. Then, the total scattering fields are given by summing up the fields radiated from these PO currents.

In Chapter 4, the electromagnetic scattering fields by the wedges and rectangular cylinders are approximated from the surface equivalent current method. Firstly, the scattering fields by the conducting wedges and rectangular cylinders are derived. Here, the equivalent electric and magnetic currents are calculated from the reflected GO wave at the illuminated surface and the minus incident wave at the shadowed surface. Then the scattering fields radiated from these currents are derived using the saddle point method. The results are found to match with those obtained from the PO approximation in Chapter 3. After that, the scattering fields by the dielectric wedges and rectangular cylinders are derived. Due to the multiple bouncing effect inside the objects, the equivalent currents are calculated by the reflected/transmitted waves on the illuminated surfaces and the inci-

dent/transmitted GO waves on the shadowed surfaces. The expressions of the equivalent currents and the radiation field formulations due to the multiply bouncing transmitted waves are derived for the dielectric wedge, but those for the dielectric rectangular cylinder are omitted, except the main results, due to the complicated formulations. Also some numerical results for the dielectric rectangular cylinder are calculated to compare with those by HFSS simulation. Here, a limitation of the effect of the high order transmitted waves are used to estimate the total scattering filed. Good agreements between the analytical results and HFSS simulation to confirm the accuracy of our method.

Finally, Chapter 5 shows some conclusions and discussions on our research. In the following discussion, the time-harmonic factor $e^{-i\omega t}$ is assumed and suppressed throughout the text.

Chapter 2

Surface Equivalence Theorem

The surface equivalence theorem is a principle by which actual sources, such as an antenna and transmitter, are replaced by equivalent sources. The fictitious sources are said to be equivalent within a region because they produce within that region the same fields as the actual sources. The formulations of scattering and diffraction problems by the surface equivalence theorem are more suggestive of approximations.

By the surface equivalence theorem, the fields outside an imaginary closed surface are obtained by placing, over the closed surface, suitable electric and magnetic current densities that satisfy the boundary conditions. The current densities are selected so that the fields inside the closed surface are zero and outside are equal to the radiation produced by the actual sources.

Let us now consider electromagnetic fields $\boldsymbol{E}_1$, $\boldsymbol{H}_1$ excited by electric and/or magnetic current sources $\boldsymbol{J}_1$, $\boldsymbol{M}_1$ as shown in Fig. 2.1(a). If one encloses the sources $\boldsymbol{J}_1$, $\boldsymbol{M}_1$ by a virtual closed surface S, then the exact fields outside S can be excited by equivalent electric surface currents and magnetic surface currents as in Fig. 2.1(b) [37]

$$\boldsymbol{J}_s = \hat{\boldsymbol{n}} \times \boldsymbol{H}_1, \tag{2.1}$$

$$\boldsymbol{M}_s = \boldsymbol{E}_1 \times \hat{\boldsymbol{n}}. \tag{2.2}$$

Here $\hat{\boldsymbol{n}}$ denotes a normal unit vector on S toward the exterior. This field expression in terms of equivalent currents may be sometimes called as surface equivalence theorem. This field equivalence holds as long as the fields $\boldsymbol{E}_1$, $\boldsymbol{H}_1$ are *exact* on the virtual surface S, but it is sometimes difficult to know exact fields, and the approximated fields may be used to evaluate the radiation and scattering analyses.

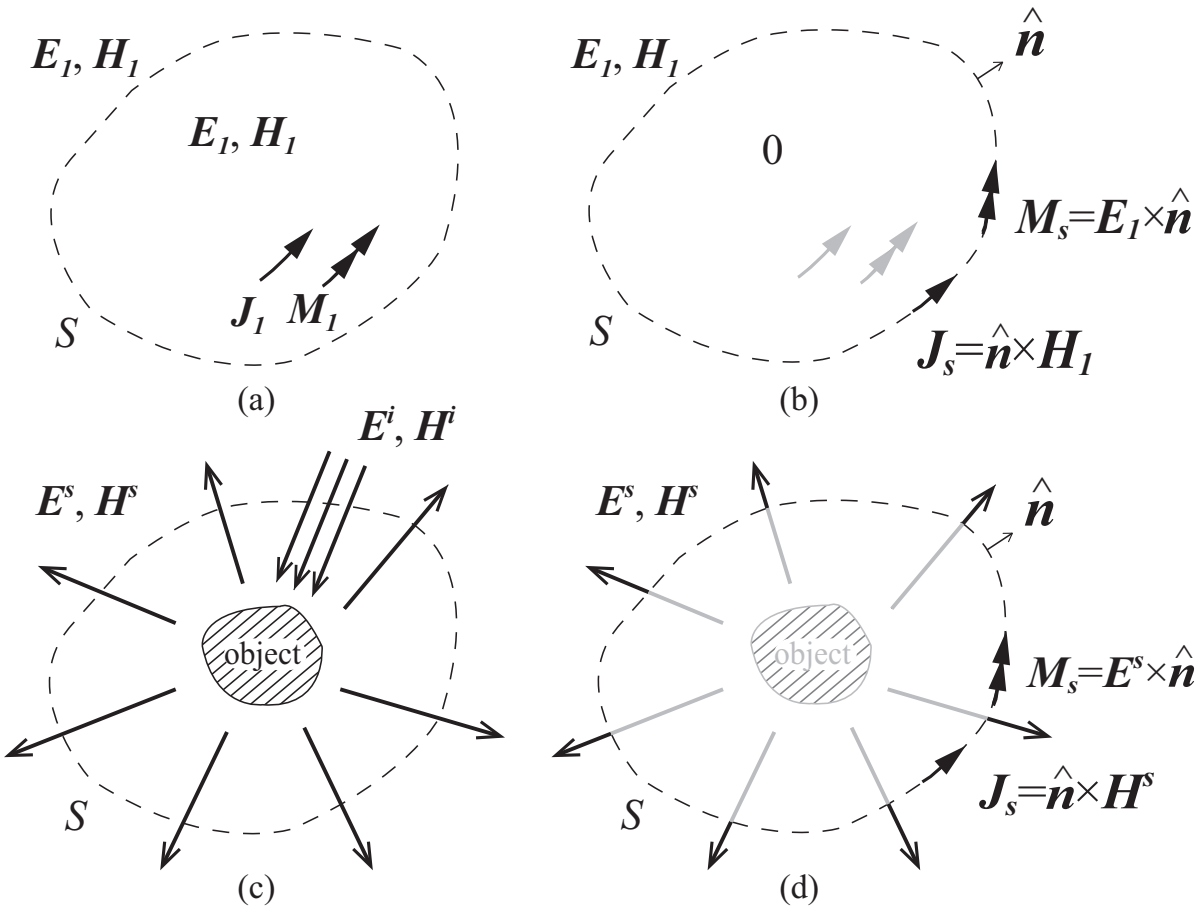

Figure 2.1: Field equivalence principle model. (a) Fields $\boldsymbol{E}_1$, $\boldsymbol{H}_1$ excited by original sources by $\boldsymbol{J}_1$, $\boldsymbol{M}_1$. (b) Fields $\boldsymbol{E}_1$, $\boldsymbol{H}_1$ excited by the equivalence surface currents $\boldsymbol{J}_s$, $\boldsymbol{M}_s$ on S. (c) Scattering fields $\boldsymbol{E}^s$, $\boldsymbol{H}^s$ by an object due to the incident wave $\boldsymbol{E}^i$, $\boldsymbol{H}^i$. (d) Scattering fields $\boldsymbol{E}^s$, $\boldsymbol{H}^s$ by the equivalence surface currents $\boldsymbol{J}_s$, $\boldsymbol{M}_s$ on S.

Let us now consider scattering field $\boldsymbol{E}^s$, $\boldsymbol{H}^s$, excited by an object upon which incident fields $\boldsymbol{E}^i$, $\boldsymbol{H}^i$ impinge from the exterior region as in Fig. 2.1(c). The total field may be written as a summation of the incident and scattering fields as

$$\boldsymbol{E} = \boldsymbol{E}^i + \boldsymbol{E}^s, \tag{2.3}$$

$$\boldsymbol{H} = \boldsymbol{H}^i + \boldsymbol{H}^s. \tag{2.4}$$

If one regards the scattering fields $\boldsymbol{E}^s$, $\boldsymbol{H}^s$ as the fields generated by the secondary sources due to the object, then the outside scattering fields can be determined from the surface

current sources:

$$\boldsymbol{J}_s = \hat{\boldsymbol{n}} \times \boldsymbol{H}^s, \tag{2.5}$$

$$\boldsymbol{M}_s = \boldsymbol{E}^s \times \hat{\boldsymbol{n}}, \tag{2.6}$$

on the virtual surface S in Fig. 2.1(d). Then the radiation field due to these surface currents can be derived from [22]

$$\boldsymbol{E}^s(\boldsymbol{r}) = \int_S \left\{ i\omega\mu_0 \boldsymbol{J}_s(\boldsymbol{r}')G - \boldsymbol{M}_s(\boldsymbol{r}') \times \nabla' G + \frac{i}{\omega\varepsilon_0} \boldsymbol{J}_s(\boldsymbol{r}') \cdot \nabla'\nabla' G \right\} dS, \tag{2.7}$$

$$\boldsymbol{H}^s(\boldsymbol{r}) = \int_S \left\{ i\omega\varepsilon_0 \boldsymbol{M}_s(\boldsymbol{r}')G + \boldsymbol{J}_s(\boldsymbol{r}') \times \nabla' G + \frac{i}{\omega\mu_0} \boldsymbol{M}_s(\boldsymbol{r}') \cdot \nabla'\nabla' G \right\} dS, \tag{2.8}$$

$$G(\boldsymbol{r}; \boldsymbol{r}') = \frac{i}{4} \mathrm{H}_0^{(1)}(k|\boldsymbol{r} - \boldsymbol{r}'|). \tag{2.9}$$

Here, $\mathrm{H}_0^{(1)}(\chi)$ denotes the zero-th order Hankel function of the first kind, ω is the angular frequency, and ∇' indicates differentiation with respect to the prime source coordinates.

Since the virtual surface S can be chosen arbitrary as long as the surface is outside the scattering object, we now choose S be just on the scattering body. By choosing so, the scattering fields $\boldsymbol{E}^s$, $\boldsymbol{H}^s$ can be obtained from the local feature of the scattering body surface on the high frequency basis. If one assumes that the radius of curvature of the surface is large compared with the wavelength, then the scattering fields $\boldsymbol{E}^s$, $\boldsymbol{H}^s$ may be given by the reflected GO fields $\boldsymbol{E}^r$, $\boldsymbol{H}^r$ of the original incident fields $\boldsymbol{E}^i$, $\boldsymbol{H}^i$ for the illuminated surface of the object. For the shadowed surface of the non-penetrable object, one could expect that the total fields $\boldsymbol{E}$, $\boldsymbol{H}$ would be almost null, therefore the scattering fields must behave to cancel the original incident fields $\boldsymbol{E}^i$, $\boldsymbol{H}^i$. Then, one shall assume $\boldsymbol{E}^s = -\boldsymbol{E}^i$, and $\boldsymbol{H}^s = -\boldsymbol{H}^i$. Accordingly, equivalent currents may be approximated as

$$\boldsymbol{J}_s = \hat{\boldsymbol{n}} \times \boldsymbol{H}^s \simeq \begin{cases} \hat{\boldsymbol{n}} \times \boldsymbol{H}^r & \text{on illuminated } S, \\ \hat{\boldsymbol{n}} \times (-\boldsymbol{H}^i) & \text{on shadowed } S, \end{cases} \tag{2.10}$$

$$\boldsymbol{M}_s = \boldsymbol{E}^s \times \hat{\boldsymbol{n}} \simeq \begin{cases} \boldsymbol{E}^r \times \hat{\boldsymbol{n}} & \text{on illuminated } S, \\ (-\boldsymbol{E}^i) \times \hat{\boldsymbol{n}} & \text{on shadowed } S. \end{cases} \tag{2.11}$$

Again, this is the high frequency approximation, since the scattering fields should have a diffracted field in addition to GO fields $\boldsymbol{E}^r$, $\boldsymbol{H}^r$ (or $-\boldsymbol{E}^i$, $-\boldsymbol{H}^i$). This diffraction contribution would be weaker than the GO fields by $\mathcal{O}(k^{-1/2})$. As will be seen in the next section, we shall show that the scattering field derived asymptotically from the equivalent

currents $\boldsymbol{J}_s$, $\boldsymbol{M}_s$ excite the same field by the PO current $\boldsymbol{J}^{PO}$, no matter how one chooses the virtual surface S in the shadowed region.

For the dielectric objects, the situation becomes more complicated than the conducting case in Eqs. (2.10) and (2.11). When the incident wave impinges on the illuminated surfaces, it excites the reflected wave ($\boldsymbol{E}^r$, $\boldsymbol{H}^r$) and the transmitted waves ($\boldsymbol{E}^t$, $\boldsymbol{H}^t$). Therefore, the scattering fields ($\boldsymbol{E}^s$, $\boldsymbol{H}^s$) on the illuminated region are given by the reflected waves ($\boldsymbol{E}^r$, $\boldsymbol{H}^r$) and the transmitted waves[1] ($\boldsymbol{E}^t$, $\boldsymbol{H}^t$), if any. On the shadowed region, one has to consider the transmitted waves ($\boldsymbol{E}^t$, $\boldsymbol{H}^t$), then the scattering fields would be $\boldsymbol{E}^s = -\boldsymbol{E}^i + \boldsymbol{E}^t$, $\boldsymbol{H}^s = -\boldsymbol{H}^i + \boldsymbol{H}^t$.

Accordingly, the equivalent current may be approximated as

$$\boldsymbol{J}_s = \hat{\boldsymbol{n}} \times \boldsymbol{H}^s \simeq \begin{cases} \hat{\boldsymbol{n}} \times (\boldsymbol{H}^r + \boldsymbol{H}^t) & \text{on illuminated } S, \\ \hat{\boldsymbol{n}} \times (-\boldsymbol{H}^i + \boldsymbol{H}^t) & \text{on shadowed } S, \end{cases} \tag{2.12}$$

$$\boldsymbol{M}_s = \boldsymbol{E}^s \times \hat{\boldsymbol{n}} \simeq \begin{cases} (\boldsymbol{E}^r + \boldsymbol{E}^t) \times \hat{\boldsymbol{n}} & \text{on illuminated } S, \\ (-\boldsymbol{E}^i + \boldsymbol{E}^t) \times \hat{\boldsymbol{n}} & \text{on shadowed } S. \end{cases} \tag{2.13}$$

In this chapter, the surface equivalence theorem based on the assumption that scattering far field is generated by the equivalent electric and magnetic currents flow on a virtual surface enclosed the scattering object. These equivalent currents may be approximated from the reflected and minus incident waves for the conducting objects, and from the reflected/transmitted GO waves for the dielectric objects.

[1] If one traces the transmitted wave through the dielectric body, some waves with multiply internal bouncing may emanate finally from the illuminated surface S too.

Chapter 3

High Frequency Scattering Analysis by Physical Optics Approximation

In this chapter, the physical optics (PO) approximation are applied to estimate electromagnetic scattering from the conducting wedge and rectangular cylinder. Physical optics (PO) approximation is a method which is known to have pretty accurate and can be efficiently used for high frequency scattering problems from the object made of conducting materials. According to the PO approximation, if the scattering objects are large compared with the wavelength, the PO currents $\boldsymbol{J}^{PO}$ are approximated from the magnetic incident field as

$$\boldsymbol{J}^{PO} = \begin{cases} 2\hat{\boldsymbol{n}} \times \boldsymbol{H}^i & \text{on illuminated surface,} \\ 0 & \text{on shadowed surface,} \end{cases} \tag{3.1}$$

and flow on the physically illuminated surfaces. This PO current $\boldsymbol{J}^{PO}$ is exact when the scattering body is made by an infinitely wide and flat electrical conductor, and $\boldsymbol{J}^{PO}$ could be a good approximation for a smoothly curved electric conducting surface whose radius of curvature is large compared with the wavelength. Then, the scattering field from this object may be derived by integrating these PO currents with the free-space Green's function. Since PO formulation involves the information of the incident wave and the scattering object's surface, it is easy to construct the equivalent currents for scattering field. This chapter starts by applying the PO method to derive diffraction field from a conducting wedge in Section 3.1. Here, the scattering field is obtained from only one PO current flowing on the illuminated surface. In Section 3.2, the conducting rectangular

cylinder has been considered. In this case, the incident wave impinges on the cylinder at two surfaces and excites two PO currents on these illuminated surfaces. Then, the total scattering fields are given by summing up the fields radiated from these PO currents.

3.1 Diffraction by a Conducting Wedge

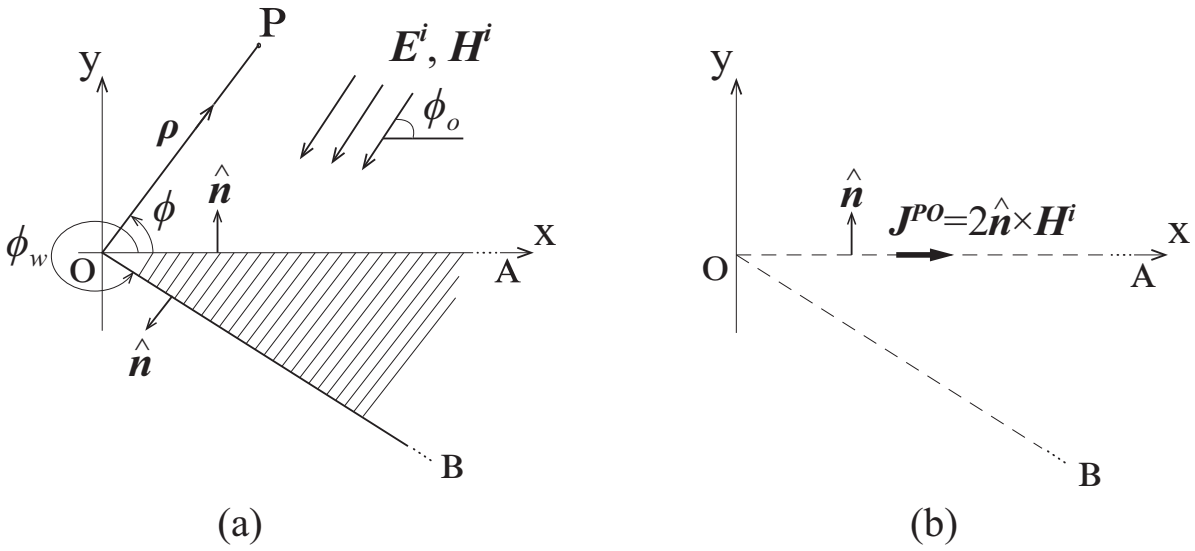

Figure 3.1: Diffraction by a conducting wedge. (a) Wedge diffraction by plane waves $\boldsymbol{E}^i$, $\boldsymbol{H}^i$. (b) PO current $\boldsymbol{J}^{PO}$ due to the incident field on the illuminated surface OA.

Figure 3.1(a) shows a two-dimensional conducting wedge of the wedge angle ϕ_w illuminated by a plane wave.

The scattering formulation may be separated into two polarizations.

3.1.1 E Polarization

An E polarized incident plane wave can be written as

$$\boldsymbol{E}^i = E_0 e^{-ik(x\cos\phi_0 + y\sin\phi_0)}\hat{\boldsymbol{z}}, \tag{3.2}$$

$$\boldsymbol{H}^i = E_0\sqrt{\frac{\varepsilon_0}{\mu_0}}e^{-ik(x\cos\phi_0 + y\sin\phi_0)}(-\sin\phi_0\hat{\boldsymbol{x}} + \cos\phi_0\hat{\boldsymbol{y}}), \tag{3.3}$$

where $k = \omega\sqrt{\varepsilon_0\mu_0}$ denotes the free space wave number. For simplicity, let us assume that the incident plane wave illuminates surface OA only ($0 < \phi_0 < \phi_w - \pi$) and the

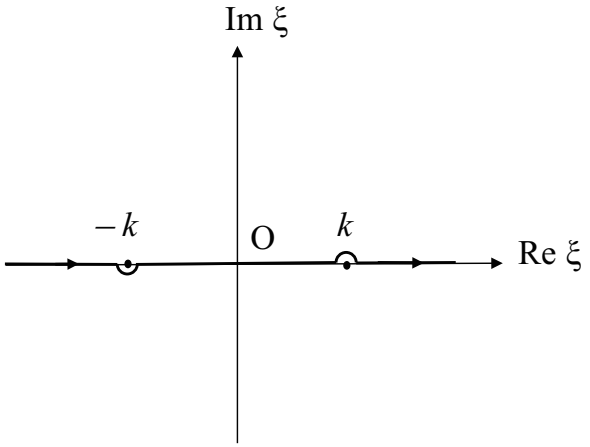

Figure 3.2: Integration contour in the complex ξ plane.

observation angle is taken as $0 < |\phi| < \pi$. The PO current $\boldsymbol{J}^{PO}$ on the illuminated wedge surface OA can be found from incident wave as Eq. (3.1)

$$\boldsymbol{J}^{PO}(x) \;= 2\hat{\boldsymbol{y}} \times \boldsymbol{H}^i\Big|_{y=0} = 2E_0\sqrt{\frac{\varepsilon_0}{\mu_0}}\sin\phi_0 e^{-ikx\cos\phi_0}\hat{\boldsymbol{z}}, \qquad (x>0). \tag{3.4}$$

The scattering field can be obtained by integrating $\boldsymbol{J}^{PO}$ with the two-dimensional Green's function G as

$$E_z^{PO} = -\int_S \frac{\omega\mu_0}{4} J^{PO}(x')\mathrm{H}_0^{(1)}(k\sqrt{(x-x')^2+(y-y')^2})\Big|_{y'=0} dS, \tag{3.5}$$

where $\mathrm{H}_0^{(1)}\left(k\sqrt{(x-x)^2+(y-y')^2}\right)$ denotes the zero-th order Hankel function of the first kind. Spectral representation of this Hankel function is given by

$$\mathrm{H}_0^{(1)}\left(k\sqrt{(x-x')^2+(y-y')^2}\right) = \frac{1}{\pi}\int_{-\infty}^{\infty} \frac{e^{i\xi(x-x')+i\sqrt{k^2-\xi^2}|y-y'|}}{\sqrt{k^2-\xi^2}}\, d\xi, \tag{3.6}$$

where the integration in the complex ξ plane is shown in Fig. 3.2. From Eqs. (3.4) and (3.6), we have

$$\begin{aligned} E_z^{PO} &= -\int_0^{\infty}\left[\frac{\omega\mu_0}{2\pi}E_0\sqrt{\frac{\varepsilon_0}{\mu_0}}\sin\phi_0 e^{-ikx'\cos\phi_0}\int_{-\infty}^{\infty}\frac{e^{i\xi(x-x')+i\sqrt{k^2-\xi^2}|y|}}{\sqrt{k^2-\xi^2}}\,d\xi\right]dx' \\ &= -E_0\frac{ik}{2\pi}\sin\phi_0\int_{-\infty}^{\infty}\left(\int_0^{\infty}e^{-ix'(k\cos\phi_0+\xi)}\,dx'\right)\frac{e^{i\xi x\pm i\sqrt{k^2-\xi^2}y}}{\sqrt{k^2-\xi^2}}\,d\xi \\ &= E_0\frac{ik}{2\pi}\sin\phi_0\int_{-\infty}^{\infty}\frac{e^{i\xi x\pm i\sqrt{k^2-\xi^2}y}}{(k\cos\phi_0+\xi)\sqrt{k^2-\xi^2}}\,d\xi, \quad (y\gtrless 0). \end{aligned} \tag{3.7}$$

Since the integral in Eq. (3.7) cannot be analytically evaluated, the saddle point method is used. Converting to complex angle w plane using the transformation $\xi = k\sin w$, with

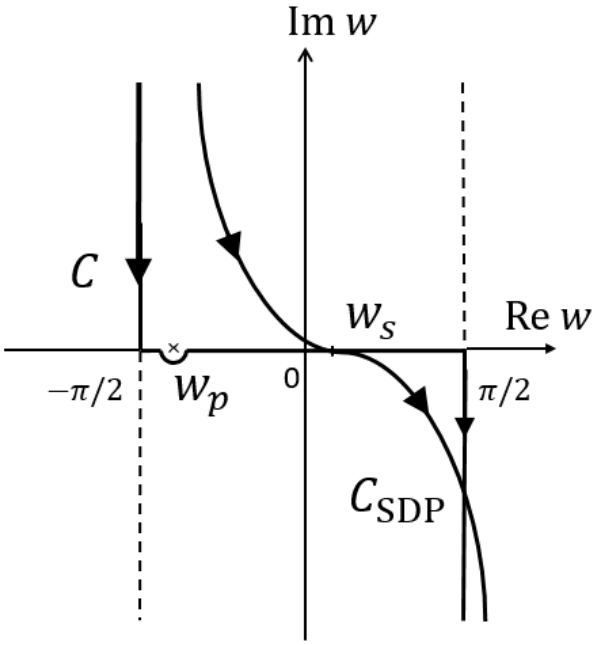

Figure 3.3: Integration contour C and C_{SDP} in the complex angular w plane.

the cylindrical coordinates (ρ, θ) with $x = \rho\cos\phi, y = \rho\sin\phi$, we have

$$\begin{aligned} E_z^{PO} &= E_0 \frac{ik}{2\pi} \sin\phi_0 \int_C \frac{e^{ik\rho(\cos\phi\sin w \pm \sin\phi\cos w)}}{k(\cos\phi_0 + \sin w)k\cos w} k\cos w\, dw \\ &= E_0 \frac{i}{2\pi} \sin\phi_0 \int_C \frac{e^{ik\rho\sin(w\pm\phi)}}{\cos\phi_0 + \sin w}\, dw, \end{aligned} \tag{3.8}$$

where contour C is given in Fig. 3.3.

One finds the saddle point from the following equation:

$$\frac{\partial}{\partial w}\left[ik\rho\sin(w \pm \phi)\right] = ik\rho\cos(w \pm \phi) = 0, \tag{3.9}$$

we obtain $w_s = \pi/2 \mp \phi$ as a possible saddle point on the contour. At the saddle point, we have

$$\sin w_s = \sin(\pi/2 \mp \phi) = \cos\phi, \tag{3.10}$$

$$\cos w_s = \cos(\pi/2 \mp \phi) = \pm\sin\phi, \tag{3.11}$$

$$ik\rho\sin(w_s + \phi) = ik\rho\sin(\pi/2) = ik\rho, \tag{3.12}$$

$$\frac{\partial^2}{\partial^2 w}\left[ik\rho\sin(w \pm \phi)\right]\Big|_{w=w_s} = -ik\rho\sin(w \pm \phi)\Big|_{w=w_s} = -ik\rho. \tag{3.13}$$

Then, by deforming the integration contour C to SDP in Fig. 3.3, Eq. (3.8) can be

approximated as

$$
\begin{aligned}
E_d^{PO} &= E_0 \frac{i}{2\pi} \sin\phi_0 \int_C \frac{e^{ik\rho\sin(w\pm\phi)}}{\cos\phi_0 + \sin w}\, dw \\
&\sim E_0 \frac{i}{2\pi} \frac{\sin\phi_0}{\cos\phi_0 + \sin w_s} e^{ik\rho} \int_{C_{SDP}} e^{-ik\rho(w-w_s)^2/2}\, dw \\
&= E_0 \frac{i}{2\pi} \frac{\sin\phi_0}{\cos\phi_0 + \cos\phi} e^{ik\rho} \sqrt{\frac{2\pi}{ik\rho}} = E_0 \frac{2\sin\phi_0}{\cos\phi_0 + \cos\phi} \sqrt{\frac{1}{8\pi k\rho}} e^{ik\rho + i\pi/4}. \quad (3.14)
\end{aligned}
$$

There are some cases where the pole $w_p = \phi_0 - \pi/2$ included in the integral. When $0 < |\phi| < \pi - \phi_0$, it is necessary to add the contribution of the pole. With $\sin w_p = \sin(\phi_0 - \pi/2) = -\cos\phi_0$, $\cos w_p = \cos(\phi_0 - \pi/2) = \sin\phi_0$, then

$$
\begin{aligned}
E_p^{PO} &= 2\pi i \frac{iE_0}{2\pi} \sin\phi_0 \frac{e^{ik\rho(\sin w_p \cos\phi \pm \cos w_p \sin\phi)}}{\cos w_p} = -E_0 \frac{\sin\phi_0}{\sin\phi_0} e^{-ik\rho(\cos\phi_0\cos\phi \pm \sin\phi_0 \sin\phi)} \\
&= -E_0 e^{-ikx\cos\phi \mp iky\sin\phi_0}, \quad (y \gtrless 0). \quad (3.15)
\end{aligned}
$$

Therefore, the diffraction from the conducting wedge becomes

$$
\begin{aligned}
E_z^{PO} &= E_d^{PO} + E_p^{PO} \\
&= E_0 \frac{2\sin\phi_0}{\cos\phi_0 + \cos\phi} C(k\rho) - E_0 e^{-ikx\cos\phi \mp iky\sin\phi_0} U(\pi - \phi_0 - |\phi|), (y \gtrless 0), \quad (3.16)
\end{aligned}
$$

where $C(\chi) = \sqrt{\frac{1}{8\pi\chi}} e^{i\chi + i\pi/4}$ is the asymptotic form of the two-dimensional free space Green's function for large χ, and $U(x) = \begin{cases} 1 & x > 0 \\ 0 & x < 0 \end{cases}$ is a step function.

3.1.2 H Polarization

A H polarization incident plane wave is given by

$$
\boldsymbol{H}^i = H_0 e^{-ik(x\cos\phi_0 + y\sin\phi_0)} \hat{\boldsymbol{z}}, \quad (3.17)
$$

$$
\boldsymbol{E}^i = H_0 \sqrt{\frac{\mu_0}{\varepsilon_0}} e^{-ik(x\cos\phi_0 + y\sin\phi_0)} (\sin\phi_0 \hat{\boldsymbol{x}} - \cos\phi_0 \hat{\boldsymbol{y}}). \quad (3.18)
$$

The PO current $\boldsymbol{J}^{PO}$ on the illuminated wedge surface OA can be found from incident wave as Eq. (3.1)

$$
\boldsymbol{J}^{PO}(x) \;= 2\hat{\boldsymbol{y}} \times \boldsymbol{H}^i\Big|_{y=0} = 2H_0 e^{jkx\cos\phi_0} \hat{\boldsymbol{x}}, \qquad (x > 0). \quad (3.19)
$$

The scattering field can be obtained by integrating $\boldsymbol{J}^{PO}$ with the two-dimensional Green's function G as

$$H_z^{PO} = \int_S \frac{i}{4} J^{PO}(x') \frac{\partial}{\partial y'} \mathrm{H}_0^{(1)}(k\sqrt{(x-x')^2+(y-y')^2})\Big|_{y'=0} dS, \tag{3.20}$$

$$\begin{aligned}\frac{\partial}{\partial y'} \mathrm{H}_0^{(1)}(k\sqrt{(x-x')^2+(y-y')^2}) &= \frac{\partial}{\partial y'}\left(\frac{1}{\pi}\int_{-\infty}^{\infty} \frac{e^{i\xi(x-x')+i\sqrt{k^2-\xi^2}|y-y'|}}{\sqrt{k^2-\xi^2}}\, d\xi\right) \\ &= \mp\frac{i}{\pi}\int_{-\infty}^{\infty} e^{i\xi(x-x')\pm i\sqrt{k^2-\xi^2}(y-y')}\, d\xi, \ (y \gtrless y'). \end{aligned} \tag{3.21}$$

$$\begin{aligned} H_z^{PO} &= \int_0^{\infty} \Big[\pm \frac{H_0}{2\pi} e^{-ikx'\cos\phi_0} \int_{-\infty}^{\infty} e^{i\xi(x-x')\pm i\sqrt{k^2-\xi^2}y}\, d\xi \Big]\, dx' \\ &= \pm\frac{H_0}{2\pi}\int_{-\infty}^{\infty}\left(\int_0^{\infty} e^{-ix'(k\cos\phi_0+\xi)}\, dx'\right) e^{i\xi x\pm i\sqrt{k^2-\xi^2}y}\, d\xi \\ &= \mp\frac{iH_0}{2\pi}\int_{-\infty}^{\infty}\frac{e^{i\xi x\pm i\sqrt{k^2-\xi^2}y}}{k\cos\phi_0+\xi}\, d\xi, \quad (y \gtrless 0). \end{aligned} \tag{3.22}$$

Since the integral in Eq. (3.22) cannot be analytically evaluated, the saddle point method is used. Converting to complex angle w plane using the transformation $\xi = k\sin w$, with the cylindrical coordinates (ρ, θ) with $x = \rho\cos\phi, y = \rho\sin\phi$, we have

$$\begin{aligned} H_z^{PO} &= \mp\frac{iH_0}{2\pi}\int_C \frac{e^{ik\rho(\cos\phi\sin w\pm\sin\phi\cos w)}}{k\cos\phi_0+k\sin w} k\cos w\, dw \\ &= \mp\frac{iH_0}{2\pi}\int_C \frac{\cos w e^{ik\rho\sin(w\pm\phi)}}{\cos\phi_0+\sin w}\, dw. \end{aligned} \tag{3.23}$$

We obtain $w_s = \pi/2 \mp \phi$ as a possible saddle point on the contour. At the saddle point, Eq. (3.23) becomes [22]

$$\begin{aligned} H_d^{PO} &= \mp\frac{iH_0}{2\pi}\int_C \frac{\cos w}{\cos\phi_0+\sin w} e^{ik\rho\sin(w\pm\phi)}\, dw \\ &\sim \mp\frac{iH_0}{2\pi}\frac{\cos w_s}{\cos\phi_0+\sin w_s} e^{ik\rho}\int_{C_{SDP}} e^{-ik\rho(w-w_s)^2/2}\, dw \\ &= \mp\frac{iH_0}{2\pi}\frac{\pm\sin\phi}{\cos\phi_0+\cos\phi} e^{ik\rho}\sqrt{\frac{2\pi}{ik\rho}} = -H_0\frac{2\sin\phi}{\cos\phi_0+\cos\phi} C(k\rho). \end{aligned} \tag{3.24}$$

There are some cases where the pole $w_p = \phi_0 - \pi/2$ included in the integral. When $0 < |\phi| < \pi - \phi_0$, it is necessary to add the contribution of the pole. With $\sin w_p = \sin(\phi_0 - \pi/2) = -\cos\phi_0$, $\cos w_p = \cos(\phi_0 - \pi/2) = \sin\phi_0$, then

$$\begin{aligned} H_p^{PO} &= 2\pi i \mp \frac{iH_0}{2\pi}\frac{\cos w_p}{\cos w_p} e^{ik\rho(\sin w_p\cos\phi\pm\cos w_p\sin\phi)} \\ &= \pm H_0 e^{-ik\rho(\cos\phi_0\cos\phi\mp\sin\phi_0\sin\phi)} \\ &= \pm H_0 e^{-ikx\cos\phi\pm iky\sin\phi_0}, \quad (y \gtrless 0). \end{aligned} \tag{3.25}$$

Therefore, the diffraction from the conducting wedge becomes

$$\begin{aligned} H_z^{PO} &= H_d^{PO} + H_p^{PO} \\ &= -H_0 \frac{2\sin\phi}{\cos\phi_0 + \cos\phi} C(k\rho) \pm H_0 e^{-ikx\cos\phi \pm iky\sin\phi_0} U(\pi - \phi_0 - |\phi|), (y \gtrless 0) \end{aligned} \tag{3.26}$$

with U is a step function.

3.2 Scattering by a Rectangular Cylinder

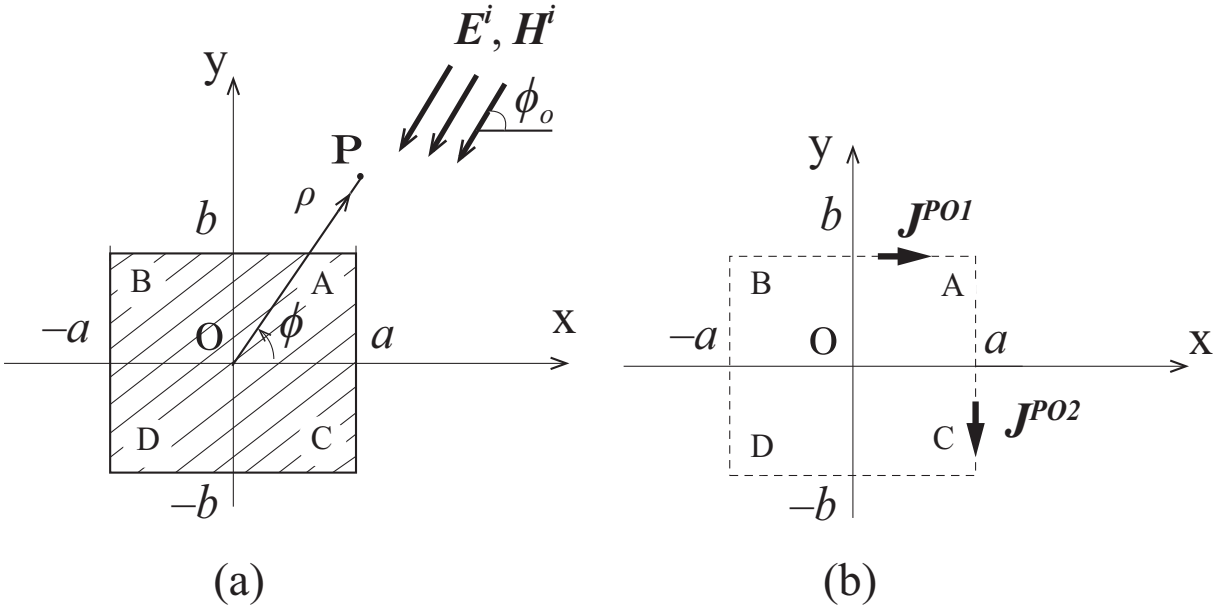

Figure 3.4: Scattering by a conducting wedge. (a) Scattering by plane waves $\boldsymbol{E}^i$, $\boldsymbol{H}^i$. (b) PO current $\boldsymbol{J}^{PO}$ due to the incident field on the illuminated surfaces.

Let us consider that a plane wave impinges upon a surface of a conducting rectangular cylinder whose dimensions are $2a \times 2b$ as shown in Fig. 3.4(a). Because of the symmetry of the scattering object, the incident angle ϕ_0 is assumed as $0 < \phi_0 < 90^o$ without losing the generality.

The scattering formulation may be separated into two polarizations.

3.2.1 E Polarization

An E polarized incident plane wave can be written as

$$\boldsymbol{E}^i = E_0 e^{-ik(x\cos\phi_0 + y\sin\phi_0)}\hat{\boldsymbol{z}}, \tag{3.27}$$

$$\boldsymbol{H}^i = E_0\sqrt{\frac{\varepsilon_0}{\mu_0}}e^{-ik(x\cos\phi_0 + y\sin\phi_0)}(-\sin\phi_0\hat{\boldsymbol{x}} + \cos\phi_0\hat{\boldsymbol{y}}), \tag{3.28}$$

where $k = \omega\sqrt{\varepsilon_0\mu_0}$ denotes the free space wave number.

The PO current $\boldsymbol{J}^{PO}$ on the illuminated cylinder surface AB can be found from incident wave as Eq. (3.1)

$$\boldsymbol{J}^{PO1}(x) \;= 2\hat{\boldsymbol{y}} \times \boldsymbol{H}^i\Big|_{y=b} = 2E_0\sqrt{\frac{\varepsilon_0}{\mu_0}}\sin\phi_0 e^{-ik(x\cos\phi_0 + b\sin\phi_0)}\hat{\boldsymbol{z}}, (-a < x < a), \tag{3.29}$$

and on surface AC,

$$\boldsymbol{J}^{PO2}(y) \;= 2\hat{\boldsymbol{x}} \times \boldsymbol{H}^i\Big|_{x=a} = 2E_0\sqrt{\frac{\varepsilon_0}{\mu_0}}\cos\phi_0 e^{-ik(a\cos\phi_0 + y\sin\phi_0)}\hat{\boldsymbol{z}}, (-b < y < b). \tag{3.30}$$

The scattering field can be obtained by integrating $\boldsymbol{J}^{PO1}$, $\boldsymbol{J}^{PO2}$ with the two-dimensional Green's function G as

$$E_z^{PO1} = -\int_S \frac{\omega\mu_0}{4} J^{PO1}\mathrm{H}_0^{(1)}(k\sqrt{(x-x')^2 + (y-y')^2})\Big|_{y'=b}\, dS, \tag{3.31}$$

$$E_z^{PO2} = -\int_S \frac{\omega\mu_0}{4} J^{PO2}\mathrm{H}_0^{(1)}(k\sqrt{(x-x')^2 + (y-y')^2})\Big|_{x'=a}\, dS. \tag{3.32}$$

From Eqs. (3.29), (3.30) and (3.6), we have

$$\begin{aligned}
E_z^{PO1} &= -\int_{-a}^{a}\left[E_0\frac{k}{2\pi}\sin\phi_0 e^{-ik(x'\cos\phi_0 + b\sin\phi_0)}\int_{-\infty}^{\infty}\frac{e^{i\xi(x-x') + i\sqrt{k^2-\xi^2}|y-b|}}{\sqrt{k^2-\xi^2}}\,d\xi\right]dx' \\
&= -E_0\frac{k}{2\pi}\sin\phi_0 e^{-ikb\sin\phi_0}\int_{-\infty}^{\infty}\left(\int_{-a}^{a}e^{-ix'(k\cos\phi_0+\xi)}\,dx'\right)\frac{e^{i\xi x \pm i\sqrt{k^2-\xi^2}(y-b)}}{\sqrt{k^2-\xi^2}}\,d\xi \\
&= -E_0\frac{ik}{2\pi}\sin\phi_0 e^{-ikb\sin\phi_0}\int_{-\infty}^{\infty}\frac{(e^{-ia(k\cos\phi_0+\xi)} - e^{ia(k\cos\phi_0+\xi)})e^{i\xi x \pm i\sqrt{k^2-\xi^2}(y-b)}}{(k\cos\phi_0+\xi)\sqrt{k^2-\xi^2}}\,d\xi \\
&= -E_0\frac{ik}{2\pi}\sin\phi_0 e^{-ikb\sin\phi_0}e^{-ika\cos\phi_0}\int_{-\infty}^{\infty}\frac{e^{i\xi(x-a) \pm i\sqrt{k^2-\xi^2}(y-b)}}{(k\cos\phi_0+\xi)\sqrt{k^2-\xi^2}}\,d\xi \\
&\quad + E_0\frac{ik}{2\pi}\sin\phi_0 e^{-ikb\sin\phi_0}e^{ika\cos\phi_0}\int_{-\infty}^{\infty}\frac{e^{i\xi(x+a) \pm i\sqrt{k^2-\xi^2}(y-b)}}{(k\cos\phi_0+\xi)\sqrt{k^2-\xi^2}}\,d\xi, \quad (y \gtrless b),
\end{aligned} \tag{3.33}$$

$$E_z^{PO2} = -\int_{-b}^{b}\left[E_0\frac{k}{2\pi}\cos\phi_0 e^{-ik(a\cos\phi_0 + y\sin\phi_0)}\int_{-\infty}^{\infty}\frac{e^{i\xi(x-a) + i\sqrt{k^2-\xi^2}|y-y'|}}{\sqrt{k^2-\xi^2}}\,d\xi\right]dy'$$

$$= -E_0\frac{k}{2\pi}\cos\phi_0 e^{-ika\cos\phi_0}\int_{-\infty}^{\infty}\left(\int_{-b}^{b}e^{-iy'(k\sin\phi_0 \pm\sqrt{k^2-\xi^2})}\,dy'\right)\frac{e^{i\xi(x-a) \pm i\sqrt{k^2-\xi^2}y}}{\sqrt{k^2-\xi^2}}\,d\xi, \tag{3.34}$$

For $y > b$, one gets

$$E_z^{PO2} = -E_0 \frac{ik}{2\pi} \cos\phi_0 e^{-ika\cos\phi_0} e^{-ikb\sin\phi_0} \int_{-\infty}^{\infty} \frac{e^{i\xi(x-a)\pm i\sqrt{k^2-\xi^2}(y-b)}}{(k\sin\phi_0 \pm \sqrt{k^2-\xi^2})\sqrt{k^2-\xi^2}}\, d\xi \quad (3.35)$$

and for $y < -b$

$$E_z^{PO2} = E_0 \frac{ik}{2\pi} \cos\phi_0 e^{-ika\cos\phi_0} e^{ikb\sin\phi_0} \int_{-\infty}^{\infty} \frac{e^{i\xi(x-a)\pm i\sqrt{k^2-\xi^2}(y+b)}}{(k\sin\phi_0 \pm \sqrt{k^2-\xi^2})\sqrt{k^2-\xi^2}}\, d\xi. \quad (3.36)$$

Converting to complex angle w plane using the transformation $\xi = k\sin w$, with the cylindrical coordinates $(x-a = \rho_A\cos\phi_A, y-b = \rho_A\sin\phi_A)$, and $(x+a = \rho_B\cos\phi_B, y-b = \rho_B\sin\phi_B)$ for surface AB, Eq. (3.33) becomes

$$\begin{aligned} E_z^{PO1} &= -E_0 \frac{ik}{2\pi} \sin\phi_0 e^{-ikb\sin\phi_0} e^{-ika\cos\phi_0} \int_C \frac{e^{ik\rho_A(\cos\phi_A\sin w \pm \sin\phi_A\cos w)}}{(k\cos\phi_0 + k\sin w)k\cos w} k\cos w\, dw \\ &\quad + E_0 \frac{ik}{2\pi} \sin\phi_0 e^{-ikb\sin\phi_0} e^{ika\cos\phi_0} \int_C \frac{e^{ik\rho_B(\cos\phi_B\sin w \pm \sin\phi_B\cos w)}}{(k\cos\phi_0 + k\sin w)k\cos w} k\cos w\, dw \\ &= -E_0 \frac{i}{2\pi} \sin\phi_0 e^{-ikb\sin\phi_0} e^{-ika\cos\phi_0} \int_C \frac{e^{ik\rho_A\sin(w\pm\phi_A)}}{\cos\phi_0 + \sin w} dw \\ &\quad + E_0 \frac{i}{2\pi} \sin\phi_0 e^{-ikb\sin\phi_0} e^{ika\cos\phi_0} \int_C \frac{e^{ik\rho_B\sin(w\pm\phi_B)}}{\cos\phi_0 + \sin w} dw. \end{aligned} \quad (3.37)$$

Similarly, converting to complex angle w plane using the transformation $\xi = k\sin w$, with the cylindrical coordinates $(x-a = \rho_A\cos\phi_A, y-b = \rho_A\sin\phi_A)$, and $(x-a = \rho_C\cos\phi_C, y+b = \rho_C\sin\phi_C)$ for surface AC, Eq. (3.36) becomes

$$\begin{aligned} E_z^{PO2} &= -E_0 \frac{ik}{2\pi} \cos\phi_0 e^{-ikb\sin\phi_0} e^{-ika\cos\phi_0} \int_C \frac{e^{ik\rho_A(\cos\phi_A\sin w \pm \sin\phi_A\cos w)}}{(k\sin\phi_0 \pm k\cos w)k\cos w} k\cos w\, dw \\ &\quad + E_0 \frac{ik}{2\pi} \cos\phi_0 e^{ikb\sin\phi_0} e^{-ika\cos\phi_0} \int_C \frac{e^{ik\rho_C(\cos\phi_B\sin w \pm \sin\phi_C\cos w)}}{(k\sin\phi_0 \pm k\cos w)k\cos w} k\cos w\, dw \\ &= -E_0 \frac{i}{2\pi} \cos\phi_0 e^{-ikb\sin\phi_0} e^{-ika\cos\phi_0} \int_C \frac{e^{ik\rho_A\sin(w\pm\phi_A)}}{\sin\phi_0 \pm \cos w} dw \\ &\quad + E_0 \frac{i}{2\pi} \cos\phi_0 e^{ikb\sin\phi_0} e^{-ika\cos\phi_0} \int_C \frac{e^{ik\rho_C\sin(w\pm\phi_C)}}{\sin\phi_0 \pm \cos w} dw. \end{aligned} \quad (3.38)$$

We obtain$w_s = \pi/2 \mp \phi_A$ and $w_s = \pi/2 \mp \phi_B$ as a saddle point on the contour. At the saddle point, Eq. (3.37) becomes

$$\begin{aligned} E_z^{PO1} &\sim -\frac{iE_0}{2\pi} e^{-ikb\sin\phi_0} e^{-ika\cos\phi_0} \frac{\sin\phi_0}{\cos\phi_0 + \sin(\pi/2 \mp \phi_A)} e^{ik\rho_A} \int_{C_{SDP}} e^{-ik\rho_A(w-w_s)^2/2}\, dw \\ &\quad + \frac{iE_0}{2\pi} e^{-ikb\sin\phi_0} e^{ika\cos\phi_0} \frac{\sin\phi_0}{\cos\phi_0 + \sin(\pi/2 \mp \phi_B)} e^{ik\rho_B} \int_{C_{SDP}} e^{-ik\rho_B(w-w_s)^2/2}\, dw \\ &= -E_0 \frac{i}{2\pi} e^{-ikb\sin\phi_0} e^{-ika\cos\phi_0} \frac{\sin\phi_0}{\cos\phi_0 + \cos\phi_A} e^{ik\rho_A} \sqrt{\frac{2\pi}{ik\rho_A}} \\ &\quad + E_0 \frac{i}{2\pi} e^{-ikb\sin\phi_0} e^{ika\cos\phi_0} \frac{\sin\phi_0}{\cos\phi_0 + \cos\phi_B} e^{ik\rho_B} \sqrt{\frac{2\pi}{ik\rho_B}}. \end{aligned} \quad (3.39)$$

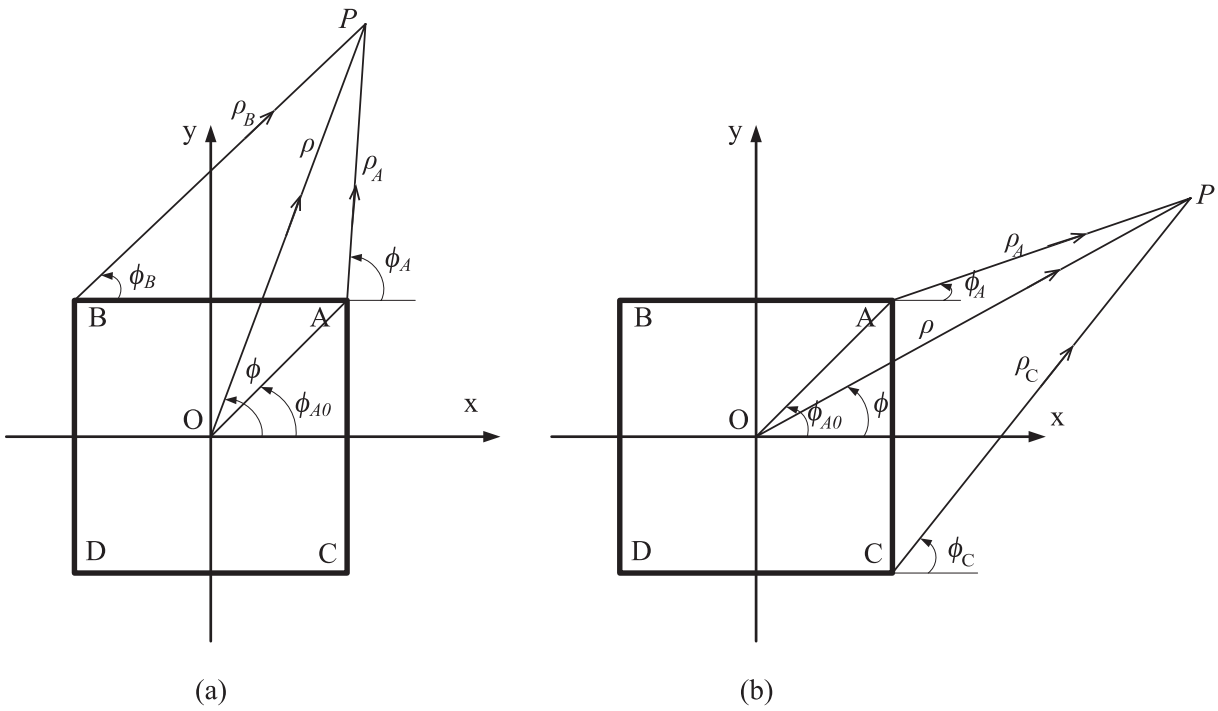

Figure 3.5: Observation point from surfaces AB (a) and AC (b).

At the saddle point $w_s = \pi/2 \mp \phi_A$ and $w_s = \pi/2 \mp \phi_C$, Eq. (3.38) becomes

$$\begin{aligned} E_z^{PO2} \sim & -\frac{iE_0}{2\pi} e^{-ikb\sin\phi_0} e^{-ika\cos\phi_0} \frac{\cos\phi_0}{\sin\phi_0 \pm \cos(\pi/2 \mp \phi_A)} e^{ik\rho_A} \int_{C_{SDP}} e^{-ik\rho_A (w-w_s)^2/2}\, dw \\ & + \frac{iE_0}{2\pi} e^{ikb\sin\phi_0} e^{-ika\cos\phi_0} \frac{\cos\phi_0}{\sin\phi_0 \pm \cos(\pi/2 \mp \phi_C)} e^{ik\rho_C} \int_{C_{SDP}} e^{-ik\rho_C (w-w_s)^2/2}\, dw \\ = & -E_0 \frac{i}{2\pi} e^{-ikb\sin\phi_0} e^{-ika\cos\phi_0} \frac{\cos\phi_0}{\sin\phi_0 + \sin\phi_A} e^{ik\rho_A} \sqrt{\frac{2\pi}{ik\rho_A}} \\ & + E_0 \frac{i}{2\pi} e^{ikb\sin\phi_0} e^{-ika\cos\phi_0} \frac{\cos\phi_0}{\sin\phi_0 + \sin\phi_C} e^{ik\rho_C} \sqrt{\frac{2\pi}{ik\rho_C}}. \end{aligned} \tag{3.40}$$

For far-field ($k\rho \gg 1$), assuming that

$$\begin{cases} \phi_A = \phi_B = \phi_C \sim \phi \\ \rho_A = \rho_B = \rho_C \sim \rho \end{cases} \quad \text{for amplitude variations,}$$

$$\begin{cases} \rho_A = \rho - d\cos(\phi - \phi_{A0}) = \rho - a\cos\phi - b\sin\phi \\ \rho_B = \rho - d\cos(\pi - \phi - \phi_{A0}) = \rho + a\cos\phi - b\sin\phi \\ \rho_C = \rho - d\cos(\phi + \phi_{A0}) = \rho - a\cos\phi + b\sin\phi \end{cases} \quad \text{for phase variations,} \tag{3.41}$$

then, Eqs. (3.39) and (3.40) can be approximated as

$$\begin{aligned} E_z^{PO1} &= -E_0\frac{i}{2\pi}e^{-ikb(\sin\phi+\sin\phi_0)}e^{-ika(\cos\phi+\cos\phi_0)}\frac{\sin\phi_0}{\cos\phi_0+\cos\phi}e^{ik\rho}\sqrt{\frac{2\pi}{ik\rho}} \\ &\quad +E_0\frac{i}{2\pi}e^{-ikb(\sin\phi+\sin\phi_0)}e^{ika(\cos\phi+\cos\phi_0)}\frac{\sin\phi_0}{\cos\phi_0+\cos\phi}e^{ik\rho}\sqrt{\frac{2\pi}{ik\rho}} \\ &= 4iE_0e^{-ikb(\sin\phi+\sin\phi_0)}\sin[ka(\cos\phi_0+\cos\phi)]\frac{\sin\phi_0}{\cos\phi_0+\cos\phi}C(k\rho), \end{aligned} \tag{3.42}$$

$$\begin{aligned} E_z^{PO2} &= -E_0\frac{i}{2\pi}e^{-ika(\cos\phi+\cos\phi_0)}e^{-ikb(\sin\phi_0+\sin\phi)}\frac{\cos\phi_0}{\sin\phi_0+\sin\phi}e^{ik\rho}\sqrt{\frac{2\pi}{ik\rho}} \\ &\quad +E_0\frac{i}{2\pi}e^{-ika(\cos\phi+\cos\phi_0)}e^{ikb(\sin\phi_0+\sin\phi)}\frac{\cos\phi_0}{\sin\phi_0+\sin\phi}e^{ik\rho}\sqrt{\frac{2\pi}{ik\rho}} \\ &= 4iE_0e^{-ika(\cos\phi+\cos\phi_0)}\sin[kb(\sin\phi_0+\sin\phi)]\frac{\cos\phi_0}{\sin\phi_0+\sin\phi}C(k\rho). \end{aligned} \tag{3.43}$$

Then, the total scattering field is

$$\begin{aligned} E_z^{PO} &= E_z^{JPO1}+E_z^{JPO2} \\ &= 4iE_0\sin\phi_0\frac{\sin[ka(\cos\phi_0+\cos\phi)]}{\cos\phi_0+\cos\phi}e^{-ikb(\sin\phi+\sin\phi_0)}C(k\rho) \\ &\quad +4iE_0\cos\phi_0\frac{\sin[kb(\sin\phi_0+\sin\phi)]}{\sin\phi_0+\sin\phi}e^{-ika(\cos\phi+\cos\phi_0)}C(k\rho). \end{aligned} \tag{3.44}$$

3.2.2 H Polarization

An H polarized incident plane wave can be written as

$$\boldsymbol{H}^i = H_0e^{-ik(x\cos\phi_0+y\sin\phi_0)}\hat{\boldsymbol{z}}, \tag{3.45}$$

$$\boldsymbol{E}^i = H_0\sqrt{\frac{\mu_0}{\varepsilon_0}}e^{-ik(x\cos\phi_0+y\sin\phi_0)}(\sin\phi_0\hat{\boldsymbol{x}}-\cos\phi_0\hat{\boldsymbol{y}}). \tag{3.46}$$

The PO current $\boldsymbol{J}^{PO}$ on the illuminated cylinder surface AB can be found from incident wave as Eq. (3.1)

$$\boldsymbol{J}^{PO1}(x) \;= 2\hat{\boldsymbol{y}}\times\boldsymbol{H}^i\Big|_{y=b} = 2H_0e^{-ik(x\cos\phi_0+b\sin\phi_0)}\hat{\boldsymbol{x}}, (x>0), \tag{3.47}$$

and on surface AC,

$$\boldsymbol{J}^{PO2}(y) \;= 2\hat{\boldsymbol{x}}\times\boldsymbol{H}^i\Big|_{x=a} = -2H_0e^{-ik(a\cos\phi_0+y\sin\phi_0)}\hat{\boldsymbol{y}}, (x>0). \tag{3.48}$$

The scattering field can be obtained by integrating $\boldsymbol{J}^{PO1}$, $\boldsymbol{J}^{PO2}$ with the two-dimensional

Green's function G as

$$H_z^{PO1} = \int_S \frac{i}{4} J^{PO1} \frac{\partial}{\partial y'} \mathrm{H}_0^{(1)}(k\sqrt{(x-x')^2+(y-y')^2})\Big|_{y'=b} dS, \tag{3.49}$$

$$H_z^{PO2} = -\int_S \frac{i}{4} J^{PO2} \frac{\partial}{\partial x'} \mathrm{H}_0^{(1)}(k\sqrt{(x-x')^2+(y-y')^2})\Big|_{x'=a} dS, \tag{3.50}$$

$$\begin{aligned}\frac{\partial}{\partial x'} \mathrm{H}_0^{(1)}(k\sqrt{(x-x')^2+(y-y')^2}) &= \frac{\partial}{\partial x'}\left(\frac{1}{\pi}\int_{-\infty}^{\infty} \frac{e^{i\xi(x-x')+i\sqrt{k^2-\xi^2}|y-y'|}}{\sqrt{k^2-\xi^2}}\, d\xi\right) \\ &= -\frac{i}{\pi}\int_{-\infty}^{\infty} \frac{\xi e^{i\xi(x-x')\pm i\sqrt{k^2-\xi^2}(y-y')}}{\sqrt{k^2-\xi^2}}\, d\xi, \ (y \gtrless y'),\end{aligned} \tag{3.51}$$

From Eqs. (3.47), (3.48), (3.51) and (3.21) we have

$$\begin{aligned}H_z^{PO1} &= \pm\int_{-a}^{a}\left[H_0\frac{1}{2\pi}e^{-ik(x\cos\phi_0+b\sin\phi_0)}\int_{-\infty}^{\infty} e^{i\xi(x-x')+i\sqrt{k^2-\xi^2}|y-b|}\, d\xi\right] dx' \\ &= \pm H_0\frac{1}{2\pi}e^{-ikb\sin\phi_0}\int_{-\infty}^{\infty}\left(\int_{-a}^{a} e^{-ix'(k\cos\phi_0+\xi)}\, dx'\right) e^{i\xi x\pm i\sqrt{k^2-\xi^2}(y-b)}\, d\xi \\ &= \pm H_0\frac{i}{2\pi}e^{-ikb\sin\phi_0}\int_{-\infty}^{\infty}\frac{(e^{-ia(k\cos\phi_0+\xi)}-e^{ia(k\cos\phi_0+\xi)})e^{i\xi x\pm i\sqrt{k^2-\xi^2}(y-b)}}{k\cos\phi_0+\xi}\, d\xi \\ &= \pm H_0\frac{i}{2\pi}e^{-ikb\sin\phi_0}e^{-ika\cos\phi_0}\int_{-\infty}^{\infty}\frac{e^{i\xi(x-a)\pm i\sqrt{k^2-\xi^2}(y-b)}}{k\cos\phi_0+\xi}\, d\xi \\ &\quad \mp H_0\frac{i}{2\pi}e^{-ikb\sin\phi_0}e^{ika\cos\phi_0}\int_{-\infty}^{\infty}\frac{e^{i\xi(x+a)\pm i\sqrt{k^2-\xi^2}(y-b)}}{k\cos\phi_0+\xi}\, d\xi, \quad (y \gtrless b),\end{aligned} \tag{3.52}$$

$$\begin{aligned}H_z^{PO2} &= \int_{-b}^{b}\left[H_0\frac{1}{2\pi}e^{-ik(a\cos\phi_0+y\sin\phi_0)}\int_{-\infty}^{\infty}\frac{\xi e^{i\xi(x-a)+i\sqrt{k^2-\xi^2}|y-y'|}}{\sqrt{k^2-\xi^2}}\, d\xi\right] dy' \\ &= H_0\frac{1}{2\pi}e^{-ika\cos\phi_0}\int_{-\infty}^{\infty}\left(\int_{-b}^{b} e^{-iy'(k\sin\phi_0\pm\sqrt{k^2-\xi^2})}\, dy'\right)\frac{\xi e^{i\xi(x-a)\pm i\sqrt{k^2-\xi^2}y}}{\sqrt{k^2-\xi^2}}\, d\xi \\ &= H_0\frac{i}{2\pi}e^{-ika\cos\phi_0}e^{-ikb\cos\phi_0}\int_{-\infty}^{\infty}\frac{\xi e^{i\xi(x-a)\pm i\sqrt{k^2-\xi^2}(y-b)}}{(k\sin\phi_0\pm\sqrt{k^2-\xi^2})\sqrt{k^2-\xi^2}}\, d\xi \\ &\quad -H_0\frac{ik}{2\pi}e^{-ika\cos\phi_0}e^{ikb\cos\phi_0}\int_{-\infty}^{\infty}\frac{\xi e^{i\xi(x-a)\pm i\sqrt{k^2-\xi^2}(y+b)}}{(k\sin\phi_0\pm\sqrt{k^2-\xi^2})\sqrt{k^2-\xi^2}}\, d\xi.\end{aligned} \tag{3.53}$$

Converting to complex angle w plane using the transformation $\xi = k\sin w$, with the cylindrical coordinates with ($x-a = \rho_A\cos\phi_A, y-b = \rho_A\sin\phi_A$), and ($x+a = \rho_B\cos\phi_B, y-b =$

$\rho_B \sin\phi_B$) for surface AB, Eq. (3.52) becomes

$$\begin{aligned}
H_z^{PO1} &= \pm H_0 \frac{i}{2\pi} e^{-ikb\sin\phi_0} e^{-ika\cos\phi_0} \int_C \frac{e^{ik\rho_A(\cos\phi_A \sin w \pm \sin\phi_A \cos w)}}{k\cos\phi_0 + k\sin w} k\cos w\, dw \\
&\quad \mp H_0 \frac{ik}{2\pi} e^{-ikb\sin\phi_0} e^{ika\cos\phi_0} \int_C \frac{e^{ik\rho_B(\cos\phi_B \sin w \pm \sin\phi_B \cos w)}}{k\cos\phi_0 + k\sin w} k\cos w\, dw \\
&= \pm H_0 \frac{i}{2\pi} e^{-ikb\sin\phi_0} e^{-ika\cos\phi_0} \int_C \frac{\cos w e^{ik\rho_A \sin(w\pm\phi_A)}}{\cos\phi_0 + \sin w} dw \\
&\quad \mp H_0 \frac{i}{2\pi} e^{-ikb\sin\phi_0} e^{ika\cos\phi_0} \int_C \frac{\cos w e^{ik\rho_B \sin(w\pm\phi_B)}}{\cos\phi_0 + \sin w} dw, \qquad (3.54)
\end{aligned}$$

and $(x-a = \rho_A\cos\phi_A, y-b = \rho_A\sin\phi_A)$, $(x-a = \rho_C\cos\phi_C, y+b = \rho_C\sin\phi_C)$ for surface AC, Eq. (3.53) becomes

$$\begin{aligned}
H_z^{PO2} &= H_0 \frac{ik}{2\pi} e^{-ikb\sin\phi_0} e^{-ika\cos\phi_0} \int_C \frac{k\sin w e^{ik\rho_A(\cos\phi_A \sin w \pm \sin\phi_A \cos w)}}{(k\sin\phi_0 + k\cos w)k\cos w} k\cos w\, dw \\
&\quad - H_0 \frac{ik}{2\pi} e^{-ikb\sin\phi_0} e^{ika\cos\phi_0} \int_C \frac{k\sin w e^{ik\rho_B(\cos\phi_B \sin w \pm \sin\phi_B \cos w)}}{(k\sin\phi_0 + k\cos w)k\cos w} k\cos w\, dw \\
&= H_0 \frac{i}{2\pi} \sin\phi_0 e^{-ikb\sin\phi_0} e^{-ika\cos\phi_0} \int_C \frac{e^{ik\rho_A \sin(w\pm\phi_A)}}{\sin\phi_0 + \cos w} dw \\
&\quad - H_0 \frac{i}{2\pi} \sin\phi_0 e^{-ikb\sin\phi_0} e^{ika\cos\phi_0} \int_C \frac{e^{ik\rho_B \sin(w\pm\phi_B)}}{\sin\phi_0 + \cos w} dw. \qquad (3.55)
\end{aligned}$$

We obtain $w_s = \pi/2 \mp \phi$ as a possible saddle point on the contour. At the saddle point, Eq. (3.54) becomes

$$\begin{aligned}
H_z^{PO1} &\sim \pm \frac{iH_0}{2\pi} e^{-ikb\sin\phi_0} e^{-ika\cos\phi_0} \frac{\cos(\pi/2 \mp \phi_A)}{\cos\phi_0 + \sin(\pi/2 \mp \phi_A)} e^{ik\rho_A} \int_{C_{SDP}} e^{-ik\rho_A(w-w_s)^2/2}\, dw \\
&\quad \mp \frac{iH_0}{2\pi} e^{-ikb\sin\phi_0} e^{ika\cos\phi_0} \frac{\cos(\pi/2 \mp \phi_B)}{\cos\phi_0 + \sin(\pi/2 \mp \phi_B)} e^{ik\rho_B} \int_{C_{SDP}} e^{-ik\rho_B(w-w_s)^2/2}\, dw \\
&= H_0 \frac{i}{2\pi} e^{-ikb\sin\phi_0} e^{-ika\cos\phi_0} \frac{\sin\phi_A}{\cos\phi_0 + \cos\phi_A} e^{ik\rho_A} \sqrt{\frac{2\pi}{ik\rho_A}} \\
&\quad - H_0 \frac{i}{2\pi} e^{-ikb\sin\phi_0} e^{ika\cos\phi_0} \frac{\sin\phi_B}{\cos\phi_0 + \cos\phi_B} e^{ik\rho_B} \sqrt{\frac{2\pi}{ik\rho_B}}, \qquad (3.56)
\end{aligned}$$

and $w_s = \pi/2 \mp \phi_A$ and $w_s = \pi/2 \mp \phi_C$, Eq. (3.55) becomes

$$\begin{aligned}
H_z^{PO2} &\sim \frac{iH_0}{2\pi} e^{-ikb\sin\phi_0} e^{-ika\cos\phi_0} \frac{\sin(\pi/2 \mp \phi_A)}{\sin\phi_0 \pm \cos(\pi/2 \mp \phi_A)} e^{ik\rho_A} \int_{C_{SDP}} e^{-ik\rho_A(w-w_s)^2/2}\, dw \\
&\quad \mp \frac{iH_0}{2\pi} e^{ikb\sin\phi_0} e^{-ika\cos\phi_0} \frac{\sin(\pi/2 \mp \phi_C)}{\sin\phi_0 \pm \cos(\pi/2 \mp \phi_C)} e^{ik\rho_B} \int_{C_{SDP}} e^{-ik\rho_B(w-w_s)^2/2}\, dw \\
&= H_0 \frac{i}{2\pi} e^{-ikb\sin\phi_0} e^{-ika\cos\phi_0} \frac{\cos\phi_A}{\cos\phi_0 + \sin\phi_A} e^{ik\rho_A} \sqrt{\frac{2\pi}{ik\rho_A}} \\
&\quad - H_0 \frac{i}{2\pi} e^{ikb\sin\phi_0} e^{-ika\cos\phi_0} \frac{\cos\phi_C}{\cos\phi_0 + \sin\phi_C} e^{ik\rho_C} \sqrt{\frac{2\pi}{ik\rho_B}}, \qquad (3.57)
\end{aligned}$$

Using far-field approximation in Eq. (3.41), Eqs. (3.56) and (3.57) can be approximated as

$$\begin{aligned} H_z^{PO1} &= H_0 \frac{i}{2\pi} e^{-ikb(\sin\phi+\sin\phi_0)} e^{-ika(\sin\phi+\sin\phi_0)} \frac{\sin\phi}{\cos\phi_0+\cos\phi} e^{ik\rho}\sqrt{\frac{2\pi}{ik\rho}} \\ &\quad - H_0 \frac{i}{2\pi} e^{-ikb(\sin\phi+\sin\phi_0)} e^{ika(\sin\phi+\sin\phi_0)} \frac{\sin\phi}{\cos\phi_0+\cos\phi} e^{ik\rho}\sqrt{\frac{2\pi}{ik\rho}} \\ &= -4iH_0 \sin[ka(\cos\phi_0+\cos\phi)] \frac{\sin\phi}{\cos\phi_0+\cos\phi} e^{-ikb(\sin\phi+\sin\phi_0)} C(k\rho), \quad (3.58) \end{aligned}$$

$$\begin{aligned} H_z^{PO2} &= H_0 \frac{i}{2\pi} e^{-ika(\cos\phi+\cos\phi_0)} e^{-ikb(\sin\phi_0+\sin\phi)} \frac{\cos\phi}{\sin\phi_0+\sin\phi} e^{ik\rho}\sqrt{\frac{2\pi}{ik\rho}} \\ &\quad - H_0 \frac{i}{2\pi} e^{-ika(\cos\phi+\cos\phi_0)} e^{ikb(\sin\phi_0+\sin\phi)} \frac{\cos\phi_0}{\sin\phi_0+\sin\phi} e^{ik\rho}\sqrt{\frac{2\pi}{ik\rho}} \\ &= -4iH_0 e^{-ika(\cos\phi+\cos\phi_0)} \sin[kb(\sin\phi_0+\sin\phi)] \frac{\cos\phi}{\sin\phi_0+\sin\phi} C(k\rho). \quad (3.59) \end{aligned}$$

Then, the total scattering field is

$$\begin{aligned} H_z^{PO} &= H_z^{JPO1} + H_z^{JPO2} \\ &= -4iH_0 \sin[ka(\cos\phi_0+\cos\phi)] \frac{\sin\phi}{\cos\phi_0+\cos\phi} e^{-ikb(\sin\phi+\sin\phi_0)} C(k\rho) \\ &\quad - 4iH_0 \sin[kb(\sin\phi_0+\sin\phi)] \frac{\cos\phi}{\sin\phi_0+\sin\phi} e^{-ika(\cos\phi+\cos\phi_0)} C(k\rho). \quad (3.60) \end{aligned}$$

In this chapter, the PO approximation are applied to estimate electromagnetic scattering from the conducting wedge and rectangular cylinder. According to the PO approximation, if the scattering objects are large compared with the wavelength, the PO currents $\boldsymbol{J}^{PO}$ are approximated from the incident magnetic field as $\boldsymbol{J}^{PO} = 2\hat{\boldsymbol{n}} \times \boldsymbol{H}^i$ and flow on the physically illuminated surfaces. Then, the scattering field from this object may be derived by integrating these PO currents with the free-space Green's function. In Section 3.1, the scattering field by the conducting wedge is obtained from only one PO current flowing on the illuminated surface OA. The results include the edge diffracted field and the GO field which gives a reflected field in the illuminated region or a field to cancel the incident field in the shadow region. In Section 3.2, when the incident wave impinges on the cylinder at two surfaces AB and AC, it excites two PO currents on these illuminated surfaces. Then, the total scattering fields are given by summing up the fields radiated from these PO currents.

Chapter 4

High Frequency Scattering Analysis by Equivalent Current Method

In this chapter, the surface equivalence theorem is applied to derive the scattering fields by the wedge and rectangular cylinder. According to the surface equivalence theorem in Chapter 2, the scattering field by the scattering objects are approximated by the radiations from the equivalent currents calculated by the reflected/transmitted GO waves. Firstly, the scattering fields by the conducting wedge and rectangular cylinder are formulated to compare with those obtained from the PO approximation in Chapter 3 (Section 4.1). Then, the scattering fields by the dielectric wedge and rectangular cylinder are consider in Section 4.2.

4.1 Scattering by a Conducting Edged Object

In this section, the scattering fields by a conducting wedge and rectangular cylinder are formulated. According to the surface equivalence theorem, the corresponding equivalent electric and magnetic currents $\boldsymbol{J}_s$, $\boldsymbol{M}_s$ are calculated the GO rays on a postulated surface enclosing the scattering object. While currents $\boldsymbol{J}_s$, $\boldsymbol{M}_s$ on the illuminated surface are approximated by the GO reflected waves $\boldsymbol{E}^r$, $\boldsymbol{H}^r$, those on the shadow surface are obtained

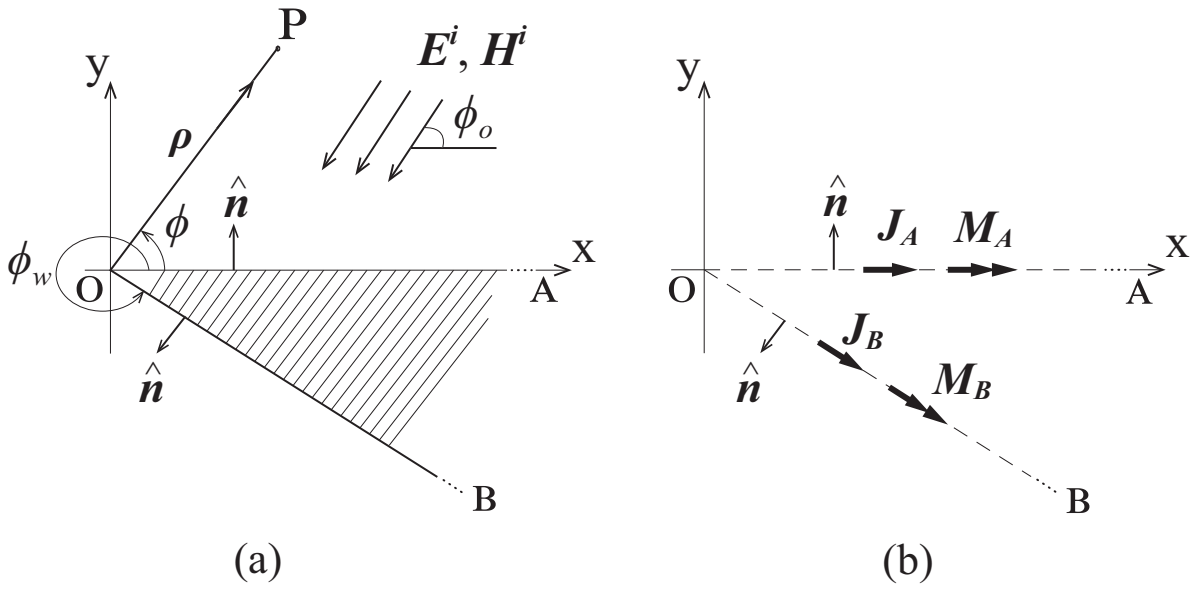

Figure 4.1: Diffraction by a conducting wedge. (a) Wedge diffraction by plane waves $\boldsymbol{E}^i$, $\boldsymbol{H}^i$. (b) Equivalent currents $\boldsymbol{J}_A$, $\boldsymbol{M}_A$, $\boldsymbol{J}_B$, $\boldsymbol{M}_B$ due to the scattering field on the wedge surfaces OA and OB.

from the incident GO wave $-\boldsymbol{E}^i$, $-\boldsymbol{H}^i$

$$\boldsymbol{J}_s = \hat{\boldsymbol{n}} \times \boldsymbol{H}^s \simeq \begin{cases} \hat{\boldsymbol{n}} \times \boldsymbol{H}^r & \text{on illuminated } S, \\ \hat{\boldsymbol{n}} \times (-\boldsymbol{H}^i) & \text{on shadowed } S, \end{cases} \tag{4.1}$$

$$\boldsymbol{M}_s = \boldsymbol{E}^s \times \hat{\boldsymbol{n}} \simeq \begin{cases} \boldsymbol{E}^r \times \hat{\boldsymbol{n}} & \text{on illuminated } S, \\ (-\boldsymbol{E}^i) \times \hat{\boldsymbol{n}} & \text{on shadowed } S. \end{cases} \tag{4.2}$$

Then, the total scattering field are given by summing up the all contributions radiated from these equivalent currents.

This section starts by formulating the diffraction by a conducting wedge. After that, the scattering by a conducting rectangular cylinder is considered.

4.1.1 Diffraction by a Conducting Wedge

Figure 4.1(a) shows a two-dimensional conducting wedge of the wedge angle ϕ_w illuminated by a plane wave. For simplicity, let us assume that the incident plane wave illuminates surface OA only ($0 < \phi_0 < \phi_w - \pi$) and the observation angle is taken as $0 < |\phi| < \pi$.

The scattering formulation may be separated into two polarizations.

E Polarization

An E polarized incident plane wave can be written as

$$\boldsymbol{E}^i = E_0 e^{-ik(x\cos\phi_0 + y\sin\phi_0)}\hat{\boldsymbol{z}}, \tag{4.3}$$

$$\boldsymbol{H}^i = E_0\sqrt{\frac{\varepsilon_0}{\mu_0}}e^{-ik(x\cos\phi_0 + y\sin\phi_0)}(-\sin\phi_0\hat{\boldsymbol{x}} + \cos\phi_0\hat{\boldsymbol{y}}). \tag{4.4}$$

The reflected wave at OA surface can be written as

$$\boldsymbol{E}^r = -E_0 e^{-ik(x\cos\phi_0 - y\sin\phi_0)}\hat{\boldsymbol{z}}, \tag{4.5}$$

$$\boldsymbol{H}^r = E_0\sqrt{\frac{\varepsilon_0}{\mu_0}}e^{-ik(x\cos\phi_0 - y\sin\phi_0)}(-\sin\phi_0\hat{\boldsymbol{x}} - \cos\phi_0\hat{\boldsymbol{y}}). \tag{4.6}$$

Then, the equivalent currents $\boldsymbol{J}_s$, $\boldsymbol{M}_s$ as in Fig. 4.1(b) can be derived from Eqs. (4.1), (4.2). On the illuminated surface OA, one finds

$$\boldsymbol{J}_A = \hat{\boldsymbol{y}} \times \boldsymbol{H}^r\Big|_{y=0} = E_0\sqrt{\frac{\varepsilon_0}{\mu_0}}\sin\phi_0 e^{-ikx\cos\phi_0}\hat{\boldsymbol{z}}, \tag{4.7}$$

$$\boldsymbol{M}_A = \boldsymbol{E}^r \times \hat{\boldsymbol{y}}\Big|_{y=0} = E_0 e^{-ikx\cos\phi_0}\hat{\boldsymbol{x}}, \tag{4.8}$$

and on the shadowed surface OB,

$$\boldsymbol{J}_B = \hat{\boldsymbol{n}} \times (-\boldsymbol{H}^i)\Big|_{y=x\tan\phi_w} = E_0\sqrt{\frac{\varepsilon_0}{\mu_0}}\sin(\phi_0 - \phi_w)e^{-ikx(\cos\phi_0 + \tan\phi_w\sin\phi_0)}\hat{\boldsymbol{z}}, \tag{4.9}$$

$$\boldsymbol{M}_B = (-\boldsymbol{E}^i) \times \hat{\boldsymbol{n}}\Big|_{y=x\tan\phi_w} = -E_0 e^{-ikx(\cos\phi_0 + \tan\phi_w\sin\phi_0)}(\cos\phi_w\hat{\boldsymbol{x}} + \sin\phi_w\hat{\boldsymbol{y}}). \tag{4.10}$$

The scattering field can be obtained by integrating $\boldsymbol{J}_s$, $\boldsymbol{M}_s$ with the two-dimensional Green's function G as

$$E_z^{JA} = -\int_S \frac{\omega\mu_0}{4}J_A \mathrm{H}_0^{(1)}(k\sqrt{(x-x')^2 + (y-y')^2})\Big|_{y'=0} dS, \tag{4.11}$$

$$E_z^{MA} = -\int_S \frac{i}{4}M_{Ax}\frac{\partial}{\partial y'}\mathrm{H}_0^{(1)}(k\sqrt{(x-x')^2 + (y-y')^2})\Big|_{y'=0} dS, \tag{4.12}$$

$$E_z^{JB} = -\int_S \frac{\omega\mu_0}{4}J_B \mathrm{H}_0^{(1)}(k\sqrt{(x-x')^2 + (y-y')^2})\Big|_{y'=x'\tan\phi_w} dS, \tag{4.13}$$

$$E_z^{MB} = -\int_S \frac{i}{4}(M_{Bx}\frac{\partial}{\partial y'} - M_{By}\frac{\partial}{\partial x'})\mathrm{H}_0^{(1)}(k\sqrt{(x-x')^2 + (y-y')^2})\Big|_{y'=x'\tan\phi_w} dS \tag{4.14}$$

with

$$\frac{\partial}{\partial x'}\mathrm{H}_0^{(1)}(k\sqrt{(x-x')^2+(y-y')^2}) = \frac{\partial}{\partial x'}(\frac{1}{\pi}\int_{-\infty}^{\infty}\frac{e^{i\xi(x-x')+i\sqrt{k^2-\xi^2}|y-y'|}}{\sqrt{k^2-\xi^2}}\,d\xi)$$
$$= -\frac{i}{\pi}\int_{-\infty}^{\infty}\frac{\xi e^{i\xi(x-x')\pm i\sqrt{k^2-\xi^2}(y-y')}}{\sqrt{k^2-\xi^2}}\,d\xi,\ (y \gtrless y'), \tag{4.15}$$

$$\frac{\partial}{\partial y'}\mathrm{H}_0^{(1)}(k\sqrt{(x-x')^2+(y-y')^2}) = \frac{\partial}{\partial y'}(\frac{1}{\pi}\int_{-\infty}^{\infty}\frac{e^{i\xi(x-x')+i\sqrt{k^2-\xi^2}|y-y'|}}{\sqrt{k^2-\xi^2}}\,d\xi)$$
$$= \mp\frac{i}{\pi}\int_{-\infty}^{\infty}e^{i\xi(x-x')\pm i\sqrt{k^2-\xi^2}(y-y')}\,d\xi,\ (y \gtrless y'). \tag{4.16}$$

From Eqs. (3.6), (4.7), (4.8) and (4.16), Eqs. (4.12) and (4.11)can be expressed as

$$E_z^{JA} = -\int_0^{\infty}\Big[\frac{\omega\mu_0}{4\pi}E_0\sqrt{\frac{\varepsilon_0}{\mu_0}}\sin\phi_0 e^{-ikx'\cos\phi_0}\int_{-\infty}^{\infty}\frac{e^{i\xi(x-x')+i\sqrt{k^2-\xi^2}|y|}}{\sqrt{k^2-\xi^2}}\,d\xi\Big]\,dx'$$
$$= -E_0\frac{ik}{4\pi}\sin\phi_0\int_{-\infty}^{\infty}\left(\int_0^{\infty}e^{-ix'(k\cos\phi_0+\xi)}\,dx'\right)\frac{e^{i\xi x\pm i\sqrt{k^2-\xi^2}y}}{\sqrt{k^2-\xi^2}}\,d\xi$$
$$= E_0\frac{ik}{4\pi}\sin\phi_0\int_{-\infty}^{\infty}\frac{e^{i\xi x\pm i\sqrt{k^2-\xi^2}y}}{(k\cos\phi_0+\xi)\sqrt{k^2-\xi^2}}\,d\xi,\quad (y \gtrless 0), \tag{4.17}$$

$$E_z^{MA} = \mp\int_0^{\infty}\Big[E_0\frac{1}{4\pi}e^{-ikx'\cos\phi_0}\int_{-\infty}^{\infty}e^{i\xi(x-x')\pm i\sqrt{k^2-\xi^2}y}\,d\xi\Big]\,dx'$$
$$= \mp E_0\frac{1}{4\pi}\int_{-\infty}^{\infty}\left(\int_0^{\infty}e^{-ix'(k\cos\phi_0+\xi)}\,dx'\right)e^{i\xi x\pm i\sqrt{k^2-\xi^2}y}\,d\xi$$
$$= \pm E_0\frac{i}{4\pi}\int_{-\infty}^{\infty}\frac{e^{i\xi x\pm i\sqrt{k^2-\xi^2}y}}{k\cos\phi_0+\xi}\,d\xi,\quad (y \gtrless 0). \tag{4.18}$$

From Eqs. (3.6), (4.9), (4.10), (4.15) and (4.16), Eqs. (4.13) and (4.14) can be expressed as

$$E_z^{JB} = -\int_0^{\infty}\Big[\frac{\omega\mu_0}{4\pi}E_0\sqrt{\frac{\varepsilon_0}{\mu_0}}\sin(\phi_0-\phi_w)e^{-ikx'(\cos\phi_0+\tan\phi_w\sin\phi_0)}$$
$$\cdot\int_{-\infty}^{\infty}\frac{e^{i\xi(x-x')\pm i\sqrt{k^2-\xi^2}(y-x'\tan\phi_w)}}{\sqrt{k^2-\xi^2}}\,d\xi\Big]\sqrt{1+\tan^2\phi_w}\,dx'$$
$$= -E_0\frac{k}{4\pi}\frac{\sin(\phi_0-\phi_w)}{\cos\phi_w}$$
$$\cdot\int_{-\infty}^{\infty}\Big(\int_0^{\infty}e^{-ix'(k\cos\phi_0+k\tan\phi_w\sin\phi_0+\xi\pm\sqrt{k^2-\xi^2}\tan\phi_w)}\,dx'\Big)\frac{e^{i\xi x\pm i\sqrt{k^2-\xi^2}y}}{\sqrt{k^2-\xi^2}}\,d\xi$$
$$= E_0\frac{ik}{4\pi}\int_{-\infty}^{\infty}\frac{\sin(\phi_0-\phi_w)e^{i\xi x\pm i\sqrt{k^2-\xi^2}y}}{\cos\phi_w(k\cos\phi_0+k\tan\phi_w\sin\phi_0+\xi\pm\sqrt{k^2-\xi^2}\tan\phi_w)\sqrt{k^2-\xi^2}}\,d\xi,$$
$$(y \gtrless x'\tan\phi_w), \tag{4.19}$$

$$
\begin{aligned}
E_z^{MB} &= -\int_0^\infty \Big[\frac{1}{4\pi}E_0 e^{-ikx'(\cos\phi_0+\tan\phi_w\sin\phi_0)}\int_{-\infty}^{\infty} e^{i\xi(x-x')\pm i\sqrt{k^2-\xi^2}(y-x'\tan\phi_w)} \\
&\qquad \cdot\Big(\mp\cos\phi_w+\sin\phi_w\frac{\xi}{\sqrt{k^2-\xi^2}}\Big)\,d\xi\Big]\sqrt{1+\tan^2\phi_w}\,dx' \\
&= \pm\frac{1}{4\pi}E_0\int_{-\infty}^{\infty}\Big(\int_0^\infty e^{-ix'(k\cos\phi_0+k\tan\phi_w\sin\phi_0+\xi\pm\sqrt{k^2-\xi^2}\tan\phi_w)}\,dx'\Big)e^{i\xi x\pm i\sqrt{k^2-\xi^2}y}\,d\xi \\
&-\frac{1}{4\pi}E_0\frac{\sin\phi_w}{\cos\phi_w}\int_{-\infty}^{\infty}\Big(\int_0^\infty e^{-ix'(k\cos\phi_0+k\tan\phi_w\sin\phi_0+\xi\pm\sqrt{k^2-\xi^2}\tan\phi_w)}\,dx'\Big)\frac{\xi e^{i\xi x\pm i\sqrt{k^2-\xi^2}y}}{\sqrt{k^2-\xi^2}}\,d\xi \\
&= \frac{i}{4\pi}E_0\frac{\sin\phi_w}{\cos\phi_w}\int_{-\infty}^{\infty}\frac{\xi e^{i\xi x\pm i\sqrt{k^2-\xi^2}y}}{(k\cos\phi_0+k\tan\phi_w\sin\phi_0+\xi\pm\sqrt{k^2-\xi^2}\tan\phi_w)\sqrt{k^2-\xi^2}}\,d\xi \\
&\mp\frac{iE_0}{4\pi}\int_{-\infty}^{\infty}\frac{e^{i\xi x\pm i\sqrt{k^2-\xi^2}y}}{(k\cos\phi_0+k\tan\phi_w\sin\phi_0+\xi\pm\sqrt{k^2-\xi^2}\tan\phi_w)}\,d\xi,(y\gtrless x'\tan\phi_w). \qquad (4.20)
\end{aligned}
$$

Since these integrals cannot be analytically evaluated, the saddle point method is used. Converting to complex angle w plane using the transformation $\xi = k\sin w$, with the cylindrical coordinates (ρ,θ) with $x=\rho\cos\phi, y=\rho\sin\phi$, Eqs. (4.17)–(4.20) can be expressed as

$$
\begin{aligned}
E_z^{JA} &= E_0\frac{ik}{4\pi}\sin\phi_0\int_C\frac{e^{ik\rho(\cos\phi\sin w\pm\sin\phi\cos w)}}{k(\cos\phi_0+\sin w)k\cos w}k\cos w\,dw \\
&= E_0\frac{i}{4\pi}\int_C\frac{\sin\phi_0}{\cos\phi_0+\sin w}e^{ik\rho(\sin(w\pm\phi)}\,dw, \qquad (4.21)
\end{aligned}
$$

$$
\begin{aligned}
E_z^{MA} &= \pm E_0\frac{i}{4\pi}\int_C\frac{e^{ik\rho(\cos\phi\sin w\pm\sin\phi\cos w)}}{k(\cos\phi_0+\sin w)k}k\cos w\,dw \\
&= \pm E_0\frac{i}{4\pi}\int_C\frac{\cos w}{\cos\phi_0+\sin w}e^{ik\rho(\sin(w\pm\phi)}\,dw, \qquad (4.22) \\
E_z^{JB} &= E_0\frac{ik}{4\pi}\frac{\sin(\phi_0-\phi_w)}{\cos\phi_w} \\
&\qquad\cdot\int_C\frac{e^{ik\rho(\cos\phi\sin w\pm\sin\phi\cos w)}}{(k\cos\phi_0+k\tan\phi_w\sin\phi_0+k\sin w\pm k\cos w\tan\phi_w)k\cos w}k\cos w\,dw \\
&= E_0\frac{i}{4\pi}\int_C\frac{\sin(\phi_0-\phi_w)}{\cos(\phi_0-\phi_w)+\sin(w\pm\phi_w)}e^{ik\rho(\sin(w\pm\phi)}\,dw, \qquad (4.23)
\end{aligned}
$$

$$
\begin{aligned}
E_z^{MB} &= \mp E_0\frac{i}{4\pi}\int_C\frac{e^{ik\rho(\cos\phi\sin w\pm\sin\phi\cos w)}}{(k\cos\phi_0+k\tan\phi_w\sin\phi_0+k\sin w\pm k\cos w\tan\phi_w)}k\cos w\,dw \\
&+ E_0\frac{i}{4\pi}\frac{\sin\phi_w}{\cos\phi_w}\int_C\frac{k\sin w e^{ik\rho(\cos\phi\sin w\pm\sin\phi\cos w)}}{(k\cos\phi_0+k\tan\phi_w\sin\phi_0+k\sin w\pm k\cos w\tan\phi_w)}k\cos w\,dw \\
&= \mp E_0\frac{i}{4\pi}\int_C\frac{\cos(w\pm\phi_w)}{\cos(\phi_0-\phi_w)+\sin(w\pm\phi_w)}e^{ik\rho(\sin(w\pm\phi)}\,dw, \qquad (4.24)
\end{aligned}
$$

where contour C is given in Fig. 3.3.

We obtain $w_s = \pi/2 \mp \phi$ as a possible saddle point. At saddle point, Eqs. (4.21)– (4.24) become

$$\begin{aligned}
E_d^{JA} &= E_0 \frac{i}{4\pi} \int_C \frac{\sin\phi_0}{\cos\phi_0 + \sin w} e^{ik\rho(\sin(w\pm\phi)} \, dw \\
&= E_0 \frac{i}{4\pi} \frac{\sin\phi_0}{\cos\phi_0 + \sin w_s} e^{ik\rho} \int_{C_{SDP}} e^{-ik\rho(w-w_s)^2/2} \, dw \\
&= E_0 \frac{\sin\phi_0}{\cos\phi_0 + \cos\phi} C(k\rho), \qquad (4.25) \\
E_d^{MA} &= \pm E_0 \frac{i}{4\pi} \int_C \frac{\cos w}{\cos\phi_0 + \sin w} e^{ik\rho(\sin(w\pm\phi)} \, dw \\
&= \pm E_0 \frac{i}{4\pi} \frac{\cos w_s}{\cos\phi_0 + \sin w_s} e^{ik\rho} \int_{C_{SDP}} e^{-ik\rho(w-w_s)^2/2} \, dw \\
&= E_0 \frac{\sin\phi}{\cos\phi_0 + \cos\phi} C(k\rho), \qquad (4.26) \\
E_d^{JB} &= E_0 \frac{i}{4\pi} \int_C \frac{\sin(\phi_0 - \phi_w)}{\cos(\phi_0 - \phi_w) + \sin(w \mp \phi_w)} e^{ik\rho(\sin(w\pm\phi)} \, dw \\
&= E_0 \frac{i}{4\pi} \frac{\sin(\phi_0 - \phi_w)}{\cos(\phi_0 - \phi_w) + \sin(w_s \mp \phi_w)} e^{ik\rho} \int_{C_{SDP}} e^{-ik\rho(w-w_s)^2/2} \, dw \\
&= E_0 \frac{\sin(\phi_0 - \phi_w)}{\cos(\phi_0 - \phi_w) + \cos(\phi - \phi_w)} C(k\rho), \qquad (4.27) \\
E_d^{MB} &= \mp E_0 \frac{i}{4\pi} \int_C \frac{\cos(w \pm \phi_w)}{\cos(\phi_0 - \phi_w) + \sin(w \mp \phi_w)} e^{ik\rho(\sin(w\pm\phi)} \, dw \\
&= \mp E_0 \frac{i}{4\pi} \frac{\cos(w_s \pm \phi_w)}{\cos(\phi_0 - \phi_w) + \sin(w_s \mp \phi_w)} e^{ik\rho} \int_{C_{SDP}} e^{-ik\rho(w-w_s)^2/2} \, dw \\
&= -E_0 \frac{\sin(\phi - \phi_w)}{\cos(\phi_0 - \phi_w) + \cos(\phi - \phi_w)} C(k\rho). \qquad (4.28)
\end{aligned}$$

The contribution of the pole $w_p = \phi_0 - \pi/2$ for surface OA with $0 < |\phi| < \pi - \phi_0$ as

$$\begin{aligned}
E_p^{JA} &= 2\pi i \frac{iE_0}{4\pi} \frac{\sin\phi_0}{\cos w_p} e^{ik(\rho \sin w_p \cos\phi \pm \cos w_p \sin\phi)} \\
&= -\frac{E_0}{2} e^{-ik\rho(\cos\phi_0 \cos\phi \mp \sin\phi_0 \sin\phi)} U(\pi - \phi_0 - |\phi|) \\
&= -\frac{E_0}{2} e^{-ikx\cos\phi_0 + iky\sin\phi_0} U(\pi - \phi_0 - |\phi|), \qquad (4.29) \\
E_p^{MA} &= \pm 2\pi i \frac{iE_0}{4\pi} \frac{\cos w_p}{\cos w_p} e^{ik(\rho \sin w_p \cos\phi \pm \cos w_p \sin\phi)} \\
&= \mp \frac{E_0}{2} e^{-ik\rho(\cos\phi_0 \cos\phi \mp \sin\phi_0 \sin\phi)} U(\pi - \phi_0 - |\phi|) \\
&= \mp \frac{E_0}{2} e^{-ikx\cos\phi_0 + iky\sin\phi_0} U(\pi - \phi_0 - |\phi|). \qquad (4.30)
\end{aligned}$$

For surface OB with $w_p = \phi_0 - \pi/2$, $\phi_0 - \pi < \phi < \phi_w - 2\pi$,

$$\begin{aligned} E_p^{JB} &= 2\pi i \frac{iE_0}{4\pi} \frac{\sin(\phi_0 - \phi_w)}{\cos(w_p - \phi_w)} e^{ik(\rho \sin w_p \cos\phi - \cos w_p \sin\phi)} \\ &= -\frac{E_0}{2} e^{-ik\rho(\cos\phi_0 \cos\phi + \sin\phi_0 \sin\phi)} U(\phi + \pi - \phi_0) U(-\phi - 2\pi + \phi_w) \\ &= -\frac{E_0}{2} e^{-ikx\cos\phi_0 - iky\sin\phi_0} U(\phi + \pi - \phi_0) U(-\phi - 2\pi + \phi_w), \end{aligned} \tag{4.31}$$

$$\begin{aligned} E_p^{MB} &= 2\pi i \frac{iE_0}{4\pi} \frac{\cos(w_p - \phi_w)}{\cos(w_p - \phi_w)} e^{ik(\rho \sin w_p \cos\phi - \cos w_p \sin\phi)} \\ &= -\frac{E_0}{2} e^{-ik\rho(\cos\phi_0 \cos\phi + \sin\phi_0 \sin\phi)} U(\phi + \pi - \phi_0) U(-\phi - 2\pi + \phi_w) \\ &= -\frac{E_0}{2} e^{-ikx\cos\phi_0 - iky\sin\phi_0} U(\phi + \pi - \phi_0) U(-\phi - 2\pi + \phi_w), \end{aligned} \tag{4.32}$$

and for $w_p = \phi_0 - 2\phi_w - \pi/2$, $\phi_w - 2\pi < \phi < 2\phi_w - \phi_0 - 3\pi$

$$\begin{aligned} E_p^{JB} &= 2\pi i \frac{iE_0}{4\pi} \frac{\sin(\phi_0 - \phi_w)}{\cos(w_p + \phi_w)} e^{ik(\rho \sin w_p \cos\phi + \cos w_p \sin\phi)} \\ &= -\frac{E_0}{2} e^{-ik\rho(\cos(2\phi_w - \phi_0)\cos\phi - \sin(2\phi_w - \phi_0)\sin\phi)} U(\phi + 2\pi - \phi_w) U(-\phi - 3\pi + 2\phi_w - \phi_0) \\ &= -\frac{E_0}{2} e^{-ikx\cos(2\phi_w - \phi_0) - iky\sin(2\phi_w - \phi_0)} U(\phi + 2\pi - \phi_w) U(-\phi - 3\pi + 2\phi_w - \phi_0), \end{aligned} \tag{4.33}$$

$$\begin{aligned} E_p^{MB} &= -2\pi i \frac{iE_0}{4\pi} \frac{\cos(w_p + \phi_w)}{\cos(w_p + \phi_w)} e^{ik(\rho \sin w_p \cos\phi + \cos w_p \sin\phi)} \\ &= \frac{E_0}{2} e^{-ik\rho(\cos(2\phi_w - \phi_0)\cos\phi - \sin(2\phi_w - \phi_0)\sin\phi)} U(\phi + 2\pi - \phi_w) U(-\phi - 3\pi + 2\phi_w - \phi_0) \\ &= \frac{E_0}{2} e^{-ikx\cos(2\phi_w - \phi_0) - iky\sin(2\phi_w - \phi_0)} U(\phi + 2\pi - \phi_w) U(-\phi - 3\pi + 2\phi_w - \phi_0). \end{aligned} \tag{4.34}$$

Then the scattering field from the surface OA is

$$\begin{aligned} E_z^{\mathrm{OA}} &= E_d^{\mathrm{OA}} + E_p^{\mathrm{OA}} \\ &= E_0 \frac{\sin\phi_0 + \sin\phi}{\cos\phi_0 + \cos\phi} C(k\rho) - E_0 e^{-ikx\cos\phi_0 + iky\sin\phi_0} U(\pi - \phi_0 - \phi) U(\phi), \end{aligned} \tag{4.35}$$

and from the surface OB is

$$\begin{aligned} E_z^{\mathrm{OB}} &= E_d^{\mathrm{OB}} + E_p^{\mathrm{OB}} \\ &= E_0 \frac{\sin(\phi_0 - \phi_w) - \sin(\phi - \phi_w)}{\cos(\phi_0 - \phi_w) + \cos(\phi - \phi_w)} C(k\rho) \\ &\quad - E_0 e^{-ikx\cos\phi_0 - iky\sin\phi_0} U(\phi + \pi - \phi_0) U(-\phi - 2\pi + \phi_w). \end{aligned} \tag{4.36}$$

Then, the total scattering field E_z^s is defined by the summation of the above contributions

in Eqs. (4.35), (4.36) as

$$\begin{aligned} E_z^s &= E_z^{\mathrm{OA}} + E_z^{\mathrm{OB}} \\ &= E_0\Big(\frac{\sin\phi_0+\sin\phi}{\cos\phi_0+\cos\phi} + \frac{\sin(\phi_0-\phi_w)-\sin(\phi-\phi_w)}{\cos(\phi_0-\phi_w)+\cos(\phi-\phi_w)}\Big)C(k\rho) \\ &\quad - E_0 e^{-ikx\cos\phi_0+iky\sin\phi_0}U(\pi-\phi_0-\phi)U(\phi) \\ &\quad - E_0 e^{-ikx\cos\phi_0-iky\sin\phi_0}U(\phi+\pi-\phi_0)U(-\phi-2\pi+\phi_w). \end{aligned} \tag{4.37}$$

The term A in the big parentheses of the first line in Eq. (4.37) becomes

$$\begin{aligned} A &= \frac{\sin\phi_0+\sin\phi}{\cos\phi_0+\cos\phi} + \frac{\sin(\phi_0-\phi_w)-\sin(\phi-\phi_w)}{\cos(\phi_0-\phi_w)+\cos(\phi-\phi_w)}\Big) \\ &= \frac{\begin{array}{l}(\sin\phi_0+\sin\phi)[\cos(\phi_0-\phi_w)+\cos(\phi-\phi_w)] \\ +[\sin(\phi_0-\phi_w)-\sin(\phi-\phi_w)](\cos\phi_0+\cos\phi)\end{array}}{(\cos\phi_0+\cos\phi)[\cos(\phi_0-\phi_w)+\cos(\phi-\phi_w)]} \\ &= \frac{\begin{array}{l}\sin[\phi_0+(\phi_0-\phi_w)]+\sin[\phi_0-(\phi_0-\phi_w)] \\ +\sin[\phi_0+(\phi-\phi_w)]+\sin[\phi_0-(\phi-\phi_w)]\end{array}}{(\cos\phi_0+\cos\phi)[\cos(\phi_0-\phi_w)+\cos(\phi-\phi_w)]} \\ &= \frac{2\sin\phi_0[\cos(\phi_0-\phi_w)+\cos(\phi-\phi_w)]}{(\cos\phi_0+\cos\phi)[\cos(\phi_0-\phi_w)+\cos(\phi-\phi_w)]} \\ &= \frac{2\sin\phi_0}{(\cos\phi_0+\cos\phi)}. \end{aligned} \tag{4.38}$$

Therefore, this results matches exactly with the one by the PO approximation in Eq. (3.16).

H Polarization

The same observation can be applied for the H polarization case when the incident plane wave is given by

$$\boldsymbol{H}^i = H_0 e^{-ik(x\cos\phi_0+y\sin\phi_0)}\hat{\boldsymbol{z}}, \tag{4.39}$$

$$\boldsymbol{E}^i = H_0\sqrt{\frac{\mu_0}{\varepsilon_0}}e^{-ik(x\cos\phi_0+y\sin\phi_0)}(\sin\phi_0\hat{\boldsymbol{x}}-\cos\phi_0\hat{\boldsymbol{y}}), \tag{4.40}$$

and the reflected waves at illuminated surface OA can be expressed as

$$\boldsymbol{H}^r = H_0 e^{-ik(x\cos\phi_0-y\sin\phi_0)}\hat{\boldsymbol{z}}, \tag{4.41}$$

$$\boldsymbol{E}^r = H_0\sqrt{\frac{\mu_0}{\varepsilon_0}}e^{-ik(x\cos\phi_0-y\sin\phi_0)}(-\sin\phi_0\hat{\boldsymbol{x}}-\cos\phi_0\hat{\boldsymbol{y}}). \tag{4.42}$$

Then, the equivalent currents $\boldsymbol{J}_s$, $\boldsymbol{M}_s$ can be derived from Eqs. (4.1), (4.2). On the illuminated surface OA, one finds

$$\boldsymbol{J}_A = \hat{\boldsymbol{y}} \times \boldsymbol{H}^r\Big|_{y=0} = H_0 e^{-ikx\cos\phi_0}\hat{\boldsymbol{x}}, \tag{4.43}$$

$$\boldsymbol{M}_A = \boldsymbol{E}^r \times \hat{\boldsymbol{y}}\Big|_{y=0} = -H_0\sqrt{\frac{\mu_0}{\varepsilon_0}}\sin\phi_0 e^{-ikx\cos\phi_0}\hat{\boldsymbol{z}}, \tag{4.44}$$

and on the shadowed surface OB,

$$\boldsymbol{J}_B = \hat{\boldsymbol{n}} \times (-\boldsymbol{H}^i)\Big|_{y=x\tan\phi_w} = H_0 e^{-ikx(\cos\phi_0+\tan\phi_w\sin\phi_0)}(\cos\phi_w\hat{\boldsymbol{x}} + \sin\phi_w\hat{\boldsymbol{y}}), \tag{4.45}$$

$$\boldsymbol{M}_B = (-\boldsymbol{E}^i) \times \hat{\boldsymbol{n}}\Big|_{y=x\tan\phi_w} = -H_0\sqrt{\frac{\mu_0}{\varepsilon_0}}\sin(\phi_0-\phi_w)e^{-ikx(\cos\phi_0+\tan\phi_w\sin\phi_0)}\hat{\boldsymbol{z}}. \tag{4.46}$$

The scattering field can be obtained by integrating $\boldsymbol{J}_s$, $\boldsymbol{M}_s$ with the two-dimensional Green's function G as

$$H_z^{JA} = \int_S \frac{i}{4}J_{Ax}\frac{\partial}{\partial y'}\mathrm{H}_0^{(1)}(k\sqrt{(x-x')^2+(y-y')^2})\Big|_{y'=0} dS, \tag{4.47}$$

$$H_z^{MA} = -\int_S \frac{\omega\varepsilon_0}{4}M_{Az}\mathrm{H}_0^{(1)}(k\sqrt{(x-x')^2+(y-y')^2})\Big|_{y'=0} dS, \tag{4.48}$$

$$H_z^{JB} = \int_S \frac{i}{4}(J_{Bx}\frac{\partial}{\partial y'} - J_{By}\frac{\partial}{\partial x'})\mathrm{H}_0^{(1)}(k\sqrt{(x-x')^2+(y-y')^2})\Big]\Big|_{y'=x'\tan\phi_w} dS, \tag{4.49}$$

$$H_z^{MB} = -\int_S \frac{\omega\varepsilon_0}{4}M_{Bz}\mathrm{H}_0^{(1)}(k\sqrt{(x-x')^2+(y-y')^2})\Big|_{y'=x'\tan\phi_w} dS. \tag{4.50}$$

From Eqs. (3.6), (4.43), (4.44) and (4.16), Eqs. (4.47), (4.48) can be expressed as

$$\begin{aligned} H_z^{JA} &= \int_0^\infty \Big[\pm H_0\frac{1}{4\pi}e^{-ikx'\cos\phi_0}\int_{-\infty}^\infty e^{i\xi(x-x')\pm i\sqrt{k^2-\xi^2}y}\,d\xi\Big]\,dx' \\ &= \pm H_0\frac{1}{4\pi}\int_{-\infty}^\infty \left(\int_0^\infty e^{-ix'(k\cos\phi_0+\xi)}\,dx'\right) e^{i\xi x\pm i\sqrt{k^2-\xi^2}y}\,d\xi \\ &= \mp H_0\frac{i}{4\pi}\int_{-\infty}^\infty \frac{e^{i\xi x\pm i\sqrt{k^2-\xi^2}y}}{k\cos\phi_0+\xi}\,d\xi, \quad (y \gtrless 0), \end{aligned} \tag{4.51}$$

$$\begin{aligned} H_z^{MA} &= -\int_0^\infty \Big[\frac{\omega\varepsilon_0}{4\pi}\sqrt{\frac{\mu_0}{\varepsilon_0}}H_0\sin\phi_0 e^{jkx'\cos\phi_0}\frac{1}{\pi}\int_{-\infty}^\infty \frac{e^{i\xi(x-x')+i\sqrt{k^2-\xi^2}|y|}}{\sqrt{k^2-\xi^2}}\,d\xi\Big]\,dx' \\ &= H_0\frac{k}{4\pi}\sin\phi_0\int_{-\infty}^\infty \left(\int_0^\infty e^{-ix'(k\cos\phi_0+\xi)}\,dx'\right)\frac{e^{i\xi x\pm i\sqrt{k^2-\xi^2}y}}{\sqrt{k^2-\xi^2}}\,d\xi \\ &= -H_0\frac{ik}{4\pi}\sin\phi_0\int_{-\infty}^\infty \frac{e^{i\xi x\pm i\sqrt{k^2-\xi^2}y}}{(k\cos\phi_0+\xi)\sqrt{k^2-\xi^2}}\,d\xi, \quad (y \gtrless 0). \end{aligned} \tag{4.52}$$

From Eqs. (3.6), (4.45), (4.46), (4.15) and (4.16), Eqs. (4.49) and (4.50)can be expressed as

$$
\begin{aligned}
H_z^{JB} &= \int_0^{\infty} \Big[\frac{1}{4\pi} H_0 e^{-ikx'(\cos\phi_0+\tan\phi_w\sin\phi_0)} \int_{-\infty}^{\infty} e^{i\xi(x-x')\pm i\sqrt{k^2-\xi^2}(y-x'\tan\phi_w)} \\
&\qquad \cdot\Big(\pm\cos\phi_w - \sin\phi_w \frac{\xi}{\sqrt{k^2-\xi^2}}\,d\xi\Big)\Big]\sqrt{1+\tan^2\phi_w}\,dx' \\
&= \pm\frac{H_0}{4\pi}\int_{-\infty}^{\infty}\Big(\int_0^{\infty} e^{-ix'(k\cos\phi_0+k\tan\phi_w\sin\phi_0+\xi\pm\sqrt{k^2-\xi^2}\tan\phi_w)}\,dx'\Big)e^{i\xi x\pm i\sqrt{k^2-\xi^2}y}\,d\xi \\
&\quad -\frac{H_0}{4\pi}\frac{\sin\phi_w}{\cos\phi_w}\int_{-\infty}^{\infty}\Big(\int_0^{\infty} e^{-ix'(k\cos\phi_0+k\tan\phi_w\sin\phi_0+\xi\pm\sqrt{k^2-\xi^2}\tan\phi_w)}\,dx'\Big)\frac{\xi e^{i\xi x\pm i\sqrt{k^2-\xi^2}y}}{\sqrt{k^2-\xi^2}}\,d\xi \\
&= -\frac{iH_0}{4\pi}\frac{\sin\phi_w}{\cos\phi_w}\int_{-\infty}^{\infty}\frac{\xi e^{i\xi x\pm i\sqrt{k^2-\xi^2}y}}{(k\cos\phi_0+k\tan\phi_w\sin\phi_0+\xi\pm\sqrt{k^2-\xi^2}\tan\phi_w)\sqrt{k^2-\xi^2}}\,d\xi \\
&\quad \mp\frac{iH_0}{4\pi}\int_{-\infty}^{\infty}\frac{e^{i\xi x\pm i\sqrt{k^2-\xi^2}y}}{(k\cos\phi_0+k\tan\phi_w\sin\phi_0+\xi\pm\sqrt{k^2-\xi^2}\tan\phi_w)}\,d\xi, \\
&\qquad\qquad (y \gtrless x'\tan\phi_w), \qquad (4.53)
\end{aligned}
$$

$$
\begin{aligned}
H_z^{MB} &= -\int_0^{\infty}\Big[\frac{\omega\varepsilon_0}{4\pi}\sqrt{\frac{\mu_0}{\varepsilon_0}}H_0\sin(\phi_0-\phi_w)e^{jkx'(\cos\phi_0+\tan\phi_w\sin\phi_0)} \\
&\qquad \cdot\int_{-\infty}^{\infty}\frac{e^{i\xi(x-x')\pm i\sqrt{k^2-\xi^2}(y-x'\tan\phi_w)}}{\sqrt{k^2-\xi^2}}\,d\xi\Big]\sqrt{1+\tan^2\phi_w}\,dx' \\
&= -H_0\frac{k}{4\pi}\frac{\sin(\phi_0-\phi_w)}{\cos\phi_w} \\
&\qquad \cdot\int_{-\infty}^{\infty}\Big(\int_0^{\infty} e^{-ix'(k\cos\phi_0+k\tan\phi_w\sin\phi_0+\xi\pm\sqrt{k^2-\xi^2}\tan\phi_w)}\,dx'\Big)\frac{e^{i\xi x\pm i\sqrt{k^2-\xi^2}y}}{\sqrt{k^2-\xi^2}}\,d\xi \\
&= H_0\frac{ik}{4\pi}\int_{-\infty}^{\infty}\frac{\sin(\phi_0-\phi_w)e^{i\xi x\pm i\sqrt{k^2-\xi^2}y}}{\cos\phi_w(k\cos\phi_0+k\tan\phi_w\sin\phi_0+\xi\pm\sqrt{k^2-\xi^2}\tan\phi_w)\sqrt{k^2-\xi^2}}\,d\xi, \\
&\qquad\qquad (y \gtrless x'\tan\phi_w). \qquad (4.54)
\end{aligned}
$$

Since these integrals cannot be analytically evaluated, the saddle point method is used. Converting to complex angle w plane using the transformation $\xi = k\sin w$, with the cylindrical coordinates (ρ,θ) with $x = \rho\cos\phi, y = \rho\sin\phi$, Eqs. (4.51)–(4.54) can be expressed as

$$
\begin{aligned}
H_z^{JA} &= \mp H_0\frac{i}{4\pi}\int_C \frac{e^{ik\rho(\cos\phi\sin w\pm\sin\phi\cos w)}}{k(\cos\phi_0+\sin w)k}k\cos w\,dw \\
&= \mp H_0\frac{i}{4\pi}\int_C\frac{\cos w}{\cos\phi_0+\sin w}e^{ik\rho(\sin(w\pm\phi)}\,dw, \qquad (4.55)\\
H_z^{MA} &= -H_0\frac{ik}{4\pi}\sin\phi_0\int_C\frac{e^{ik\rho(\cos\phi\sin w\pm\sin\phi\cos w)}}{k(\cos\phi_0+\sin w)k\cos w}k\cos w\,dw \\
&= -H_0\frac{i}{4\pi}\int_C\frac{\sin\phi_0}{\cos\phi_0+\sin w}e^{ik\rho(\sin(w\pm\phi)}\,dw, \qquad (4.56)
\end{aligned}
$$

$$H_z^{JB} = \pm H_0 \frac{i}{4\pi} \int_C \frac{e^{ik\rho(\cos\phi \sin w \pm \sin\phi \cos w)}}{(k\cos\phi_0 + k\tan\phi_w \sin\phi_0 + k\sin w \pm k\cos w \tan\phi_w)} k\cos w\, dw$$
$$- H_0 \frac{i}{4\pi} \frac{\sin\phi_w}{\cos\phi_w} \int_C \frac{k\sin w e^{ik\rho(\cos\phi \sin w \pm \sin\phi \cos w)}}{(k\cos\phi_0 + k\tan\phi_w \sin\phi_0 + k\sin w \pm k\cos w \tan\phi_w)} k\cos w\, dw$$
$$= \pm H_0 \frac{i}{4\pi} \int_C \frac{\cos(w \pm \phi_w)}{\cos(\phi_0 - \phi_w) + \sin(w \pm \phi_w)} e^{ik\rho(\sin(w\pm\phi)}\, dw, \tag{4.57}$$

$$H_z^{MB} = H_0 \frac{ik}{4\pi} \frac{\sin(\phi_0 - \phi_w)}{\cos\phi_w}$$
$$\cdot \int_C \frac{e^{ik\rho(\cos\phi \sin w \pm \sin\phi \cos w)}}{(k\cos\phi_0 + k\tan\phi_w \sin\phi_0 + k\sin w \pm k\cos w \tan\phi_w) k\cos w} k\cos w\, dw$$
$$= H_0 \frac{i}{4\pi} \int_C \frac{\sin(\phi_0 - \phi_w)}{\cos(\phi_0 - \phi_w) + \sin(w \pm \phi_w)} e^{ik\rho(\sin(w\pm\phi)}\, dw. \tag{4.58}$$

we obtain $w_s = \pi/2 \mp \phi$ as a possible saddle point on the contour. At the saddle point, Eqs. (4.55)– (4.58) becomes

$$H_d^{JA} = \mp H_0 \frac{i}{4\pi} \int_C \frac{\cos w}{\cos\phi_0 + \sin w} e^{ik\rho(\sin(w\pm\phi)}\, dw$$
$$= \mp H_0 \frac{i}{4\pi} \frac{\cos w_s}{\cos\phi_0 + \sin w_s} e^{ik\rho} \int_{C_{SDP}} e^{-ik\rho(w-w_s)^2/2}\, dw$$
$$= -H_0 \frac{\sin\phi}{\cos\phi_0 + \cos\phi} C(k\rho), \tag{4.59}$$

$$H_d^{MA} = -H_0 \frac{i}{4\pi} \int_C \frac{\sin\phi_0}{\cos\phi_0 + \sin w} e^{ik\rho(\sin(w\pm\phi)}\, dw$$
$$= -H_0 \frac{i}{4\pi} \frac{\sin\phi_0}{\cos\phi_0 + \sin w_s} e^{ik\rho} \int_{C_{SDP}} e^{-ik\rho(w-w_s)^2/2}\, dw$$
$$= -H_0 \frac{\sin\phi_0}{\cos\phi_0 + \cos\phi} C(k\rho), \tag{4.60}$$

$$H_d^{JB} = \mp H_0 \frac{i}{4\pi} \int_C \frac{\cos(w \pm \phi_w)}{\cos(\phi_0 - \phi_w) + \sin(w \mp \phi_w)} e^{ik\rho(\sin(w\pm\phi)}\, dw$$
$$= \mp H_0 \frac{i}{4\pi} \frac{\cos(w_s \pm \phi_w)}{\cos(\phi_0 - \phi_w) + \sin(w_s \mp \phi_w)} e^{ik\rho} \int_{C_{SDP}} e^{-ik\rho(w-w_s)^2/2}\, dw$$
$$= -H_0 \frac{\sin(\phi - \phi_w)}{\cos(\phi_0 - \phi_w) + \cos(\phi - \phi_w)} C(k\rho), \tag{4.61}$$

$$H_d^{MB} = H_0 \frac{i}{4\pi} \int_C \frac{\sin(\phi_0 - \phi_w)}{\cos(\phi_0 - \phi_w) + \sin(w \mp \phi_w)} e^{ik\rho(\sin(w\pm\phi)}\, dw$$
$$= H_0 \frac{i}{4\pi} \frac{\sin(\phi_0 - \phi_w)}{\cos(\phi_0 - \phi_w) + \sin(w_s \mp \phi_w)} e^{ik\rho} \int_{C_{SDP}} e^{-ik\rho(w-w_s)^2/2}\, dw$$
$$= H_0 \frac{\sin(\phi_0 - \phi_w)}{\cos(\phi_0 - \phi_w) + \cos(\phi - \phi_w)} C(k\rho). \tag{4.62}$$

The contribution of the pole $w_p = \phi_0 - \pi/2$ for surface OA with $0 < |\phi| < \pi - \phi_0$ as

$$\begin{aligned} H_p^{JA} &= 2\pi i \frac{\mp i H_0}{4\pi} \frac{\cos w_p}{\cos w_p} e^{ik(\rho \sin w_p \cos\phi \pm \cos w_p \sin\phi)} \\ &= \pm \frac{H_0}{2} e^{-ik\rho(\cos\phi_0 \cos\phi \mp \sin\phi_0 \sin\phi)} U(\pi - \phi_0 - |\phi|) \\ &= \pm \frac{H_0}{2} e^{-ikx\cos\phi_0 + iky\sin\phi_0} U(\pi - \phi_0 - |\phi|), \end{aligned} \tag{4.63}$$

$$\begin{aligned} H_p^{MA} &= 2\pi i \frac{-iH_0}{4\pi} \frac{\sin\phi_0}{\cos w_p} e^{ik(\rho \sin w_p \cos\phi \pm \cos w_p \sin\phi)} \\ &= \frac{H_0}{2} e^{-ik\rho(\cos\phi_0 \cos\phi \mp \sin\phi_0 \sin\phi)} U(\pi - \phi_0 - |\phi|) \\ &= \frac{H_0}{2} e^{-ikx\cos\phi_0 + iky\sin\phi_0} U(\pi - \phi_0 - |\phi|). \end{aligned} \tag{4.64}$$

For surface OB with $w_p = \phi_0 - \pi/2$, $\phi_0 - \pi < \phi < \phi_w - 2\pi$,

$$\begin{aligned} H_p^{JB} &= 2\pi i \frac{iH_0}{4\pi} \frac{\cos(w_p - \phi_w)}{\cos(w_p - \phi_w)} e^{ik(\rho \sin w_p \cos\phi - \cos w_p \sin\phi)} \\ &= -\frac{H_0}{2} e^{-ik\rho(\cos\phi_0 \cos\phi + \sin\phi_0 \sin\phi)} U(\phi + \pi - \phi_0) U(-\phi - 2\pi + \phi_w) \\ &= -\frac{H_0}{2} e^{-ikx\cos\phi_0 - iky\sin\phi_0} U(\phi + \pi - \phi_0) U(-\phi - 2\pi + \phi_w), \end{aligned} \tag{4.65}$$

$$\begin{aligned} H_p^{MB} &= 2\pi i \frac{iH_0}{4\pi} \frac{\sin(\phi_0 - \phi_w)}{\cos(w_p - \phi_w)} e^{ik(\rho \sin w_p \cos\phi - \cos w_p \sin\phi)} \\ &= -\frac{H_0}{2} e^{-ik\rho(\cos\phi_0 \cos\phi + \sin\phi_0 \sin\phi)} U(\phi + \pi - \phi_0) U(-\phi - 2\pi + \phi_w) \\ &= -\frac{H_0}{2} e^{-ikx\cos\phi_0 - iky\sin\phi_0} U(\phi + \pi - \phi_0) U(-\phi - 2\pi + \phi_w), \end{aligned} \tag{4.66}$$

and for $w_p = \phi_0 - 2\phi_w - \pi/2$, $\phi_w - 2\pi < \phi < 2\phi_w - \phi_0 - 3\pi$

$$\begin{aligned} H_p^{JB} &= -2\pi i \frac{iH_0}{4\pi} \frac{\cos(w_p + \phi_w)}{\cos(w_p + \phi_w)} e^{ik(\rho \sin w_p \cos\phi + \cos w_p \sin\phi)} \\ &= \frac{H_0}{2} e^{-ik\rho(\cos(2\phi_w - \phi_0)\cos\phi - \sin(2\phi_w - \phi_0)\sin\phi)} U(\phi + 2\pi - \phi_w) U(-\phi - 3\pi + 2\phi_w - \phi_0) \\ &= \frac{H_0}{2} e^{-ikx\cos(2\phi_w - \phi_0) - iky\sin(2\phi_w - \phi_0)} U(\phi + 2\pi - \phi_w) U(-\phi - 3\pi + 2\phi_w - \phi_0), \end{aligned} \tag{4.67}$$

$$\begin{aligned} H_p^{MB} &= 2\pi i \frac{iH_0}{4\pi} \frac{\sin(\phi_0 - \phi_w)}{\cos(w_p + \phi_w)} e^{ik(\rho \sin w_p \cos\phi + \cos w_p \sin\phi)} \\ &= -\frac{H_0}{2} e^{-ik\rho(\cos(2\phi_w - \phi_0)\cos\phi - \sin(2\phi_w - \phi_0)\sin\phi)} U(\phi + 2\pi - \phi_w) U(-\phi - 3\pi + 2\phi_w - \phi_0) \\ &= -\frac{H_0}{2} e^{-ikx\cos(2\phi_w - \phi_0) - iky\sin(2\phi_w - \phi_0)} U(\phi + 2\pi - \phi_w) U(-\phi - 3\pi + 2\phi_w - \phi_0). \end{aligned} \tag{4.68}$$

Then the scattering field from the surface OA is

$$\begin{aligned} H_z^{\mathrm{OA}} &= H_d^{JA} + H_d^{MA} + H_p^{JA} + H_p^{MA} \\ &= -H_0 \frac{\sin\phi_0 + \sin\phi}{\cos\phi_0 + \cos\phi} C(k\rho) + H_0 e^{-ikx\cos\phi_0 + iky\sin\phi_0} U(\pi - \phi_0 - \phi) U(\phi) \end{aligned} \tag{4.69}$$

and from the surface OB is

$$\begin{aligned} H_z^{\mathrm{OB}} &= H_d^{JB} + H_d^{MB} + H_p^{JB} + H_p^{MB} \\ &= H_0 \frac{\sin(\phi_0 - \phi_w) - \sin(\phi - \phi_w)}{\cos(\phi_0 - \phi_w) + \cos(\phi - \phi_w)} C(k\rho) \\ &\quad - H_0 e^{-ikx\cos\phi_0 - iky\sin\phi_0} U(\phi + \pi - \phi_0) U(-\phi - 2\pi + \phi_w). \end{aligned} \tag{4.70}$$

Then, the total scattering field E_z^s is defined by the summation of the above contributions in Eqs. (4.69), (4.70) as

$$\begin{aligned} H_z^{\mathrm{OB}} &= H_z^{\mathrm{OA}} + H_z^{\mathrm{OB}} \\ &= -H_0 \Big(\frac{\sin\phi_0 + \sin\phi}{\cos\phi_0 + \cos\phi} - \frac{\sin(\phi_0 - \phi_w) - \sin(\phi - \phi_w)}{\cos(\phi_0 - \phi_w) + \cos(\phi - \phi_w)} \Big) C(k\rho) \\ &\quad - H_0 e^{-ikx\cos\phi_0 + iky\sin\phi_0} U(\pi - \phi_0 - \phi) U(\phi) \\ &\quad - H_0 e^{-ikx\cos\phi_0 - iky\sin\phi_0} U(\phi + \pi - \phi_0) U(-\phi - 2\pi + \phi_w). \end{aligned} \tag{4.71}$$

The term B in the big parentheses of the first line in Eq. (4.71) becomes

$$\begin{aligned} B &= \frac{\sin\phi_0 + \sin\phi}{\cos\phi_0 + \cos\phi} - \frac{\sin(\phi_0 - \phi_w) - \sin(\phi - \phi_w)}{\cos(\phi_0 - \phi_w) + \cos(\phi - \phi_w)} \\ &= \frac{\begin{array}{r}(\sin\phi_0 + \sin\phi)[\cos(\phi_0 - \phi_w) + \cos(\phi - \phi_w)] \\ - [\sin(\phi_0 - \phi_w) - \sin(\phi - \phi_w)](\cos\phi_0 + \cos\phi)\end{array}}{(\cos\phi_0 + \cos\phi)[\cos(\phi_0 - \phi_w) + \cos(\phi - \phi_w)]} \\ &= \frac{\begin{array}{r}\sin[\phi + (\phi_0 - \phi_w)] + \sin[\phi - (\phi_0 - \phi_w)] \\ + \sin[\phi + (\phi - \phi_w)] + \sin[\phi - (\phi - \phi_w)]\end{array}}{(\cos\phi_0 + \cos\phi)[\cos(\phi_0 - \phi_w) + \cos(\phi - \phi_w)]} \\ &= \frac{2\sin\phi[\cos(\phi_0 - \phi_w) + \cos(\phi - \phi_w)]}{(\cos\phi_0 + \cos\phi)[\cos(\phi_0 - \phi_w) + \cos(\phi - \phi_w)]} \\ &= \frac{2\sin\phi}{(\cos\phi_0 + \cos\phi)}. \end{aligned} \tag{4.72}$$

This results is found to match with the one by the PO approximation in Eq. (3.26).

It is also interesting to observed that the reflected GO field is excited from the currents $\boldsymbol{J}_A$ and $\boldsymbol{M}_A$ on the illuminated surface, while the negative incident field which cancels the original incident field is from the currents $\boldsymbol{J}_B$ and $\boldsymbol{M}_B$ on the shadowed surface. Also the contributions $\boldsymbol{J}_B$, $\boldsymbol{M}_B$ on the shadow surface yield the same results regardless of the wedge angle. This matches the observation of PO approximation which assumes zero surface current on the shadow side. According to the surface equivalence theorem, the equivalent currents excite null field inside the enclosed surface as in Fig. 2.1(b). The total field E_z^s in Eqs. (4.37) and (4.71) does not vanish inside the conducting wedge region

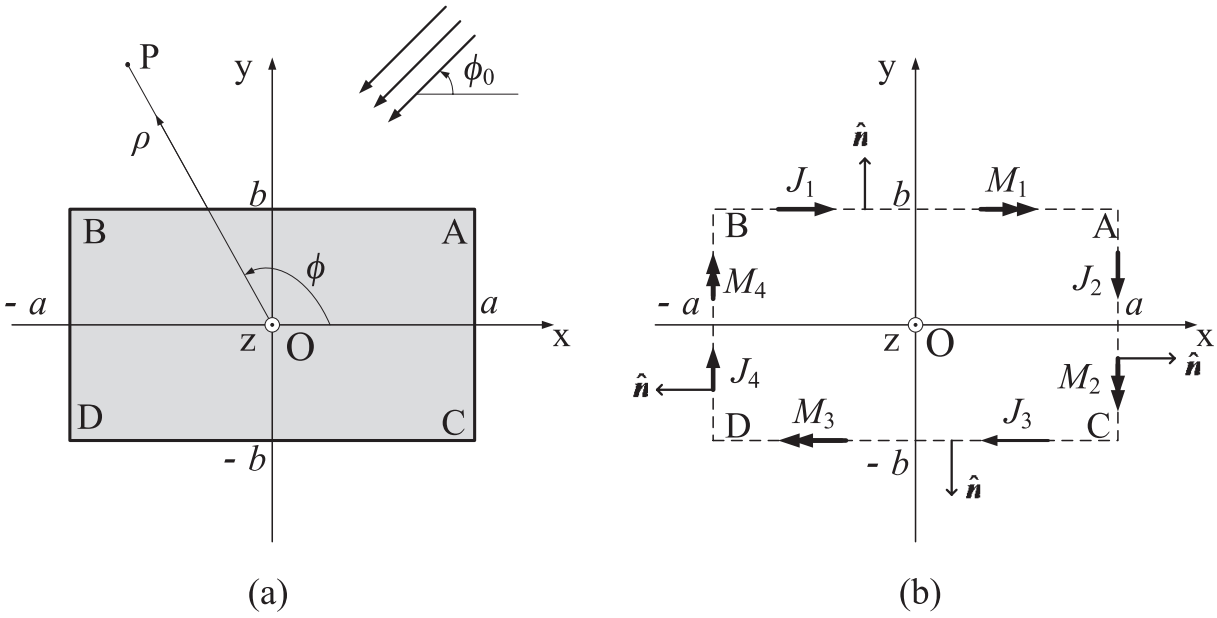

Figure 4.2: Scattering by a conducting rectangular cylinder. (a) Scattering by plane waves $\boldsymbol{E}^i$, $\boldsymbol{H}^i$. (b) Equivalent currents $\boldsymbol{J}_s$, $\boldsymbol{M}_s$ on the cylinder surfaces.

($\phi_w - 2\pi < \phi < 0$), but it would be asymptotically $\mathcal{O}\ (k^{-1/2})$, since the all GO fields cancel and the only edge diffracted fields from the edges exist. This is due to the fact that the equivalent surface currents are derived from the incident and reflected GO fields with ignoring the possible edge diffracted field.

One may also find that $E_z^{JA} = E_z^{JB}$, $E_z^{MA} = -E_z^{MB}$ for a half-plane ($\phi_w = 2\pi$). Accordingly, one does not need magnetic currents $\boldsymbol{M}_A$ and $\boldsymbol{M}_B$, and the electric current $\boldsymbol{J}_B$ on the shadow side contributes one half of the total scattering field.

4.1.2 Scattering by a Conducting Rectangular Cylinder

Let us consider that a plane wave impinges upon a surface of a conducting rectangular cylinder whose dimensions are $2a \times 2b$ as shown in Fig. 4.2(a). Because of the symmetry of the scattering object, the incident angle ϕ_0 is assumed as $0 < \phi_0 < 90^o$ without losing the generality. shows a two-dimensional conducting wedge of the wedge angle ϕ_w illuminated by a plane wave.

The scattering formulation may be separated into two polarizations.

E Polarization

When an E polarized incident plane wave can be written as in Eqs. (4.3), (4.4) impinges on the surfaces of the conducting rectangular cylinder, the reflected waves at the surface AB can be obtained as

$$\boldsymbol{E}^{rAB} = -E_0 e^{-ik(x\cos\phi_0+(2b-y)\sin\phi_0)}\hat{\boldsymbol{z}}, \tag{4.73}$$

$$\boldsymbol{H}^{rAB} = E_0\sqrt{\frac{\varepsilon_0}{\mu_0}}e^{-ik(x\cos\phi_0+(2b-y)\sin\phi_0)}(-\sin\phi_0\hat{\boldsymbol{x}} - \cos\phi_0\hat{\boldsymbol{y}}), \tag{4.74}$$

and at the surface AC,

$$\boldsymbol{E}^{rAC} = -E_0 e^{-ik((2a-x)\cos\phi_0+y\sin\phi_0)}\hat{\boldsymbol{z}}, \tag{4.75}$$

$$\boldsymbol{H}^{rAC} = E_0\sqrt{\frac{\varepsilon_0}{\mu_0}}e^{-ik((2a-x)\cos\phi_0+y\sin\phi_0)}(\sin\phi_0\hat{\boldsymbol{x}} + \cos\phi_0\hat{\boldsymbol{y}}). \tag{4.76}$$

Considering to the surfaces of the cylinder, the equivalent currents $\boldsymbol{J}_s$ and $\boldsymbol{M}_s$ can be derived as

$$\boldsymbol{J}_1 = \hat{\boldsymbol{y}} \times \boldsymbol{H}^{rAB}\Big|_{y=b} = E_0\sqrt{\frac{\varepsilon_0}{\mu_0}}\sin\phi_0 e^{-ik(x\cos\phi_0+b\sin\phi_0)}\hat{\boldsymbol{z}}, \tag{4.77}$$

$$\boldsymbol{M}_1 = \boldsymbol{E}^{rAB} \times \hat{\boldsymbol{y}}\Big|_{y=b} = E_0 e^{-ik(x\cos\phi_0+b\sin\phi_0)}\hat{\boldsymbol{x}}, \tag{4.78}$$

$$\boldsymbol{J}_2 = \hat{\boldsymbol{x}} \times \boldsymbol{H}^{rAC}\Big|_{x=a} = E_0\sqrt{\frac{\varepsilon_0}{\mu_0}}\cos\phi_0 e^{-ik(a\cos\phi_0+y\sin\phi_0)}\hat{\boldsymbol{z}}, \tag{4.79}$$

$$\boldsymbol{M}_2 = \boldsymbol{E}^{rAC} \times \hat{\boldsymbol{x}}\Big|_{x=a} = -E_0 e^{-ik(a\cos\phi_0+y\sin\phi_0)}\hat{\boldsymbol{y}}, \tag{4.80}$$

$$\boldsymbol{J}_3 = -\hat{\boldsymbol{y}} \times (-\boldsymbol{H}^i)\Big|_{y=-b} = E_0\sqrt{\frac{\varepsilon_0}{\mu_0}}\sin\phi_0 e^{-ik(x\cos\phi_0+b\sin\phi_0)}\hat{\boldsymbol{z}}, \tag{4.81}$$

$$\boldsymbol{M}_3 = (-\boldsymbol{E}^i) \times (-\hat{\boldsymbol{y}})\Big|_{y=-b} = -E_0 e^{-ik(x\cos\phi_0+b\sin\phi_0)}\hat{\boldsymbol{x}}, \tag{4.82}$$

$$\boldsymbol{J}_4 = (-\hat{\boldsymbol{x}}) \times (-\boldsymbol{H}^i)\Big|_{x=-a} = E_0\sqrt{\frac{\varepsilon_0}{\mu_0}}\cos\phi_0 e^{-ik(-a\cos\phi_0+y\sin\phi_0)}\hat{\boldsymbol{z}}, \tag{4.83}$$

$$\boldsymbol{M}_4 = (-\boldsymbol{E}^i) \times (-\hat{\boldsymbol{x}})\Big|_{x=-a} = E_0 e^{-ik(-a\cos\phi_0+y\sin\phi_0)}\hat{\boldsymbol{y}}. \tag{4.84}$$

The scattering field can be obtained by integrating $\boldsymbol{J}_1 \sim \boldsymbol{M}_4$ with the two-dimensional

Green's function G as

$$E_z^{J1} = -\int_S \frac{\omega\mu_0}{4} J_1 \mathrm{H}_0^{(1)}(k\sqrt{(x-x')^2+(y-y')^2})\Big|_{y'=b} dS, \tag{4.85}$$

$$E_z^{M1} = -\int_S \frac{i}{4} M_1 \frac{\partial}{\partial y'} \mathrm{H}_0^{(1)}(k\sqrt{(x-x')^2+(y-y')^2})\Big|_{y'=b} dS, \tag{4.86}$$

$$E_z^{J2} = -\int_S \frac{\omega\mu_0}{4} J_2 \mathrm{H}_0^{(1)}(k\sqrt{(x-x')^2+(y-y')^2})\Big|_{x'=a} dS, \tag{4.87}$$

$$E_z^{M2} = \int_S \frac{i}{4} M_2 \frac{\partial}{\partial x'} \mathrm{H}_0^{(1)}(k\sqrt{(x-x')^2+(y-y')^2})\Big|_{x'=a} dS, \tag{4.88}$$

$$E_z^{J3} = -\int_S \frac{\omega\mu_0}{4} J_3 \mathrm{H}_0^{(1)}(k\sqrt{(x-x')^2+(y-y')^2})\Big|_{y'=-b} dS, \tag{4.89}$$

$$E_z^{M3} = -\int_S \frac{i}{4} M_3 \frac{\partial}{\partial y'} \mathrm{H}_0^{(1)}(k\sqrt{(x-x')^2+(y-y')^2})\Big|_{y'=-b} dS, \tag{4.90}$$

$$E_z^{J4} = -\int_S \frac{\omega\mu_0}{4} J_4 \mathrm{H}_0^{(1)}(k\sqrt{(x-x')^2+(y-y')^2})\Big|_{x'=-a} dS, \tag{4.91}$$

$$E_z^{M4} = \int_S \frac{i}{4} M_4 \frac{\partial}{\partial x'} \mathrm{H}_0^{(1)}(k\sqrt{(x-x')^2+(y-y')^2})\Big|_{x'=-a} dS. \tag{4.92}$$

From Eqs. (4.77)–(4.84), we have

$$\begin{aligned} E_z^{J1} &= -\int_{-a}^{a} \Big[E_0 \frac{k}{4\pi} \sin\phi_0 e^{-ik(x\cos\phi_0 + b\sin\phi_0)} \int_{-\infty}^{\infty} \frac{e^{i\xi(x-x')+i\sqrt{k^2-\xi^2}|y-b|}}{\sqrt{k^2-\xi^2}} d\xi \Big] dx' \\ &= -E_0 \frac{ik}{4\pi} \sin\phi_0 e^{-ikb\sin\phi_0} e^{-ika\cos\phi_0} \int_{-\infty}^{\infty} \frac{e^{i\xi(x-a)\pm i\sqrt{k^2-\xi^2}(y-b)}}{(k\cos\phi_0+\xi)\sqrt{k^2-\xi^2}} d\xi \\ &\quad + E_0 \frac{ik}{4\pi} \sin\phi_0 e^{-ikb\sin\phi_0} e^{ika\cos\phi_0} \int_{-\infty}^{\infty} \frac{e^{i\xi(x+a)\pm i\sqrt{k^2-\xi^2}(y-b)}}{(k\cos\phi_0+\xi)\sqrt{k^2-\xi^2}} d\xi, (y \gtrless b), \end{aligned} \tag{4.93}$$

$$\begin{aligned} E_z^{M1} &= \mp \int_{-a}^{a} \Big[H_0 \frac{1}{4\pi} e^{-ik(x\cos\phi_0 + b\sin\phi_0)} \int_{-\infty}^{\infty} e^{i\xi(x-x')+i\sqrt{k^2-\xi^2}|y-b|} d\xi \Big] dx' \\ &= \mp E_0 \frac{i}{4\pi} e^{-ikb\sin\phi_0} e^{-ika\cos\phi_0} \int_{-\infty}^{\infty} \frac{e^{i\xi(x-a)\pm i\sqrt{k^2-\xi^2}(y-b)}}{k\cos\phi_0+\xi} d\xi \\ &\quad \pm E_0 \frac{i}{4\pi} e^{-ikb\sin\phi_0} e^{ika\cos\phi_0} \int_{-\infty}^{\infty} \frac{e^{i\xi(x+a)\pm i\sqrt{k^2-\xi^2}(y-b)}}{k\cos\phi_0+\xi} d\xi, \qquad (y \gtrless b), \end{aligned} \tag{4.94}$$

$$\begin{aligned} E_z^{J2} &= -\int_{-b}^{b} \Big[E_0 \frac{k}{4\pi} \cos\phi_0 e^{-ik(a\cos\phi_0 + y\sin\phi_0)} \int_{-\infty}^{\infty} \frac{e^{i\xi(x-a)+i\sqrt{k^2-\xi^2}|y-y'|}}{\sqrt{k^2-\xi^2}} d\xi \Big] dy' \\ &= -E_0 \frac{ik}{4\pi} \cos\phi_0 e^{-ika\cos\phi_0} e^{-ikb\cos\phi_0} \int_{-\infty}^{\infty} \frac{e^{i\xi(x-a)\pm i\sqrt{k^2-\xi^2}(y-b)}}{(k\cos\phi_0+\sqrt{k^2-\xi^2})\sqrt{k^2-\xi^2}} d\xi \\ &\quad + E_0 \frac{ik}{4\pi} \cos\phi_0 e^{-ika\cos\phi_0} e^{ikb\cos\phi_0} \int_{-\infty}^{\infty} \frac{e^{i\xi(x-a)\pm i\sqrt{k^2-\xi^2}(y+b)}}{(k\cos\phi_0+\sqrt{k^2-\xi^2})\sqrt{k^2-\xi^2}} d\xi, \\ &\qquad\qquad (y \gtrless y'), \end{aligned} \tag{4.95}$$

$$E_z^{M2} = -\int_{-b}^{b}\Big[E_0\frac{1}{4\pi}e^{-ik(a\cos\phi_0+y\sin\phi_0)}\int_{-\infty}^{\infty}\frac{\xi e^{i\xi(x-a)+i\sqrt{k^2-\xi^2}|y-y'|}}{\sqrt{k^2-\xi^2}}\,d\xi\Big]\,dy'$$
$$= -E_0\frac{i}{4\pi}e^{-ika\cos\phi_0}e^{-ikb\cos\phi_0}\int_{-\infty}^{\infty}\frac{\xi e^{i\xi(x-a)\pm i\sqrt{k^2-\xi^2}(y-b)}}{(k\cos\phi_0+\sqrt{k^2-\xi^2})\sqrt{k^2-\xi^2}}\,d\xi$$
$$+ E_0\frac{ik}{4\pi}e^{-ika\cos\phi_0}e^{ikb\cos\phi_0}\int_{-\infty}^{\infty}\frac{\xi e^{i\xi(x-a)\pm i\sqrt{k^2-\xi^2}(y+b)}}{(k\cos\phi_0+\sqrt{k^2-\xi^2})\sqrt{k^2-\xi^2}}\,d\xi,$$
$$(y \gtrless y'), \tag{4.96}$$

$$E_z^{J3} = -\int_{-a}^{a}\Big[E_0\frac{k}{4\pi}\sin\phi_0 e^{-ik(x\cos\phi_0+b\sin\phi_0)}\int_{-\infty}^{\infty}\frac{e^{i\xi(x-x')+i\sqrt{k^2-\xi^2}|y+b|}}{\sqrt{k^2-\xi^2}}\,d\xi\Big]\,dx'$$
$$= -E_0\frac{ik}{4\pi}\sin\phi_0 e^{ikb\sin\phi_0}e^{-ika\cos\phi_0}\int_{-\infty}^{\infty}\frac{e^{i\xi(x-a)\pm i\sqrt{k^2-\xi^2}(y+b)}}{(k\cos\phi_0+\xi)\sqrt{k^2-\xi^2}}\,d\xi$$
$$+ E_0\frac{ik}{4\pi}\sin\phi_0 e^{ikb\sin\phi_0}e^{ika\cos\phi_0}\int_{-\infty}^{\infty}\frac{e^{i\xi(x+a)\pm i\sqrt{k^2-\xi^2}(y+b)}}{(k\cos\phi_0+\xi)\sqrt{k^2-\xi^2}}\,d\xi, (y \gtrless -b) \tag{4.97}$$

$$E_z^{M3} = \pm\int_{-a}^{a}\Big[H_0\frac{1}{4\pi}e^{-ik(x\cos\phi_0+b\sin\phi_0)}\int_{-\infty}^{\infty}e^{i\xi(x-x')+i\sqrt{k^2-\xi^2}|y-b|}\,d\xi\Big]\,dx'$$
$$= \pm E_0\frac{i}{4\pi}e^{ikb\sin\phi_0}e^{-ika\cos\phi_0}\int_{-\infty}^{\infty}\frac{e^{i\xi(x-a)\pm i\sqrt{k^2-\xi^2}(y+b)}}{k\cos\phi_0+\xi}\,d\xi$$
$$\mp E_0\frac{i}{4\pi}e^{ikb\sin\phi_0}e^{ika\cos\phi_0}\int_{-\infty}^{\infty}\frac{e^{i\xi(x+a)\pm i\sqrt{k^2-\xi^2}(y+b)}}{k\cos\phi_0+\xi}\,d\xi, \qquad (y \gtrless -b), \tag{4.98}$$

$$E_z^{J4} = \int_{-b}^{b}\Big[E_0\frac{k}{4\pi}\cos\phi_0 e^{-ik(a\cos\phi_0+y\sin\phi_0)}\int_{-\infty}^{\infty}\frac{e^{i\xi(x-a)+i\sqrt{k^2-\xi^2}|y-y'|}}{\sqrt{k^2-\xi^2}}\,d\xi\Big]\,dy'$$
$$= -E_0\frac{ik}{4\pi}\cos\phi_0 e^{-ika\cos\phi_0}e^{-ikb\cos\phi_0}\int_{-\infty}^{\infty}\frac{e^{i\xi(x-a)\pm i\sqrt{k^2-\xi^2}(y-b)}}{(k\cos\phi_0+\sqrt{k^2-\xi^2})\sqrt{k^2-\xi^2}}\,d\xi$$
$$+ E_0\frac{ik}{4\pi}\cos\phi_0 e^{-ika\cos\phi_0}e^{ikb\cos\phi_0}\int_{-\infty}^{\infty}\frac{e^{i\xi(x-a)\pm i\sqrt{k^2-\xi^2}(y+b)}}{(k\cos\phi_0+\sqrt{k^2-\xi^2})\sqrt{k^2-\xi^2}}\,d\xi,$$
$$(y \gtrless y'), \tag{4.99}$$

$$E_z^{M4} = \int_{-b}^{b}\Big[E_0\frac{1}{4\pi}e^{-ik(a\cos\phi_0+y\sin\phi_0)}\int_{-\infty}^{\infty}\frac{\xi e^{i\xi(x-a)+i\sqrt{k^2-\xi^2}|y-y'|}}{\sqrt{k^2-\xi^2}}\,d\xi\Big]\,dy'$$
$$= E_0\frac{i}{4\pi}e^{-ika\cos\phi_0}e^{-ikb\cos\phi_0}\int_{-\infty}^{\infty}\frac{\xi e^{i\xi(x-a)\pm i\sqrt{k^2-\xi^2}(y-b)}}{(k\cos\phi_0+\sqrt{k^2-\xi^2})\sqrt{k^2-\xi^2}}\,d\xi$$
$$- E_0\frac{ik}{4\pi}e^{-ika\cos\phi_0}e^{ikb\cos\phi_0}\int_{-\infty}^{\infty}\frac{\xi e^{i\xi(x-a)\pm i\sqrt{k^2-\xi^2}(y+b)}}{(k\cos\phi_0+\sqrt{k^2-\xi^2})\sqrt{k^2-\xi^2}}\,d\xi,$$
$$(y \gtrless y'). \tag{4.100}$$

Similarly, converting to complex angle w plane using the transformation $\xi = k\sin w$, with the cylindrical coordinates $(x-a = \rho_A\cos\phi_A, y-b = \rho_A\sin\phi_A)$, $(x+a = \rho_B\cos\phi_C, y-b =$

$\rho_B \sin\phi_C)$ for surface AB, then

$$E_z^{J1} = -E_0 \frac{i}{2\pi} \sin\phi_0 e^{-ikb\sin\phi_0} e^{-ika\cos\phi_0} \int_C \frac{e^{ik\rho_A \sin(w\pm\phi_A)}}{\cos\phi_0 + \sin w} dw$$

$$+ E_0 \frac{i}{2\pi} \sin\phi_0 e^{-ikb\sin\phi_0} e^{ika\cos\phi_0} \int_C \frac{e^{ik\rho_B \sin(w\pm\phi_B)}}{\cos\phi_0 + \sin w} dw, \quad (y \gtrless b), \tag{4.101}$$

$$E_z^{M1} = \mp E_0 \frac{i}{2\pi} e^{-ikb\sin\phi_0} e^{-ika\cos\phi_0} \int_C \frac{\cos w e^{ik\rho_A \sin(w\pm\phi_A)}}{\cos\phi_0 + \sin w} dw$$

$$\pm E_0 \frac{i}{2\pi} e^{-ikb\sin\phi_0} e^{ika\cos\phi_0} \int_C \frac{\cos w e^{ik\rho_B \sin(w\pm\phi_B)}}{\cos\phi_0 + \sin w} dw, \quad (y \gtrless b), \tag{4.102}$$

and $(x - a = \rho_A \cos\phi_A, y - b = \rho_A \sin\phi_A)$, $(x - a = \rho_C \cos\phi_C, y + b = \rho_C \sin\phi_C)$ for surface AC, then

$$E_z^{J2} = -E_0 \frac{i}{2\pi} \cos\phi_0 e^{-ikb\sin\phi_0} e^{-ika\cos\phi_0} \int_C \frac{e^{ik\rho_A \sin(w\pm\phi_A)}}{\sin\phi_0 \pm \cos w} dw$$

$$+ E_0 \frac{i}{2\pi} \cos\phi_0 e^{ikb\sin\phi_0} e^{ika\cos\phi_0} \int_C \frac{e^{ik\rho_C \sin(w\pm\phi_C)}}{\sin\phi_0 \pm \cos w} dw, \quad (y \gtrless y'), \tag{4.103}$$

$$E_z^{M2} = -E_0 \frac{i}{2\pi} e^{-ikb\sin\phi_0} e^{-ika\cos\phi_0} \int_C \frac{\sin w e^{ik\rho_A \sin(w\pm\phi_A)}}{\sin\phi_0 \pm \cos w} dw$$

$$+ E_0 \frac{i}{2\pi} e^{ikb\sin\phi_0} e^{-ika\cos\phi_0} \int_C \frac{\sin w e^{ik\rho_C \sin(w\pm\phi_C)}}{\sin\phi_0 \pm \cos w} dw, \quad (y \gtrless y'), \tag{4.104}$$

and $(x - a = \rho_C \cos\phi_C, y + b = \rho_C \sin\phi_C)$, $(x + a = \rho_D \cos\phi_D, y - b = \rho_D \sin\phi_D)$ for surface CD,

$$E_z^{J3} = -E_0 \frac{i}{2\pi} \sin\phi_0 e^{ikb\sin\phi_0} e^{-ika\cos\phi_0} \int_C \frac{e^{ik\rho_C \sin(w\pm\phi_C)}}{\cos\phi_0 + \sin w} dw$$

$$+ E_0 \frac{i}{2\pi} \sin\phi_0 e^{ikb\sin\phi_0} e^{ika\cos\phi_0} \int_C \frac{e^{ik\rho_D \sin(w\pm\phi_D)}}{\cos\phi_0 + \sin w} dw, \quad (y \gtrless -b), \tag{4.105}$$

$$E_z^{M3} = \pm E_0 \frac{i}{2\pi} e^{ikb\sin\phi_0} e^{-ika\cos\phi_0} \int_C \frac{\cos w e^{ik\rho_C \sin(w\pm\phi_C)}}{\cos\phi_0 + \sin w} dw$$

$$\mp E_0 \frac{i}{2\pi} e^{ikb\sin\phi_0} e^{ika\cos\phi_0} \int_C \frac{\cos w e^{ik\rho_D \sin(w\pm\phi_D)}}{\cos\phi_0 + \sin w} dw, \quad (y \gtrless -b), \tag{4.106}$$

and $(x + a = \rho_B \cos\phi_B, y - b = \rho_B \sin\phi_B)$, $(x + a = \rho_D \cos\phi_C, y + b = \rho_D \sin\phi_C)$ for

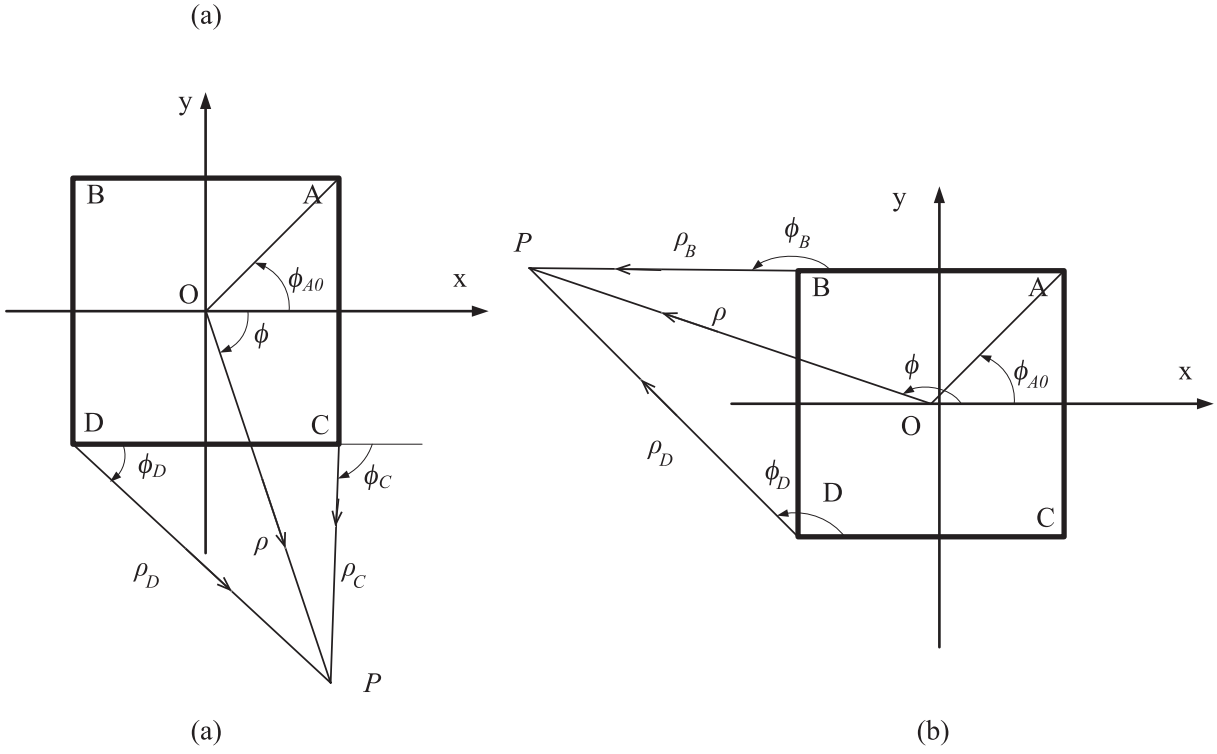

Figure 4.3: Observation point from surfaces CD (a) and BD (b).

surface BD,

$$E_z^{J4} = -E_0 \frac{i}{2\pi} \cos\phi_0 e^{-ikb\sin\phi_0} e^{ika\cos\phi_0} \int_C \frac{e^{ik\rho_B \sin(w\pm\phi_B)}}{\sin\phi_0 \pm \cos w} dw$$

$$+ E_0 \frac{i}{2\pi} \cos\phi_0 e^{ikb\sin\phi_0} e^{ika\cos\phi_0} \int_C \frac{e^{ik\rho_D \sin(w\pm\phi_D)}}{\sin\phi_0 \pm \cos w} dw, \quad (y \gtrless y'), \quad (4.107)$$

$$E_z^{M4} = E_0 \frac{i}{2\pi} e^{-ikb\sin\phi_0} e^{ika\cos\phi_0} \int_C \frac{\sin w e^{ik\rho_B \sin(w\pm\phi_B)}}{\sin\phi_0 \pm \cos w} dw$$

$$- E_0 \frac{i}{2\pi} e^{ikb\sin\phi_0} e^{ika\cos\phi_0} \int_C \frac{\sin w e^{ik\rho_B \sin(w\pm\phi_D)}}{\sin\phi_0 \pm \cos w} dw, \quad (y \gtrless y'), \quad (4.108)$$

Using saddle point method and far-field approximation

$$\begin{cases} \phi_A = \phi_B = \phi_C = \phi_D \sim \phi \\ \rho_A = \rho_B = \rho_C = \rho_D \sim \rho \end{cases} \quad \text{for amplitude variations,}$$

$$\begin{cases} \rho_A = \rho - d\cos(\phi - \phi_{A0}) = \rho - a\cos\phi - b\sin\phi \\ \rho_B = \rho - d\cos(\pi - \phi - \phi_{A0}) = \rho + a\cos\phi - b\sin\phi \\ \rho_C = \rho - d\cos(\phi + \phi_{A0}) = \rho - a\cos\phi + b\sin\phi \\ \rho_D = \rho - d\cos(\pi + \phi + \phi_{A0}) = \rho + a\cos\phi + b\sin\phi \end{cases} \quad \text{for phase variations,} \tag{4.109}$$

Eqs. (4.101)–(4.108) can be approximated as

$$E_z^{J1} = i2E_0 e^{-ikb(\sin\phi+\sin\phi_0)} \sin[ka(\cos\phi_0+\cos\phi)] \frac{\sin\phi_0}{\cos\phi_0+\cos\phi} C(k\rho), \tag{4.110}$$

$$E_z^{M1} = i2E_0 e^{-ikb(\sin\phi+\sin\phi_0)} \sin[ka(\cos\phi_0+\cos\phi)] \frac{\sin\phi}{\cos\phi_0+\cos\phi} C(k\rho), \tag{4.111}$$

$$E_z^{J2} = i2E_0 e^{-ika(\cos\phi+\cos\phi_0)} \sin[kb(\sin\phi_0+\sin\phi)] \frac{\cos\phi_0}{\sin\phi_0+\sin\phi} C(k\rho), \tag{4.112}$$

$$E_z^{M2} = i2E_0 e^{-ika(\cos\phi+\cos\phi_0)} \sin[kb(\sin\phi_0+\sin\phi)] \frac{\cos\phi}{\sin\phi_0+\sin\phi} C(k\rho), \tag{4.113}$$

$$E_z^{J3} = i2E_0 e^{ikb(\sin\phi+\sin\phi_0)} \sin[ka(\cos\phi_0+\cos\phi)] \frac{\sin\phi_0}{\cos\phi_0+\cos\phi} C(k\rho), \tag{4.114}$$

$$E_z^{M3} = -i2E_0 e^{ikb(\sin\phi+\sin\phi_0)} \sin[ka(\cos\phi_0+\cos\phi)] \frac{\sin\phi}{\cos\phi_0+\cos\phi} C(k\rho), \tag{4.115}$$

$$E_z^{J4} = i2E_0 e^{ika(\cos\phi+\cos\phi_0)} \sin[kb(\sin\phi_0+\sin\phi)] \frac{\cos\phi_0}{\sin\phi_0+\sin\phi} C(k\rho), \tag{4.116}$$

$$E_z^{M4} = -i2E_0 e^{ika(\cos\phi+\cos\phi_0)} \sin[kb(\sin\phi_0+\sin\phi)] \frac{\cos\phi}{\sin\phi_0+\sin\phi} C(k\rho). \tag{4.117}$$

Then, the total scattering field is

$$E_z^s = E_z^{J1} + E_z^{M1} + E_z^{J2} + E_z^{M2} + E_z^{J3} + E_z^{M3} + E_z^{J4} + E_z^{M4}. \tag{4.118}$$

After some manipulation, this total result is found to match with the one obtained by the PO approximation in Eq. (3.44) (see Appendix A).

$$\begin{aligned} E_z^s = {} & i4E_0 \sin\phi_0 \frac{\sin[ka(\cos\phi_0+\cos\phi)]}{\cos\phi_0+\cos\phi} e^{-ikb(\sin\phi+\sin\phi_0)} C(k\rho) \\ & + i4E_0 \cos\phi_0 \frac{\sin[kb(\sin\phi_0+\sin\phi)]}{\sin\phi_0+\sin\phi} e^{-ika(\cos\phi+\cos\phi_0)} C(k\rho). \end{aligned} \tag{4.119}$$

H Polarization

When a H polarized incident plane wave as in Eqs. (4.39), (4.40) impinges on the cylinder surfaces, the reflected waves at the surface AB can be obtained as

$$\boldsymbol{H}^{rAB} = H_0 e^{-ik(x\cos\phi_0+(2b-y)\sin\phi_0)}\hat{\boldsymbol{z}}, \tag{4.120}$$

$$\boldsymbol{E}^{rAB} = H_0\sqrt{\frac{\mu_0}{\varepsilon_0}}e^{-ik(x\cos\phi_0+(2b-y)\sin\phi_0)}(-\sin\phi_0\hat{\boldsymbol{x}}-\cos\phi_0\hat{\boldsymbol{y}}), \tag{4.121}$$

and at the surface AC,

$$\boldsymbol{H}^{rAC} = H_0 e^{-ik((2a-x)\cos\phi_0+y\sin\phi_0)}\hat{\boldsymbol{z}}, \tag{4.122}$$

$$\boldsymbol{E}^{rAC} = H_0\sqrt{\frac{\mu_0}{\varepsilon_0}}e^{-ik((2a-x)\cos\phi_0+y\sin\phi_0)}(\cos\phi_0\hat{\boldsymbol{x}}+\sin\phi_0\hat{\boldsymbol{y}}). \tag{4.123}$$

Considering to the surfaces of the cylinder, the equivalent currents $\boldsymbol{J}_s$ and $\boldsymbol{M}_s$ can be derived as

$$\boldsymbol{J}_1 = \hat{\boldsymbol{y}}\times\boldsymbol{H}^{rAB}\Big|_{y=b} = H_0 e^{-ik(x\cos\phi_0+b\sin\phi_0)}\hat{\boldsymbol{x}}, \tag{4.124}$$

$$\boldsymbol{M}_1 = \boldsymbol{E}^{rAB}\times\hat{\boldsymbol{y}}\Big|_{y=b} = -H_0\sqrt{\frac{\mu_0}{\varepsilon_0}}\sin\phi_0 e^{-ik(x\cos\phi_0+b\sin\phi_0)}\hat{\boldsymbol{z}}, \tag{4.125}$$

$$\boldsymbol{J}_2 = \hat{\boldsymbol{x}}\times\boldsymbol{H}^{rAC}\Big|_{x=a} = -H_0 e^{-ik(a\cos\phi_0+y\sin\phi_0)}\hat{\boldsymbol{y}}, \tag{4.126}$$

$$\boldsymbol{M}_2 = \boldsymbol{E}^{rAC}\times\hat{\boldsymbol{x}}\Big|_{x=a} = -H_0\sqrt{\frac{\mu_0}{\varepsilon_0}}\cos\phi_0 e^{-ik(a\cos\phi_0+y\sin\phi_0)}\hat{\boldsymbol{z}}, \tag{4.127}$$

$$\boldsymbol{J}_3 = -\hat{\boldsymbol{y}}\times(-\boldsymbol{H}^{i})\Big|_{y=-b} = H_0 e^{-ik(x\cos\phi_0+b\sin\phi_0)}\hat{\boldsymbol{x}}, \tag{4.128}$$

$$\boldsymbol{M}_3 = (-\boldsymbol{E}^{i})\times(-\hat{\boldsymbol{y}})\Big|_{y=-b} = H_0\sqrt{\frac{\mu_0}{\varepsilon_0}}\sin\phi_0 e^{-ik(x\cos\phi_0+b\sin\phi_0)}\hat{\boldsymbol{z}}, \tag{4.129}$$

$$\boldsymbol{J}_4 = (-\hat{\boldsymbol{x}})\times(-\boldsymbol{H}^{i})\Big|_{x=-a} = -H_0 e^{-ik(-a\cos\phi_0+y\sin\phi_0)}\hat{\boldsymbol{y}}, \tag{4.130}$$

$$\boldsymbol{M}_4 = (-\boldsymbol{E}^{i})\times(-\hat{\boldsymbol{x}})\Big|_{x=-a} = H_0\sqrt{\frac{\mu_0}{\varepsilon_0}}\cos\phi_0 e^{-ik(-a\cos\phi_0+y\sin\phi_0)}\hat{\boldsymbol{z}}. \tag{4.131}$$

The scattering field can be obtained by integrating $\boldsymbol{J}_1 \sim \boldsymbol{M}_4$ with the two-dimensional Green's function G as

$$H_z^{J1} = \int_S \frac{i}{4}J_1\frac{\partial}{\partial y'}\mathrm{H}_0^{(1)}(k\sqrt{(x-x')^2+(y-y')^2})\Big|_{y'=b}dS, \tag{4.132}$$

$$H_z^{M1} = -\int_S \frac{\omega\mu_0}{4}M_1\mathrm{H}_0^{(1)}(k\sqrt{(x-x')^2+(y-y')^2})\Big|_{y'=b}dS, \tag{4.133}$$

$$H_z^{J2} = -\int_S \frac{i}{4}J_2\frac{\partial}{\partial x'}\mathrm{H}_0^{(1)}(k\sqrt{(x-x')^2+(y-y')^2})\Big|_{x'=a}dS, \tag{4.134}$$

$$H_z^{M2} = -\int_S \frac{\omega\mu_0}{4}M_2\mathrm{H}_0^{(1)}(k\sqrt{(x-x')^2+(y-y')^2})\Big|_{x'=a}dS, \tag{4.135}$$

$$H_z^{J3} = \int_S \frac{i}{4} J_3 \frac{\partial}{\partial y'} \mathrm{H}_0^{(1)}(k\sqrt{(x-x')^2+(y-y')^2})\Big|_{y'=-b} dS, \tag{4.136}$$

$$H_z^{M3} = -\int_S \frac{\omega\mu_0}{4} M_3 \mathrm{H}_0^{(1)}(k\sqrt{(x-x')^2+(y-y')^2})\Big|_{y'=-b} dS, \tag{4.137}$$

$$H_z^{J4} = -\int_S \frac{i}{4} J_4 \frac{\partial}{\partial x'} \mathrm{H}_0^{(1)}(k\sqrt{(x-x')^2+(y-y')^2})\Big|_{x'=-a} dS, \tag{4.138}$$

$$H_z^{M4} = -\int_S \frac{\omega\mu_0}{4} M_4 \mathrm{H}_0^{(1)}(k\sqrt{(x-x')^2+(y-y')^2})\Big|_{x'=-a} dS. \tag{4.139}$$

From Eqs. (4.124)–(4.131), we have

$$\begin{aligned} H_z^{J1} &= \pm \int_{-a}^{a} \Big[H_0 \frac{1}{4\pi} e^{-ik(x\cos\phi_0 + b\sin\phi_0)} \int_{-\infty}^{\infty} e^{i\xi(x-x')+i\sqrt{k^2-\xi^2}|y-b|}\, d\xi \Big]\, dx' \\ &= \pm H_0 \frac{i}{4\pi} e^{-ikb\sin\phi_0} e^{-ika\cos\phi_0} \int_{-\infty}^{\infty} \frac{e^{i\xi(x-a)\pm i\sqrt{k^2-\xi^2}(y-b)}}{k\cos\phi_0+\xi}\, d\xi \\ &\quad \mp H_0 \frac{i}{4\pi} e^{-ikb\sin\phi_0} e^{ika\cos\phi_0} \int_{-\infty}^{\infty} \frac{e^{i\xi(x+a)\pm i\sqrt{k^2-\xi^2}(y-b)}}{k\cos\phi_0+\xi}\, d\xi, \qquad (y \gtrless b), \end{aligned} \tag{4.140}$$

$$\begin{aligned} H_z^{M1} &= \int_{-a}^{a} \Big[H_0 \frac{k}{4\pi} \sin\phi_0 e^{-ik(x\cos\phi_0 + b\sin\phi_0)} \int_{-\infty}^{\infty} \frac{e^{i\xi(x-x')+i\sqrt{k^2-\xi^2}|y-b|}}{\sqrt{k^2-\xi^2}}\, d\xi \Big]\, dx' \\ &= H_0 \frac{ik}{4\pi} \sin\phi_0 e^{-ikb\sin\phi_0} e^{-ika\cos\phi_0} \int_{-\infty}^{\infty} \frac{e^{i\xi(x-a)\pm i\sqrt{k^2-\xi^2}(y-b)}}{(k\cos\phi_0+\xi)\sqrt{k^2-\xi^2}}\, d\xi \\ &\quad -H_0 \frac{ik}{4\pi} \sin\phi_0 e^{-ikb\sin\phi_0} e^{ika\cos\phi_0} \int_{-\infty}^{\infty} \frac{e^{i\xi(x+a)\pm i\sqrt{k^2-\xi^2}(y-b)}}{(k\cos\phi_0+\xi)\sqrt{k^2-\xi^2}}\, d\xi, (y \gtrless b), \end{aligned} \tag{4.141}$$

$$\begin{aligned} H_z^{J2} &= \int_{-b}^{b} \Big[H_0 \frac{1}{4\pi} e^{-ik(a\cos\phi_0 + y\sin\phi_0)} \int_{-\infty}^{\infty} \frac{\xi e^{i\xi(x-a)+i\sqrt{k^2-\xi^2}|y-y'|}}{\sqrt{k^2-\xi^2}}\, d\xi \Big]\, dy' \\ &= H_0 \frac{i}{4\pi} e^{-ika\cos\phi_0} e^{-ikb\cos\phi_0} \int_{-\infty}^{\infty} \frac{\xi e^{i\xi(x-a)\pm i\sqrt{k^2-\xi^2}(y-b)}}{(k\cos\phi_0+\sqrt{k^2-\xi^2})\sqrt{k^2-\xi^2}}\, d\xi \\ &\quad -H_0 \frac{ik}{4\pi} e^{-ika\cos\phi_0} e^{ikb\cos\phi_0} \int_{-\infty}^{\infty} \frac{\xi e^{i\xi(x-a)\pm i\sqrt{k^2-\xi^2}(y+b)}}{(k\cos\phi_0+\sqrt{k^2-\xi^2})\sqrt{k^2-\xi^2}}\, d\xi, \\ &\qquad\qquad (y \gtrless y'), \end{aligned} \tag{4.142}$$

$$\begin{aligned} H_z^{M2} &= \int_{-b}^{b} \Big[H_0 \frac{k}{4\pi} \cos\phi_0 e^{-ik(a\cos\phi_0 + y\sin\phi_0)} \int_{-\infty}^{\infty} \frac{e^{i\xi(x-a)+i\sqrt{k^2-\xi^2}|y-y'|}}{\sqrt{k^2-\xi^2}}\, d\xi \Big]\, dy' \\ &= H_0 \frac{ik}{4\pi} \cos\phi_0 e^{-ika\cos\phi_0} e^{-ikb\cos\phi_0} \int_{-\infty}^{\infty} \frac{e^{i\xi(x-a)\pm i\sqrt{k^2-\xi^2}(y-b)}}{(k\cos\phi_0+\sqrt{k^2-\xi^2})\sqrt{k^2-\xi^2}}\, d\xi \\ &\quad -H_0 \frac{ik}{4\pi} \cos\phi_0 e^{-ika\cos\phi_0} e^{ikb\cos\phi_0} \int_{-\infty}^{\infty} \frac{e^{i\xi(x-a)\pm i\sqrt{k^2-\xi^2}(y+b)}}{(k\cos\phi_0+\sqrt{k^2-\xi^2})\sqrt{k^2-\xi^2}}\, d\xi, \\ &\qquad\qquad (y \gtrless y'), \end{aligned} \tag{4.143}$$

$$H_z^{J3} = \pm \int_{-a}^{a} \Big[H_0 \frac{1}{4\pi} e^{-ik(x\cos\phi_0 + b\sin\phi_0)} \int_{-\infty}^{\infty} e^{i\xi(x-x') + i\sqrt{k^2-\xi^2}|y-b|}\, d\xi \Big]\, dx'$$

$$= \pm H_0 \frac{i}{4\pi} e^{ikb\sin\phi_0} e^{-ika\cos\phi_0} \int_{-\infty}^{\infty} \frac{e^{i\xi(x-a) \pm i\sqrt{k^2-\xi^2}(y+b)}}{k\cos\phi_0 + \xi}\, d\xi$$

$$\mp H_0 \frac{i}{4\pi} e^{ikb\sin\phi_0} e^{ika\cos\phi_0} \int_{-\infty}^{\infty} \frac{e^{i\xi(x+a) \pm i\sqrt{k^2-\xi^2}(y+b)}}{k\cos\phi_0 + \xi}\, d\xi, \qquad (y \gtrless -b), \quad (4.144)$$

$$H_z^{M3} = -\int_{-a}^{a} \Big[H_0 \frac{k}{4\pi} \sin\phi_0 e^{-ik(x\cos\phi_0 + b\sin\phi_0)} \int_{-\infty}^{\infty} \frac{e^{i\xi(x-x') + i\sqrt{k^2-\xi^2}|y+b|}}{\sqrt{k^2-\xi^2}}\, d\xi \Big]\, dx'$$

$$= -H_0 \frac{ik}{4\pi} \sin\phi_0 e^{ikb\sin\phi_0} e^{-ika\cos\phi_0} \int_{-\infty}^{\infty} \frac{e^{i\xi(x-a) \pm i\sqrt{k^2-\xi^2}(y+b)}}{(k\cos\phi_0 + \xi)\sqrt{k^2-\xi^2}}\, d\xi$$

$$+H_0 \frac{ik}{4\pi} \sin\phi_0 e^{ikb\sin\phi_0} e^{ika\cos\phi_0} \int_{-\infty}^{\infty} \frac{e^{i\xi(x+a) \pm i\sqrt{k^2-\xi^2}(y+b)}}{(k\cos\phi_0 + \xi)\sqrt{k^2-\xi^2}}\, d\xi, (y \gtrless -b), \quad (4.145)$$

$$H_z^{J4} = \int_{-b}^{b} \Big[H_0 \frac{1}{4\pi} e^{-ik(a\cos\phi_0 + y\sin\phi_0)} \int_{-\infty}^{\infty} \frac{\xi e^{i\xi(x-a) + i\sqrt{k^2-\xi^2}|y-y'|}}{\sqrt{k^2-\xi^2}}\, d\xi \Big]\, dy'$$

$$= H_0 \frac{i}{4\pi} e^{-ika\cos\phi_0} e^{-ikb\cos\phi_0} \int_{-\infty}^{\infty} \frac{\xi e^{i\xi(x-a) \pm i\sqrt{k^2-\xi^2}(y-b)}}{(k\cos\phi_0 + \sqrt{k^2-\xi^2})\sqrt{k^2-\xi^2}}\, d\xi$$

$$-H_0 \frac{ik}{4\pi} e^{-ika\cos\phi_0} e^{ikb\cos\phi_0} \int_{-\infty}^{\infty} \frac{\xi e^{i\xi(x-a) \pm i\sqrt{k^2-\xi^2}(y+b)}}{(k\cos\phi_0 + \sqrt{k^2-\xi^2})\sqrt{k^2-\xi^2}}\, d\xi,$$

$$(y \gtrless y'), \quad (4.146)$$

$$H_z^{M4} = -\int_{-b}^{b} \Big[H_0 \frac{k}{4\pi} \cos\phi_0 e^{-ik(a\cos\phi_0 + y\sin\phi_0)} \int_{-\infty}^{\infty} \frac{e^{i\xi(x-a) + i\sqrt{k^2-\xi^2}|y-y'|}}{\sqrt{k^2-\xi^2}}\, d\xi \Big]\, dy'$$

$$= -H_0 \frac{ik}{4\pi} \cos\phi_0 e^{-ika\cos\phi_0} e^{-ikb\cos\phi_0} \int_{-\infty}^{\infty} \frac{e^{i\xi(x-a) \pm i\sqrt{k^2-\xi^2}(y-b)}}{(k\cos\phi_0 + \sqrt{k^2-\xi^2})\sqrt{k^2-\xi^2}}\, d\xi$$

$$+H_0 \frac{ik}{4\pi} \cos\phi_0 e^{-ika\cos\phi_0} e^{ikb\cos\phi_0} \int_{-\infty}^{\infty} \frac{e^{i\xi(x-a) \pm i\sqrt{k^2-\xi^2}(y+b)}}{(k\cos\phi_0 + \sqrt{k^2-\xi^2})\sqrt{k^2-\xi^2}}\, d\xi,$$

$$(y \gtrless y'). \quad (4.147)$$

Similarly, converting to complex angle w plane using the transformation $\xi = k\sin w$, and using saddle point method with far-filed approximation in Eq. (4.109), then Eqs. (4.140)–(4.147) becomes

$$H_z^{J1} = -i2H_0 e^{-ikb(\sin\phi + \sin\phi_0)} \sin[ka(\cos\phi_0 + \cos\phi)] \frac{\sin\phi}{\cos\phi_0 + \cos\phi} C(k\rho), \quad (4.148)$$

$$H_z^{M1} = -i2H_0 e^{-ikb(\sin\phi + \sin\phi_0)} \sin[ka(\cos\phi_0 + \cos\phi)] \frac{\sin\phi_0}{\cos\phi_0 + \cos\phi} C(k\rho), \quad (4.149)$$

$$H_z^{J2} = -i2H_0 e^{-ika(\cos\phi + \cos\phi_0)} \sin[kb(\sin\phi_0 + \sin\phi)] \frac{\cos\phi}{\sin\phi_0 + \sin\phi} C(k\rho), \quad (4.150)$$

$$H_z^{M2} = -i2H_0 e^{-ika(\cos\phi+\cos\phi_0)} \sin[kb(\sin\phi_0+\sin\phi)] \frac{\cos\phi_0}{\sin\phi_0+\sin\phi} C(k\rho), \quad (4.151)$$

$$H_z^{J3} = -i2H_0 e^{ikb(\sin\phi+\sin\phi_0)} \sin[ka(\cos\phi_0+\cos\phi)] \frac{\sin\phi}{\cos\phi_0+\cos\phi} C(k\rho), \quad (4.152)$$

$$H_z^{M3} = i2H_0 e^{ikb(\sin\phi+\sin\phi_0)} \sin[ka(\cos\phi_0+\cos\phi)] \frac{\sin\phi_0}{\cos\phi_0+\cos\phi} C(k\rho), \quad (4.153)$$

$$H_z^{J4} = -i2H_0 e^{ika(\cos\phi+\cos\phi_0)} \sin[kb(\sin\phi_0+\sin\phi)] \frac{\cos\phi}{\sin\phi_0+\sin\phi} C(k\rho), \quad (4.154)$$

$$H_z^{M4} = i2H_0 e^{ika(\cos\phi+\cos\phi_0)} \sin[kb(\sin\phi_0+\sin\phi)] \frac{\cos\phi_0}{\sin\phi_0+\sin\phi} C(k\rho). \quad (4.155)$$

Then, the total scattering field is

$$\begin{aligned} H_z^s &= H_z^{J1} + H_z^{M1} + H_z^{J2} + H_z^{M2} + H_z^{J3} + H_z^{M3} + H_z^{J4} + H_z^{M4} \\ &= -i4H_0 \sin\phi_0 \frac{\sin[ka(\cos\phi_0+\cos\phi)]}{\cos\phi_0+\cos\phi} e^{-ikb(\sin\phi+\sin\phi_0)} C(k\rho) \\ &\quad - i4H_0 \cos\phi_0 \frac{\sin[kb(\sin\phi_0+\sin\phi)]}{\sin\phi_0+\sin\phi} e^{-ika(\cos\phi+\cos\phi_0)} C(k\rho). \end{aligned} \quad (4.156)$$

After some manipulation, this total result is found to match with the one obtained by the PO approximation in Eq. (3.60) (see Appendix A).

In this section, the scattering fields by a conducting wedge and rectangular cylinder are formulated. In case of the conducting wedge, the equivalent currents $\boldsymbol{J}_A$, $\boldsymbol{M}_A$ at surface OA are approximated by the GO reflected wave, and currents $\boldsymbol{J}_B$, $\boldsymbol{M}_B$ at surface OB are calculated from the minus incident wave. Then, the total scattering field is given by summing up four contributions derived from these currents. While the diffracted component of this result is found to match with the one obtained by the PO approximation in Section 3.1, the internal field inside the wedge is found to be asymptotically zero due to the virtue of the surface equivalent theorem. For the conducting rectangular cylinder, eight equivalent currents $\boldsymbol{J}_1 \sim \boldsymbol{J}_4$ and $\boldsymbol{M}_1 \sim \boldsymbol{M}_4$ are approximated by the GO reflected and incident rays. When the resulting scattering fields radiating from these currents are combined, the final result is found to be exactly the same as the result obtained by the PO in Section 3.2. Therefore, from our derivation, one concludes that the results by surface equivalence theorem match with those obtained by the PO in Chapter 3, which utilized the induced electric currents on the illuminated physical surfaces. Then, when applying this method to estimate the scattering by the dielectric objects, one expects that this method could have the similar accuracy as PO formulation.

4.2 Scattering by a Dielectric Edged Object

In this section, the outside scattering formulations for the dielectric wedge and rectangular cylinder have been derived. Here, the situation becomes more complicated than the conducting case in Section 4.1. When the incident wave impinges on the illuminated surfaces, it excites the GO reflected wave ($\boldsymbol{E}^r$, $\boldsymbol{H}^r$), the GO transmitted waves ($\boldsymbol{E}^t$, $\boldsymbol{H}^t$), and diffracted wave ($\boldsymbol{E}^d$, $\boldsymbol{H}^d$). Since the diffracted wave is weaker than the GO ray fields, the scattering wave ($\boldsymbol{E}^s$, $\boldsymbol{H}^s$) on the illuminated region may be approximately given by the GO reflected wave ($\boldsymbol{E}^r$, $\boldsymbol{H}^r$) and the GO transmitted wave ($\boldsymbol{E}^t$, $\boldsymbol{H}^t$), if any. On the shadowed region, it is no incident wave observed, and the GO transmitted wave ($\boldsymbol{E}^t$, $\boldsymbol{H}^t$) and the diffracted wave ($\boldsymbol{E}^d$, $\boldsymbol{H}^d$). Then the scattering wave may be approximately given by $\boldsymbol{E}^s = -\boldsymbol{E}^i + \boldsymbol{E}^t$, $\boldsymbol{H}^s = -\boldsymbol{H}^i + \boldsymbol{H}^t$.

Accordingly, the equivalent current may be approximated as

$$\boldsymbol{J}_s = \hat{\boldsymbol{n}} \times \boldsymbol{H}^s \simeq \begin{cases} \hat{\boldsymbol{n}} \times (\boldsymbol{H}^r + \boldsymbol{H}^t) & \text{on illuminated } S, \\ \hat{\boldsymbol{n}} \times (-\boldsymbol{H}^i + \boldsymbol{H}^t) & \text{on shadowed } S, \end{cases} \tag{4.157}$$

$$\boldsymbol{M}_s = \boldsymbol{E}^s \times \hat{\boldsymbol{n}} \simeq \begin{cases} (\boldsymbol{E}^r + \boldsymbol{E}^t) \times \hat{\boldsymbol{n}} & \text{on illuminated } S, \\ (-\boldsymbol{E}^i + \boldsymbol{E}^t) \times \hat{\boldsymbol{n}} & \text{on shadowed } S, \end{cases} \tag{4.158}$$

where $\hat{\boldsymbol{n}}$ denotes the outward normal unit vector.

4.2.1 Diffraction by a Dielectric Wedge

Figure 4.4 shows a two-dimensional dielectric wedge of the wedge angle ϕ_w illuminated by a plane wave. For simplicity, let us assume that the incident plane wave illuminates surface OA only ($0 < \phi_0 < \phi_w - \pi$) and the observation angle is taken as $0 < \phi < 2\pi$. When the incident plane wave impinges on the illuminated surfaces of a dielectric cylinder, it excites the reflected wave at the illuminated surfaces and transmitted waves inside the wedge. In addition, the originally transmitted wave excites the internal reflected and transmitted waves $\boldsymbol{E}^t$, $\boldsymbol{H}^t$ due to the multiple bouncing effects and they radiate again from the body. Then, the contribution from the transmitted waves $\boldsymbol{E}^t$, $\boldsymbol{H}^t$ should be treated carefully, since they propagate with multiple internal bouncing in the dielectric body, then they depart from the body to all direction, as shown in Fig. 4.4. Then, the

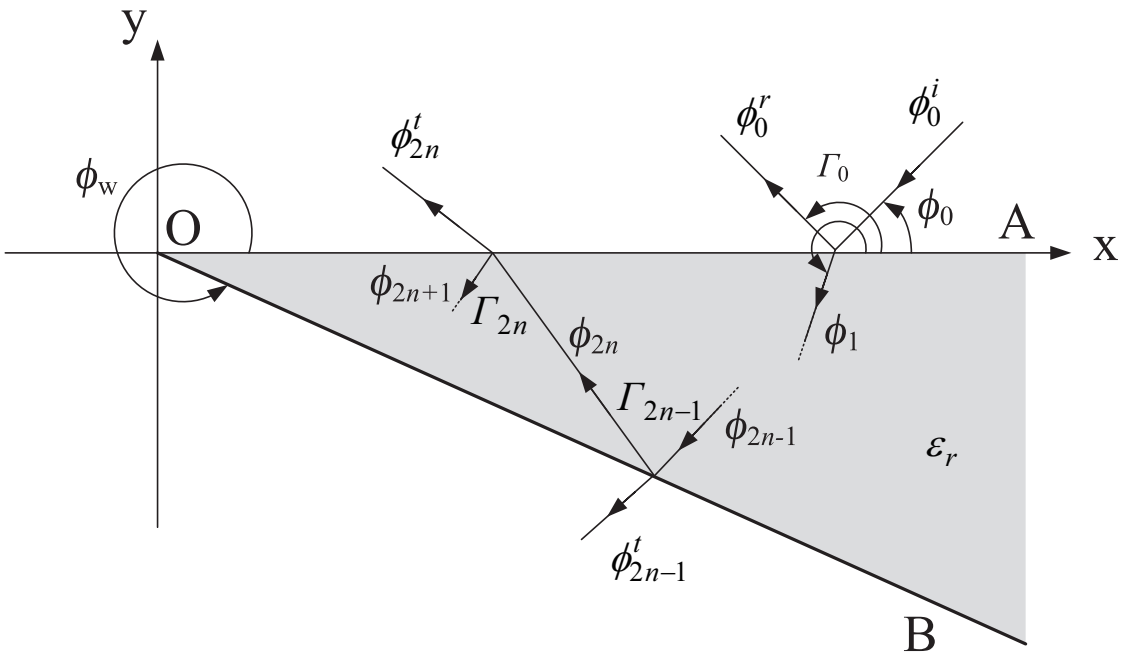

Figure 4.4: Ordinary rays traced in physical region.

total scattering field becomes

$$E_z^s = E_z^0 + \big(\text{cont. from } (\boldsymbol{E}^t, \boldsymbol{H}^t)\big), \tag{4.159}$$

$$H_z^s = H_z^0 + \big(\text{cont. from } (\boldsymbol{E}^t, \boldsymbol{H}^t)\big), \tag{4.160}$$

with E_z^0 and H_z^0 are the primary contribution derived from the reflected wave at the illuminated surface and the minus incident wave at the shadowed surface.

The scattering formulation may be separated into two polarizations.

E Polarization

When a E polarized incident plane wave impinges on the wedge's surface OA, it excites the reflected waves at illuminated surface and the transmitted wave inside the wedge. The original transmitted wave continues to experience the internal reflection and emit the outgoing transmitted waves.

At surface OA, the first reflected wave can be defined as

$$\boldsymbol{E}^r = \Gamma_0 E_0 e^{ik(x\cos\phi_0^r + y\sin\phi_0^r)}\hat{\boldsymbol{z}}, \tag{4.161}$$

$$\boldsymbol{H}^r = \Gamma_0 E_0 \sqrt{\frac{\varepsilon_0}{\mu_0}} e^{ik(x\cos\phi_0^r + y\sin\phi_0^r)}(\sin\phi_0^r\hat{\boldsymbol{x}} - \cos\phi_0^r\hat{\boldsymbol{y}}), \tag{4.162}$$

with ϕ_0^i, ϕ_0^r, ϕ_1 are the incident and reflected/transmitted angles, and Γ_0 is the reflected coefficient as

$$\phi_0^i = \pi + \phi_0, \tag{4.163}$$

$$\phi_0^r = \pi - \phi_0, \tag{4.164}$$

$$\phi_1 = \cos^{-1}\left[\frac{\cos\phi_0^i}{\sqrt{\varepsilon_r}}\right], \tag{4.165}$$

$$\Gamma_0 = \frac{\sin\phi_0 - \sqrt{\varepsilon_r - \cos^2\phi_0}}{\sin\phi_0 + \sqrt{\varepsilon_r - \cos^2\phi_0}}. \tag{4.166}$$

Comparing the reflected waves in Eqs. (4.161), (4.162) with those by conducting case in Eqs. (4.5), (4.6), the formulas of the reflected waves from the dielectric wedge have only a difference with those by conducting case at the reflection coefficient. Therefore, the contribution of the reflected waves can be obtained from Eq. (4.35) as

$$E_z^{0r} = -\Gamma_0 E_0 \frac{\sin\phi_0^r + \sin\phi}{\cos\phi_0^r - \cos\phi} C(k\rho) - \Gamma_0 E_0 e^{ikx\cos\phi_0^r + iky\sin\phi_0^r} U(\pi - \phi_0 - \phi)U(\phi) \tag{4.167}$$

Also, the contribution from the minus incident wave at the shadowed surface OB is the same as the one in Eq. (4.36)

$$\begin{aligned} E_z^{-i} = {} & E_0 \frac{\sin(\phi_0^i - \phi_w) + \sin(\phi - \phi_w)}{\cos(\phi_0^i - \phi_w) - \cos(\phi - \phi_w)} C(k\rho) \\ & - E_0 e^{ikx\cos\phi_0^i + iky\sin\phi_0^i} U(\phi + \pi - \phi_0)U(-\phi - 2\pi + \phi_w). \end{aligned} \tag{4.168}$$

The internal reflection inside the dielectric can be defined at two surfaces OA, OB, separately.

Internal Reflection at Surface OB Figure 4.5 shows the internal reflection at the surface OB. Here, ϕ_{2n-1}, ϕ_{2n} and ϕ_{2n-1}^t are the incident, reflected and outgoing transmitted angles of the $(2n-1)$-th internal reflection, respectively. Also ϕ_{2n} is the $(2n)$-th internal reflection angle. These angles and the reflected/transmitted coefficients are de-

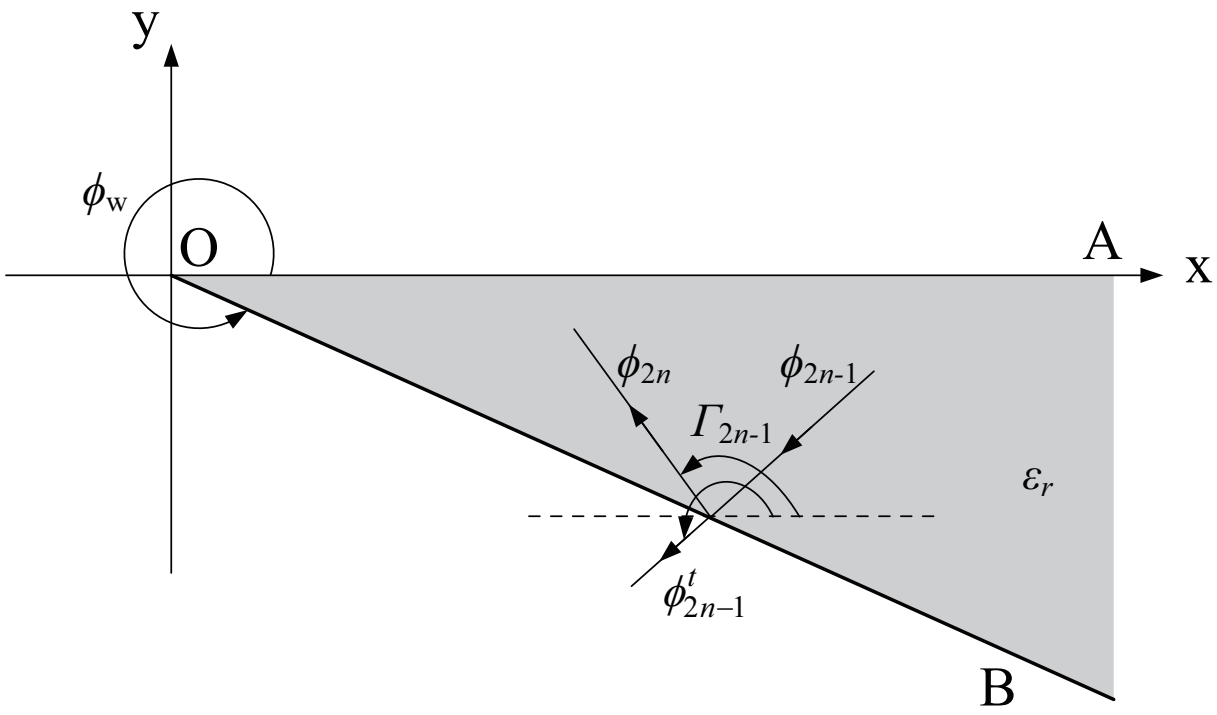

Figure 4.5: Internal reflection at surface OB.

fined as

$$\phi_{2n} = 2\phi_w - \phi_{2n-1} - 2\pi, \tag{4.169}$$

$$\phi^t_{2n-1} = \phi_w + \cos^{-1}\left[\sqrt{\varepsilon_r}\cos(\phi_{2n-1} - \phi_w)\right], \tag{4.170}$$

$$\Gamma_{2n-1} = \frac{\sin(\phi_w - \phi_{2n-1}) - \sqrt{\varepsilon_r - \cos^2(\phi_w - \phi_{2n-1})}}{\sin(\phi_w - \phi_{2n-1}) + \sqrt{\varepsilon_r - \cos^2(\phi_w - \phi_{2n-1})}}, \tag{4.171}$$

Then, the $(2n-1)$-th outgoing transmitted wave is expressed as

$$\boldsymbol{E}^{(2n-1)t} = T_{2n-1}E_0 e^{ik(x\cos\phi^t_{2n-1} + y\sin\phi^t_{2n-1})}\hat{\boldsymbol{z}}, \tag{4.172}$$

$$\boldsymbol{H}^{(2n-1)t} = T_{2n-1}E_0\sqrt{\frac{\varepsilon_0}{\mu_0}}e^{ik(x\cos\phi^t_{2n-1} + y\sin\phi^t_{2n-1})}(\sin\phi^t_{2n-1}\hat{\boldsymbol{x}} - \cos\phi^t_{2n-1}\hat{\boldsymbol{y}}), \tag{4.173}$$

and the $(2n)$-th internal reflected wave is

$$\boldsymbol{E}^{2n} = R_{2n-1}E_0 e^{ik_w(x\cos\phi_{2n} + y\sin\phi_{2n})}\hat{\boldsymbol{z}}, \tag{4.174}$$

$$\boldsymbol{H}^{2n} = R_{2n-1}E_0\sqrt{\frac{\varepsilon_0\varepsilon_r}{\mu_0}}e^{ik_w(x\cos\phi_{2n} + y\sin\phi_{2n})}(\sin\phi_{2n}\hat{\boldsymbol{x}} - \cos\phi_{2n}\hat{\boldsymbol{y}}), \tag{4.175}$$

with $k_w = k\sqrt{\varepsilon_r}$, and

$$T_{2n-1} = (1+\Gamma_0)\Gamma_1\cdots\Gamma_{2n-2}(1+\Gamma_{2n-1}), \tag{4.176}$$

$$R_{2n-1} = (1+\Gamma_0)\Gamma_1\cdots\Gamma_{2n-2}\Gamma_{2n-1}. \tag{4.177}$$

Then, the $(2n-1)$-th equivalent currents $\boldsymbol{J}_{(2n-1)t}$, $\boldsymbol{M}_{(2n-1)t}$ generated can be derived from from the $(2n-1)$-th outgoing transmitted wave as

$$\begin{aligned}
\boldsymbol{J}_{(2n-1)t} &= \hat{\boldsymbol{n}} \times \boldsymbol{H}^{(2n-1)t}\Big|_{y=x\tan\phi_w} \\
&= E_0\, T_{2n-1}\sqrt{\frac{\varepsilon_0}{\mu_0}}\sin(\phi^t_{2n-1}-\phi_w)e^{ikx(\cos\phi^t_{2n-1}+\tan\phi_w\sin\phi^t_{2n-1})}\hat{\boldsymbol{z}}, \qquad (4.178)\\
\boldsymbol{M}_{(2n-1)t} &= \boldsymbol{E}^{(2n-1)t} \times \hat{\boldsymbol{n}}\Big|_{y=x\tan\phi_w} \\
&= E_0\, T_{2n-1} e^{ikx(\cos\phi^t_{2n-1}+\tan\phi_w\sin\phi^t_{2n-1})}(\cos\phi_w\hat{\boldsymbol{x}}+\sin\phi_w\hat{\boldsymbol{y}}). \qquad (4.179)
\end{aligned}$$

The scattering field can be obtained by integrating $\boldsymbol{J}_{(2n-1)t}$, $\boldsymbol{M}_{(2n-1)t}$ with the two-dimensional Green's function G

$$\begin{aligned}
E_z^{J(2n-1)t} &= -\int_S \frac{\omega\mu_0}{4} J_{(2n-1)t}\mathrm{H}_0^{(1)}(k\sqrt{(x-x')^2+(y-y')^2})\Big|_{y'=x'\tan\phi_w} dS \\
&= -\int_0^\infty \Big[\frac{\omega\mu_0}{4}\, T_{2n-1}E_0\sqrt{\frac{\varepsilon_0}{\mu_0}}\sin(\phi^t_{2n-1}-\phi_w)e^{ikx'(\cos\phi^t_{2n-1}+\tan\phi_w\sin 2n-1^t)} \\
&\qquad \cdot\frac{1}{\pi}\int_{-\infty}^{\infty}\frac{e^{i\xi(x-x')\pm i\sqrt{k^2-\xi^2}(y-x'\tan\phi_w)}}{\sqrt{k^2-\xi^2}}\,d\xi\Big]\sqrt{1+\tan^2\phi_w}\,dx' \\
&= -T_{2n-1}E_0\frac{k}{4\pi}\frac{\sin(\phi^t_{2n-1}-\phi_w)}{\cos\phi_w} \\
&\cdot\int_{-\infty}^{\infty}\Big(\int_0^\infty e^{ix'(k\cos\phi^t_{2n-1}+k\tan\phi_w\sin\phi^t_{2n-1}-\xi\mp\sqrt{k^2-\xi^2}\tan\phi_w)}\,dx'\Big)\frac{e^{i\xi x\pm i\sqrt{k^2-\xi^2}y}}{\sqrt{k^2-\xi^2}}\,d\xi \\
&= -T_{2n-1}E_0\frac{ik}{4\pi}\frac{\sin(\phi^t_{2n-1}-\phi_w)}{\cos\phi_w} \\
&\cdot\int_{-\infty}^{\infty}\frac{e^{i\xi x\pm i\sqrt{k^2-\xi^2}y}}{(k\cos\phi^t_{2n-1}+k\tan\phi_w\sin\phi^t_{2n-1}-\xi\mp\sqrt{k^2-\xi^2}\tan\phi_w)\sqrt{k^2-\xi^2}}\,d\xi, \qquad (4.180)
\end{aligned}$$

$$
\begin{aligned}
E_z^{M(2n-1)t} &= -\int_S \frac{i}{4}(M_{(2n-1)tx}\frac{\partial}{\partial y'} - M_{(2n-1)ty}\frac{\partial}{\partial x'}) \\
&\qquad \cdot \mathrm{H}_0^{(1)}(k\sqrt{(x-x')^2+(y-y')^2})\Big|_{y'=x'\tan\phi_w} dS \\
&= \int_0^\infty \Big[\frac{1}{4\pi}\, T_{2n-1}E_0 e^{ikx'(\cos\phi_{2n-1}^t + \tan\phi_w \sin\phi_{2n-1}^t)} \int_{-\infty}^{\infty} e^{i\xi(x-x')\pm i\sqrt{k^2-\xi^2}(y-x'\tan\phi_w)} \\
&\qquad \cdot\Big(\mp\cos\phi_w + \sin\phi_w \frac{\xi}{\sqrt{k^2-\xi^2}}\, d\xi\Big)\Big] \sqrt{1+\tan^2\phi_w}\, dx' \\
&= \mp\frac{T_{2n-1}E_0}{4\pi} \int_{-\infty}^{\infty} \Big(\int_0^\infty e^{ix'(k\cos\phi_{2n-1}^t + k\tan\phi_w \sin\phi_{2n-1}^t - \xi \mp \sqrt{k^2-\xi^2}\tan\phi_w)}\, dx'\Big) \\
&\qquad \cdot\Big(e^{i\xi x\pm i\sqrt{k^2-\xi^2}y}\, d\xi \mp \frac{\sin\phi_w}{\cos\phi_w}\frac{\xi e^{i\xi x\pm i\sqrt{k^2-\xi^2}y}}{\sqrt{k^2-\xi^2}}\Big)\, d\xi \\
&= \mp\frac{i}{4\pi}\, T_{2n-1}E_0 \int_{-\infty}^{\infty} \frac{e^{i\xi x\pm i\sqrt{k^2-\xi^2}y}}{k\cos\phi_{2n-1} + k\tan\phi_w \sin\phi_{2n-1}^t - \xi \mp \sqrt{k^2-\xi^2}\tan\phi_w} \\
&\qquad \cdot\Big(1 \pm \frac{\sin\phi_w}{\cos\phi_w}\frac{\xi}{\sqrt{k^2-\xi^2}}\Big)\, d\xi, \qquad (y \gtrless x'\tan\phi_w).
\end{aligned} \tag{4.181}
$$

Converting to complex angle w plane using the transformation $\xi = k\sin w$, with the cylindrical coordinates (ρ,θ) with $x = \rho\cos\phi, y = \rho\sin\phi$, Eqs. (4.180), (4.181) can be expressed as

$$
\begin{aligned}
E_z^{J(2n-1)t} &= -T_{2n-1}E_0 \frac{ik}{4\pi}\frac{\sin(\phi_{2n-1}^t - \phi_w)}{\cos\phi_w} \\
&\cdot \int_C \frac{e^{ik\rho(\cos\phi\sin w \pm \sin\phi\cos w)}}{(k\cos\phi_{2n-1}^t + k\tan\phi_w\sin\phi_{2n-1}^t - k\sin w \mp k\cos w\tan\phi_w)k\cos w} k\cos w\, dw \\
&= -\frac{i}{4\pi}\, T_{2n-1}E_0 \int_C \frac{\sin(\phi_{2n-1}^t - \phi_w)}{\cos(\phi_{2n-1}^t - \phi_w) - \sin(w\pm\phi_w)} e^{ik\rho(\sin(w\pm\phi)}\, dw,
\end{aligned} \tag{4.182}
$$

$$
\begin{aligned}
E_z^{M(2n-1)t} &= \mp\frac{i}{4\pi}\int_C \frac{e^{ik\rho(\cos\phi\sin w \pm \sin\phi\cos w)}}{(k\cos\phi_{2n-1}^t + k\tan\phi_w\sin\phi_{2n-1}^t - k\sin w \pm k\cos w\tan\phi_w)} \\
&\qquad \cdot T_{2n-1}E_0\Big(1 \pm \frac{\sin\phi_w}{\cos\phi_w}\frac{k\sin w}{k\cos w}\Big) k\cos w\, dw \\
&= \mp\frac{i}{4\pi}\, T_{2n-1}E_0 \int_C \frac{\cos(w\pm\phi_w)}{\cos(\phi_{2n-1}^t - \phi_w) - \sin(w\pm\phi_w)} e^{ik\rho(\sin(w\pm\phi)}\, dw.
\end{aligned} \tag{4.183}
$$

Then, the contribution of the $(2n-1)$-th transmitted wave is the summation of the radiations from the currents $\boldsymbol{J}_{(2n-1)t}$, $\boldsymbol{M}_{(2n-1)t}$

$$
\begin{aligned}
E_z^{(2n-1)t} &= E_z^{J(2n-1)t} + E_z^{M(2n-1)t} \\
&= -T_{2n-1}E_0\frac{i}{4\pi}\int_C \frac{\sin(\phi_{2n-1}^t - \phi_w) \pm \cos(w\pm\phi_w)}{\cos(\phi_{2n-1}^t - \phi_w) - \sin(w\pm\phi_w)} e^{ik\rho(\sin(w\pm\phi)}\, dw.
\end{aligned} \tag{4.184}
$$

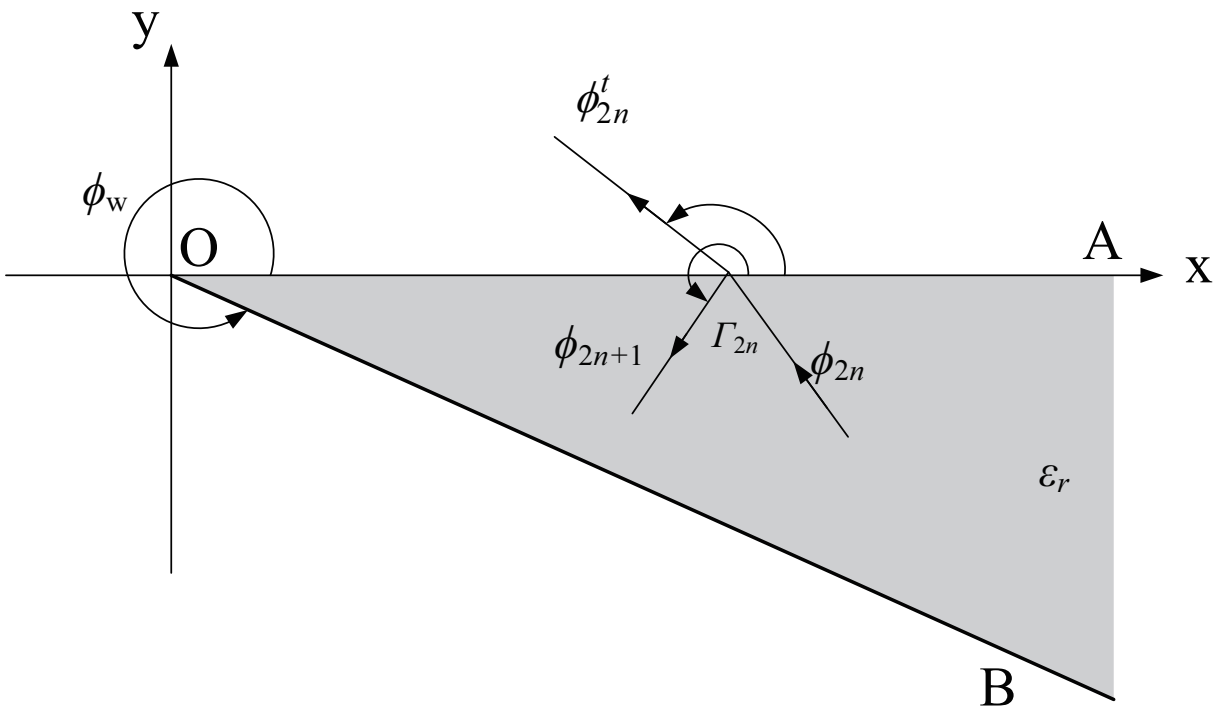

Figure 4.6: Internal reflection at surface OA.

Using saddle point method with $w_s = \pi/2 \mp \phi$, then Eq. (4.184) becomes

$$E_z^{(2n-1)t} = -T_{2n-1}E_0\frac{\sin(\phi_{2n-1}^t - \phi_w) + \sin(\phi - \phi_w)}{\cos(\phi_{2n-1}^t - \phi_w) - \cos(\phi - \phi_w)}C(k\rho) + T_{2n-1}E_0 e^{ikx\cos\phi_{2n-1}^t + iky\sin\phi_{2n-1}^t}U(\phi + \pi - \phi_0)U(-\phi - 2\pi + \phi_w). \quad (4.185)$$

Internal Reflection at Surface OA Figure 4.6 shows the internal reflection at the surface OA. Here, ϕ_{2n}, ϕ_{2n+1} and ϕ_{2n}^t are the incident, reflected and outgoing transmitted angles of the $(2n)$-th internal reflection, respectively. Also ϕ_{2n+1} is the $(2n+1)$-th internal reflection angle. These angles and the reflected/transmitted coefficients are defined as

$$\phi_{2n+1} = 2\pi - \phi_{2n}, \quad (4.186)$$

$$\phi_{2n}^t = \cos^{-1}\left[\sqrt{\varepsilon_r}\cos\phi_{2n}\right], \quad (4.187)$$

$$\Gamma_{2n} = \frac{\sin\phi_{2n} - \sqrt{\varepsilon_r - \cos^2\phi_{2n}}}{\sin\phi_{2n} + \sqrt{\varepsilon_r - \cos^2\phi_{2n}}}, \quad (4.188)$$

Then, the $(2n)$-th outgoing transmitted wave is expressed as

$$\boldsymbol{E}^{(2n)t} = T_{2n}E_0 e^{ik(x\cos\phi_{2n}^t + y\sin\phi_{2n}^t)}\hat{\boldsymbol{z}}, \quad (4.189)$$

$$\boldsymbol{H}^{(2n)t} = T_{2n}E_0\sqrt{\frac{\varepsilon_0}{\mu_0}}e^{ik(x\cos\phi_{2n}^t + y\sin\phi_{2n}^t)}(\sin\phi_{2n}^t\hat{\boldsymbol{x}} - \cos\phi_{2n}^t\hat{\boldsymbol{y}}), \quad (4.190)$$

and the $(2n+1)$-th internal reflected wave is

$$\boldsymbol{E}^{(2n+1)r} = R_{2n}E_0 e^{ik_w(x\cos\phi_{2n+1}+y\sin\phi_{2n+1})}\hat{\boldsymbol{z}}, \tag{4.191}$$

$$\boldsymbol{H}^{(2n+1)r} = R_{2n}E_0\sqrt{\frac{\varepsilon_0\varepsilon_r}{\mu_0}}e^{ik(x\cos\phi_{2n+1}+y\sin\phi_{2n+1})}(\sin\phi_{2n+1}\hat{\boldsymbol{x}} - \cos\phi_{2n+1}\hat{\boldsymbol{y}}), \tag{4.192}$$

with

$$T_{2n} = (1+\Gamma_0)\Gamma_1\cdots\Gamma_{2n-1}(1+\Gamma_{2n}), \tag{4.193}$$

$$R_{2n} = (1+\Gamma_0)\Gamma_1\cdots\Gamma_{2n-1}\Gamma_{2n}. \tag{4.194}$$

Then, the $(2n)$-th equivalent currents $\boldsymbol{J}_{(2n)t}$, $\boldsymbol{M}_{(2n)t}$ generated can be derived from from the $(2n)$-th outgoing transmitted wave as

$$\boldsymbol{J}_{(2n)t} = \hat{\boldsymbol{y}}\times\boldsymbol{H}^{(2n)t}\Big|_{y=0} = T_{2n}E_0\sqrt{\frac{\varepsilon_0}{\mu_0}}\sin\phi^t_{2n}e^{ikx\cos\phi^t_{2n}}\hat{\boldsymbol{z}}, \tag{4.195}$$

$$\boldsymbol{M}_{(2n)t} = \boldsymbol{E}^{(2n)t}\times\hat{\boldsymbol{y}}\Big|_{y=0} = T_{2n}E_0 e^{ikx\cos\phi^t_{2n}}\hat{\boldsymbol{x}}, \tag{4.196}$$

The scattering field can be obtained by integrating $\boldsymbol{J}_{(2n)t}$, $\boldsymbol{M}_{(2n)t}$ with two-dimensional Green's function G as

$$\begin{aligned}
E_z^{J(2n)t} &= -\int_S \frac{\omega\mu_0}{4}J_{(2n)t}\mathrm{H}_0^{(1)}(k\sqrt{(x-x')^2+(y-y')^2})\Big|_{y'=0}\,dS \\
&= -\int_0^\infty\Big[\frac{\omega\mu_0}{4}T_{2n}E_0\sqrt{\frac{\varepsilon_0}{\mu_0}}\sin\phi^t_{2n}e^{ikx'\cos\phi^t_{2n}}\frac{1}{\pi}\int_{-\infty}^\infty\frac{e^{i\xi(x-x')\pm i\sqrt{k^2-\xi^2}y}}{\sqrt{k^2-\xi^2}}\,d\xi\Big]\,dx' \\
&= -T_{2n}E_0\frac{k}{4\pi}\sin\phi^t_{2n}\int_{-\infty}^\infty\Big(\int_0^\infty e^{ix'(k\cos\phi^t_{2n}-\xi)}\,dx'\Big)\frac{e^{i\xi x\pm i\sqrt{k^2-\xi^2}y}}{\sqrt{k^2-\xi^2}}\,d\xi \\
&= -T_{2n}E_0\frac{ik}{4\pi}\sin\phi^t_{2n}\int_{-\infty}^\infty\frac{e^{i\xi x\pm i\sqrt{k^2-\xi^2}y}}{(k\cos\phi^t_{2n}-\xi)\sqrt{k^2-\xi^2}}\,d\xi,
\end{aligned} \tag{4.197}$$

$$\begin{aligned}
E_z^{M(2n)t} &= -\int_S\frac{i}{4}M_{(2n)tx}\frac{\partial}{\partial y'}\mathrm{H}_0^{(1)}(k\sqrt{(x-x')^2+(y-y')^2})\Big|_{y'=x'\tan\phi_w}\,dS \\
&= \mp\int_0^\infty\frac{1}{4\pi}T_{2n}E_0e^{ikx'\cos\phi^t_{2n}}\int_{-\infty}^\infty e^{i\xi(x-x')\pm i\sqrt{k^2-\xi^2}y}\,d\xi\,dx' \\
&= \mp\frac{T_{2n}E_0}{4\pi}\int_{-\infty}^\infty\Big(\int_0^\infty e^{ix'(k\cos\phi^t_{2n}-\xi)}\,dx'\Big)e^{i\xi x\pm i\sqrt{k^2-\xi^2}y}\,d\xi \\
&= \mp\frac{i}{4\pi}T_{2n}E_0\int_{-\infty}^\infty\frac{e^{i\xi x\pm i\sqrt{k^2-\xi^2}y}}{k\cos\phi^t_{2n}-\xi}\,d\xi, \qquad (y\gtrless 0).
\end{aligned} \tag{4.198}$$

Converting to complex angle w plane using the transformation $\xi = k\sin w$, with the cylindrical coordinates (ρ,θ) with $x=\rho\cos\phi, y=\rho\sin\phi$, Eqs. (4.197), (4.198) can be

expressed as

$$E_z^{J(2n)t} = -T_{2n}E_0\frac{ik}{4\pi}\sin\phi_{2n}^t\int_C \frac{e^{ik\rho(\cos\phi\sin w\pm\sin\phi\cos w)}}{(k\cos\phi_{2n}^t - k\sin w)k\cos w}k\cos w\,dw$$
$$= -T_{2n}E_0\frac{i}{4\pi}\int_C \frac{\sin\phi_{2n}^t}{\cos\phi_{2n}^t - \sin w}e^{ik\rho(\sin(w\pm\phi)}\,dw, \tag{4.199}$$

$$E_z^{M(2n)t} = \mp T_{2n}E_0\frac{i}{4\pi}\int_C \frac{e^{ik\rho(\cos\phi\sin w\pm\sin\phi\cos w)}}{(k\cos\phi_{2n}^t - k\sin w)}k\cos w\,dw$$
$$= \mp T_{2n}E_0\frac{i}{4\pi}\int_C \frac{\cos w}{\cos\phi_{2n}^t - \sin w}e^{ik\rho(\sin(w\pm\phi)}\,dw. \tag{4.200}$$

Then, the contribution of the $(2n)$-th transmitted wave is the summation of the radiations from the currents $\boldsymbol{J}_{(2n)t}$, $\boldsymbol{M}_{(2n)t}$

$$E_z^{(2n)t} = E_z^{J(2n)t} + E_z^{M(2n)t} = -T_{2n}E_0\frac{i}{4\pi}\int_C \frac{\sin\phi_{2n}^t \pm \cos w}{\cos\phi_{2n}^t - \sin w}e^{ik\rho(\sin(w\pm\phi)}\,dw. \tag{4.201}$$

Using saddle point method with $w_s = \pi/2 \mp \phi$, Eq. (4.201) becomes

$$E_z^{(2n)t} = -T_{2n}E_0\frac{\sin\phi_{2n}^t + \sin\phi}{\cos\phi_{2n}^t - \cos\phi}C(k\rho)$$
$$+ T_{2n-1}E_0e^{ikx\cos\phi_{2n}^t + iky\sin\phi_{2n}^t}U(\pi - \phi_0 - \phi)U(\phi) \tag{4.202}$$

Then, the scattering field outside the dielectric wedge is defined as in Eq. (4.159)

$$E_z^s = E_z^{0r} + E_z^{-i} + \sum_1^N E_z^{(n)t}. \tag{4.203}$$

with N is the number of internal reflections.

H Polarization

When a H polarized incident plane wave impinges on the wedge's surface OA, it excites the reflected waves at illuminated surface and the transmitted wave inside the wedge. The original transmitted wave continues to experience the internal reflection and emit the outgoing transmitted waves.

At surface OA, the first reflected wave can be defined as

$$\boldsymbol{H}^r = \bar{\Gamma}_0 H_0 e^{ik(x\cos\phi_0^r + y\sin\phi_0^r)}\hat{\boldsymbol{z}}, \tag{4.204}$$
$$\boldsymbol{E}^r = \bar{\Gamma}_0 H_0\sqrt{\frac{\varepsilon_0}{\mu_0}}e^{ik(x\cos\phi_0^r + y\sin\phi_0^r)}(-\sin\phi_0^r\hat{\boldsymbol{x}} + \cos\phi_0^r\hat{\boldsymbol{y}}). \tag{4.205}$$

with ϕ_0^i, ϕ_0^r, ϕ_1 are the incident and reflected/transmitted angles, and $\bar{\Gamma}_0$ is the reflected coefficient as

$$\phi_0^i = \pi + \phi_0, \tag{4.206}$$

$$\phi_0^r = \pi - \phi_0, \tag{4.207}$$

$$\phi_1 = \cos^{-1}\left[\frac{\cos\phi_0^i}{\sqrt{\varepsilon_r}}\right], \tag{4.208}$$

$$\bar{\Gamma}_0 = \frac{-\sqrt{\varepsilon_r}\sin\phi_0 + \sqrt{\varepsilon_r - \cos^2\phi_0}}{\sqrt{\varepsilon_r}\sin\phi_0 + \sqrt{\varepsilon_r - \cos^2\phi_0}}. \tag{4.209}$$

Comparing the reflected waves in Eqs. (4.161), (4.162) with those by conducting case in Eqs. (4.41), (4.42), the formulas of the reflected waves from the dielectric wedge have only a difference with those by conducting case at the reflection coefficient. Then, the contribution of the reflected waves can be given as in Eq. (4.55),

$$H_z^{0r} = \bar{\Gamma}_0 H_0 \frac{\sin\phi_0^r + \sin\phi}{\cos\phi_0^r - \cos\phi} C(k\rho) + \bar{\Gamma}_0 H_0 e^{ikx\cos\phi_0^r + iky\sin\phi_0^r} U(\pi - \phi_0 - \phi)U(\phi), \tag{4.210}$$

Also, the contribution from the minus incident wave at the shadowed surface OB is

$$\begin{aligned} H_z^{-i} = &-H_0 \frac{\sin(\phi_0^i - \phi_w) + \sin(\phi - \phi_w)}{\cos(\phi_0^i - \phi_w) - \cos(\phi - \phi_w)} C(k\rho) \\ &- H_0 e^{ikx\cos\phi_0^i + iky\sin\phi_0^i} U(\phi + \pi - \phi_0)U(-\phi - 2\pi + \phi_w). \end{aligned} \tag{4.211}$$

The internal reflection inside the dielectric can be defined at two surfaces OA, OB, separately.

Internal Reflection at Surface OB Figure 4.5 shows the internal reflection at the surface OB. Here, ϕ_{2n-1}, ϕ_{2n} and ϕ_{2n-1}^t are the incident, reflected and outgoing transmitted angles of the $(2n-1)$-th internal reflection, respectively. Also ϕ_{2n} is the $(2n)$-th internal reflection angle. These angles and the reflected/transmitted coefficients are defined as

$$\phi_{2n} = 2\phi_w - \phi_{2n-1} - 2\pi, \tag{4.212}$$

$$\phi_{2n-1}^t = \phi_w + \cos^{-1}\left[\sqrt{\varepsilon_r}\cos(\phi_{2n-1} - \phi_w)\right], \tag{4.213}$$

$$\bar{\Gamma}_{2n-1} = \frac{-\sin(\phi_w - \phi_{2n-1}) + \sqrt{\varepsilon_r - \varepsilon_r^2\sin^2(\phi_w - \phi_{2n-1})}}{\sin(\phi_w - \phi_{2n-1}) + \sqrt{\varepsilon_r - \varepsilon_r^2\sin^2(\phi_w - \phi_{2n-1})}}, \tag{4.214}$$

Then, the $(2n-1)$-th outgoing transmitted wave is expressed as

$$\boldsymbol{H}^{(2n-1)t} = \bar{T}_{2n-1} H_0 e^{ik(x\cos\phi_{2n-1}^t + y\sin\phi_{2n-1}^t)}\hat{\boldsymbol{z}}, \tag{4.215}$$

$$\boldsymbol{E}^{(2n-1)t} = \bar{T}_{2n-1} H_0 \sqrt{\frac{\mu_0}{\varepsilon_0}} e^{ik(x\cos\phi_{2n-1}^t + y\sin\phi_{2n-1}^t)}(-\sin\phi_{2n-1}^t\hat{\boldsymbol{x}} + \cos\phi_{2n-1}^t\hat{\boldsymbol{y}}), \tag{4.216}$$

and the $(2n)$-th internal reflected wave is

$$\boldsymbol{H}^{2n} = \bar{R}_{2n-1} H_0 e^{ik_w\sqrt{\varepsilon_r}(x\cos\phi_{2n}+y\sin\phi_{2n})}\hat{\boldsymbol{z}}, \tag{4.217}$$

$$\boldsymbol{E}^{2n} = \bar{R}_{2n-1} H_0 \sqrt{\frac{\mu_0}{\varepsilon_0\varepsilon_r}} e^{ik_w(x\cos\phi_{2n}+y\sin\phi_{2n})}(-\sin\phi_{2n}\hat{\boldsymbol{x}} + \cos\phi_{2n}\hat{\boldsymbol{y}}), \tag{4.218}$$

with $k_w = k\sqrt{\varepsilon_r}$, and

$$\bar{T}_{2n-1} = (1-\bar{\Gamma}_0)\bar{\Gamma}_1\cdots\bar{\Gamma}_{2n-2}(1-\bar{\Gamma}_{2n-1}), \tag{4.219}$$

$$\bar{R}_{2n-1} = (1-\bar{\Gamma}_0)/\sqrt{\varepsilon_r}\bar{\Gamma}_1\cdots\bar{\Gamma}_{2n-2}\bar{\Gamma}_{2n-1}. \tag{4.220}$$

Then, the $(2n-1)$-th equivalent currents $\boldsymbol{J}_{(2n-1)t}$, $\boldsymbol{M}_{(2n-1)t}$ generated can be derived from from the $(2n-1)$-th outgoing transmitted wave as

$$\begin{aligned}\boldsymbol{J}_{(2n-1)t} &= \hat{\boldsymbol{n}} \times \boldsymbol{H}^{(2n-1)t}\Big|_{y=x\tan\phi_w} \\ &= H_0\bar{T}_{2n-1}e^{ikx(\cos\phi^t_{2n-1}+\tan\phi_w\sin\phi^t_{2n-1})}(\cos\phi_w\hat{\boldsymbol{x}}+\sin\phi_w\hat{\boldsymbol{y}}), \qquad (4.221)\\ \boldsymbol{M}_{(2n-1)t} &= \boldsymbol{E}^{(2n-1)t}\times\hat{\boldsymbol{n}}\Big|_{y=x\tan\phi_w} \\ &= -H_0\bar{T}_{2n-1}\sqrt{\frac{\mu_0}{\varepsilon_0}}\sin(\phi^t_{2n-1}-\phi_w)e^{ikx(\cos\phi^t_{2n-1}+\tan\phi_w\sin\phi^t_{2n-1})}\hat{\boldsymbol{z}}. \qquad (4.222)\end{aligned}$$

The scattering field can be obtained by integrating $\boldsymbol{J}_{(2n-1)t}$, $\boldsymbol{M}_{(2n-1)t}$ with the two-dimensional Green's function G as

$$\begin{aligned}H_z^{J(2n-1)t} &= \int_S \frac{i}{4}(J_{(2n-1)tx}\frac{\partial}{\partial y'} - J_{(2n-1)ty}\frac{\partial}{\partial x'})\mathrm{H}_0^{(1)}(k\sqrt{(x-x')^2+(y-y')^2})\Big|_{y'=x'\tan\phi_w} dS \\
&= \int_0^\infty \Big[\frac{1}{4\pi}\bar{T}_{2n-1}H_0 e^{ikx'(\cos\phi^t_{2n-1}+\tan\phi_w\sin\phi^t_{2n-1})}\int_{-\infty}^{\infty} e^{i\xi(x-x')\pm i\sqrt{k^2-\xi^2}(y-x'\tan\phi_w)} \\
&\quad\cdot\Big(\pm\cos\phi_w - \sin\phi_w\frac{\xi}{\sqrt{k^2-\xi^2}}\,d\xi\Big)\Big]\sqrt{1+\tan^2\phi_w}\,dx' \\
&= \pm\frac{\bar{T}_{2n-1}H_0}{4\pi}\int_{-\infty}^{\infty}\Big(\int_0^\infty e^{ix'(k\cos\phi^t_{2n-1}+k\tan\phi_w\sin\phi^t_{2n-1}-\xi\mp\sqrt{k^2-\xi^2}\tan\phi_w)}\,dx'\Big) \\
&\quad\cdot\Big(e^{i\xi x\pm i\sqrt{k^2-\xi^2}y}\,d\xi \mp \frac{\sin\phi_w}{\cos\phi_w}\frac{\xi e^{i\xi x\pm i\sqrt{k^2-\xi^2}y}}{\sqrt{k^2-\xi^2}}\Big)\,d\xi \\
&= \pm\frac{i}{4\pi}\bar{T}_{2n-1}H_0\int_{-\infty}^{\infty}\frac{e^{i\xi x\pm i\sqrt{k^2-\xi^2}y}}{k\cos\phi_{2n-1}+k\tan\phi_w\sin\phi^t_{2n-1}-\xi\mp\sqrt{k^2-\xi^2}\tan\phi_w} \\
&\quad\cdot\Big(1\pm\frac{\sin\phi_w}{\cos\phi_w}\frac{\xi}{\sqrt{k^2-\xi^2}}\Big)\,d\xi, \qquad (y\gtrless x'\tan\phi_w), \qquad (4.223)\end{aligned}$$

$$
\begin{aligned}
H_z^{M(2n-1)t} &= -\int_S \frac{\omega\varepsilon_0}{4} M_{(2n-1)t} \mathrm{H}_0^{(1)}(k\sqrt{(x-x')^2+(y-y')^2})\Big|_{y'=x'\tan\phi_w} dS \\
&= \int_0^\infty \Big[\frac{\omega\varepsilon_0}{4}\bar{T}_{2n-1}H_0\sqrt{\frac{\mu_0}{\varepsilon_0}}\sin(\phi_{2n-1}^t-\phi_w)e^{ikx'(\cos\phi_{2n-1}^t+\tan\phi_w\sin\phi_{2n-1}^t)} \\
&\qquad \cdot\frac{1}{\pi}\int_{-\infty}^\infty \frac{e^{i\xi(x-x')\pm i\sqrt{k^2-\xi^2}(y-x'\tan\phi_w)}}{\sqrt{k^2-\xi^2}}\,d\xi\Big]\sqrt{1+\tan^2\phi_w}\,dx' \\
&= \bar{T}_{2n-1}H_0\frac{k}{4\pi}\frac{\sin(\phi_{2n-1}^t-\phi_w)}{\cos\phi_w} \\
&\cdot\int_{-\infty}^\infty\Big(\int_0^\infty e^{ix'(k\cos\phi_{2n-1}^t+k\tan\phi_w\sin\phi_{2n-1}^t-\xi\mp\sqrt{k^2-\xi^2}\tan\phi_w)}\,dx'\Big)\frac{e^{i\xi x\pm i\sqrt{k^2-\xi^2}y}}{\sqrt{k^2-\xi^2}}\,d\xi \\
&= \bar{T}_{2n-1}H_0\frac{ik}{4\pi}\frac{\sin(\phi_{2n-1}^t-\phi_w)}{\cos\phi_w} \\
&\cdot\int_{-\infty}^\infty \frac{e^{i\xi x\pm i\sqrt{k^2-\xi^2}y}}{(k\cos\phi_{2n-1}^t+k\tan\phi_w\sin\phi_{2n-1}^t-\xi\mp\sqrt{k^2-\xi^2}\tan\phi_w)\sqrt{k^2-\xi^2}}\,d\xi. \quad (4.224)
\end{aligned}
$$

Converting to complex angle w plane using the transformation $\xi = k\sin w$, with the cylindrical coordinates (ρ,θ) with $x=\rho\cos\phi, y=\rho\sin\phi$, Eqs. (4.223), (4.224) can be expressed as

$$
\begin{aligned}
H_z^{J(2n-1)t} &= \pm\frac{i}{4\pi}\int_C \frac{e^{ik\rho(\cos\phi\sin w\pm\sin\phi\cos w)}}{(k\cos\phi_{2n-1}^t+k\tan\phi_w\sin\phi_{2n-1}^t-k\sin w\pm k\cos w\tan\phi_w)} \\
&\qquad\cdot\bar{T}_{2n-1}H_0\Big(1\pm\frac{\sin\phi_w}{\cos\phi_w}\frac{k\sin w}{k\cos w}\Big)k\cos w\,dw \\
&= \pm\frac{i}{4\pi}\bar{T}_{2n-1}H_0\int_C\frac{\cos(w\pm\phi_w)}{\cos(\phi_{2n-1}^t-\phi_w)-\sin(w\pm\phi_w)}e^{ik\rho(\sin(w\pm\phi)}\,dw, \quad (4.225) \\
H_z^{M(2n-1)t} &= \bar{T}_{2n-1}H_0\frac{ik}{4\pi}\frac{\sin(\phi_{2n-1}^t-\phi_w)}{\cos\phi_w} \\
&\cdot\int_C\frac{e^{ik\rho(\cos\phi\sin w\pm\sin\phi\cos w)}}{(k\cos\phi_{2n-1}^t+k\tan\phi_w\sin\phi_{2n-1}^t-k\sin w\mp k\cos w\tan\phi_w)k\cos w}k\cos w\,dw \\
&= \frac{i}{4\pi}\bar{T}_{2n-1}H_0\int_C\frac{\sin(\phi_{2n-1}^t-\phi_w)}{\cos(\phi_{2n-1}^t-\phi_w)-\sin(w\pm\phi_w)}e^{ik\rho(\sin(w\pm\phi)}\,dw. \quad (4.226)
\end{aligned}
$$

Then, the contribution of the $(2n-1)$-th transmitted wave is the summation of the radiations from the currents $\boldsymbol{J}_{(2n-1)t}$, $\boldsymbol{M}_{(2n-1)t}$

$$
\begin{aligned}
H_z^{(2n-1)t} &= H_z^{J(2n-1)t}+H_z^{M(2n-1)t} \\
&= \bar{T}_{2n-1}H_0\frac{i}{4\pi}\int_C\frac{\sin(\phi_{2n-1}^t-\phi_w)\pm\cos(w\pm\phi_w)}{\cos(\phi_{2n-1}^t-\phi_w)-\sin(w\pm\phi_w)}e^{ik\rho(\sin(w\pm\phi)}\,dw \\
&= \bar{T}_{2n-1}H_0\frac{\sin(\phi_{2n-1}^t-\phi_w)+\sin(\phi-\phi_w)}{\cos(\phi_{2n-1}^t-\phi_w)-\cos(\phi-\phi_w)}C(k\rho) \\
&\quad +\bar{T}_{2n-1}H_0e^{ikx\cos\phi_{2n-1}^t+iky\sin\phi_{2n-1}^t}U(\phi+\pi-\phi_0)U(-\phi-2\pi+\phi_w). \quad (4.227)
\end{aligned}
$$

Internal Reflection at Surface OA Figure 4.6 shows the internal reflection at the surface OA. Here, ϕ_{2n}, ϕ_{2n+1} and ϕ^t_{2n} are the incident, reflected and outgoing transmitted angles of the $(2n)$-th internal reflection, respectively. Also ϕ_{2n+1} is the $(2n+1)$-th internal reflection angle. These angles and the reflected/transmitted coefficients are defined as

$$\phi_{2n+1} = 2\pi - \phi_{2n}, \tag{4.228}$$

$$\phi^t_{2n} = \cos^{-1}\left[\sqrt{\varepsilon_r}\cos\phi_{2n}\right], \tag{4.229}$$

$$\bar{\Gamma}_{2n} = \frac{-\sin\phi_{2n-1} + \sqrt{\varepsilon_r - \varepsilon_r^2\cos^2\phi_{2n}}}{\sin\phi_{2n} + \sqrt{\varepsilon_r - \varepsilon_r^2\cos^2\phi_{2n}}}, \tag{4.230}$$

Then, the $(2n)$-th outgoing transmitted wave is expressed as

$$\boldsymbol{E}^{(2n)t} = \bar{T}_{2n}H_0 e^{ik(x\cos\phi^t_{2n} + y\sin\phi^t_{2n})}\hat{\boldsymbol{z}}, \tag{4.231}$$

$$\boldsymbol{H}^{(2n)t} = \bar{T}_{2n}H_0\sqrt{\frac{\varepsilon_0}{\mu_0}}e^{ik(x\cos\phi^t_{2n} + y\sin\phi^t_{2n})}(\sin\phi^t_{2n}\hat{\boldsymbol{x}} - \cos\phi^t_{2n}\hat{\boldsymbol{y}}), \tag{4.232}$$

and the $(2n+1)$-th internal reflected wave is

$$\boldsymbol{E}^{(2n+1)r} = \bar{R}_{2n}H_0 e^{ik_w(x\cos\phi_{2n+1} + y\sin\phi_{2n+1})}\hat{\boldsymbol{z}}, \tag{4.233}$$

$$\boldsymbol{H}^{(2n+1)r} = \bar{R}_{2n}H_0\sqrt{\frac{\varepsilon_0\varepsilon_r}{\mu_0}}e^{ik(x\cos\phi_{2n+1} + y\sin\phi_{2n+1})}(\sin\phi_{2n+1}\hat{\boldsymbol{x}} - \cos\phi_{2n+1}\hat{\boldsymbol{y}}), \tag{4.234}$$

with

$$\bar{T}_{2n} = (1-\bar{\Gamma}_0)\bar{\Gamma}_1\cdots\Gamma_{2n-1}(1-\bar{\Gamma}_{2n}), \tag{4.235}$$

$$\bar{R}_{2n} = (1-\bar{\Gamma}_0)/\sqrt{\varepsilon_r}\bar{\Gamma}_1\cdots\bar{\Gamma}_{2n-1}\bar{\Gamma}_{2n}. \tag{4.236}$$

Then, the $(2n)$-th equivalent currents $\boldsymbol{J}_{(2n)t}$, $\boldsymbol{M}_{(2n)t}$ generated can be derived from from the $(2n)$-th outgoing transmitted wave as

$$\boldsymbol{J}_{(2n)t} = \hat{\boldsymbol{y}} \times \boldsymbol{H}^{(2n)t}\Big|_{y=0} = \bar{T}_{2n}H_0 e^{ikx\cos\phi^t_{2n}}\hat{\boldsymbol{x}}, \tag{4.237}$$

$$\boldsymbol{M}_{(2n)t} = \boldsymbol{E}^{(2n)t} \times \hat{\boldsymbol{y}}\Big|_{y=0} = -\bar{T}_{2n}H_0\sqrt{\frac{\varepsilon_0}{\mu_0}}\sin\phi^t_{2n}e^{ikx\cos\phi^t_{2n}}\hat{\boldsymbol{z}}, \tag{4.238}$$

The scattering field can be obtained by integrating $\boldsymbol{J}_{(2n)t}$, $\boldsymbol{M}_{(2n)t}$ with the two-dimensional Green's function G as

$$
\begin{aligned}
H_z^{J(2n)t} &= \int_S \frac{i}{4} J_{(2n)tx} \frac{\partial}{\partial y'} \mathrm{H}_0^{(1)}(k\sqrt{(x-x')^2+(y-y')^2})\Big|_{y'=x'\tan\phi_w} dS \\
&= \pm \int_0^\infty \frac{1}{4\pi} \bar{T}_{2n} H_0 e^{ikx'\cos\phi_{2n}^t} \int_{-\infty}^\infty e^{i\xi(x-x')\pm i\sqrt{k^2-\xi^2}y}\, d\xi\, dx' \\
&= \pm \frac{\bar{T}_{2n} H_0}{4\pi} \int_{-\infty}^\infty \Big(\int_0^\infty e^{ix'(k\cos\phi_{2n}^t-\xi)}\, dx' \Big) e^{i\xi x\pm i\sqrt{k^2-\xi^2}y}\, d\xi \\
&= \pm \frac{i}{4\pi} \bar{T}_{2n} H_0 \int_{-\infty}^\infty \frac{e^{i\xi x\pm i\sqrt{k^2-\xi^2}y}}{k\cos\phi_{2n}^t-\xi}\, d\xi, \qquad (y \gtrless 0), \qquad (4.239) \\
H_z^{M(2n)t} &= -\int_S \frac{\omega\mu_0}{4} M_{(2n)t} \mathrm{H}_0^{(1)}(k\sqrt{(x-x')^2+(y-y')^2})\Big|_{y'=0} dS \\
&= \int_0^\infty \Big[\frac{\omega\mu_0}{4} \bar{T}_{2n} H_0 \sqrt{\frac{\varepsilon_0}{\mu_0}} \sin\phi_{2n}^t e^{ikx'\cos\phi_{2n}^t} \frac{1}{\pi} \int_{-\infty}^\infty \frac{e^{i\xi(x-x')\pm i\sqrt{k^2-\xi^2}y}}{\sqrt{k^2-\xi^2}}\, d\xi \Big]\, dx' \\
&= \bar{T}_{2n} H_0 \frac{k}{4\pi} \sin\phi_{2n}^t \int_{-\infty}^\infty \Big(\int_0^\infty e^{ix'(k\cos\phi_{2n}^t-\xi)}\, dx' \Big) \frac{e^{i\xi x\pm i\sqrt{k^2-\xi^2}y}}{\sqrt{k^2-\xi^2}}\, d\xi \\
&= \bar{T}_{2n} H_0 \frac{ik}{4\pi} \sin\phi_{2n}^t \int_{-\infty}^\infty \frac{e^{i\xi x\pm i\sqrt{k^2-\xi^2}y}}{(k\cos\phi_{2n}^t-\xi)\sqrt{k^2-\xi^2}}\, d\xi. \qquad (4.240)
\end{aligned}
$$

Converting to complex angle w plane using the transformation $\xi = k\sin w$, with the cylindrical coordinates (ρ,θ) with $x = \rho\cos\phi, y = \rho\sin\phi$, Eqs. (4.239), (4.240) can be expressed as

$$
\begin{aligned}
H_z^{J(2n)t} &= \mp \bar{T}_{2n} H_0 \frac{i}{4\pi} \int_C \frac{e^{ik\rho(\cos\phi\sin w\pm\sin\phi\cos w)}}{(k\cos\phi_{2n}^t - k\sin w)} k\cos w\, dw \\
&= \mp T_{2n} H_0 \frac{i}{4\pi} \int_C \frac{\cos w}{\cos\phi_{2n}^t - \sin w} e^{ik\rho(\sin(w\pm\phi)}\, dw, \qquad (4.241) \\
H_z^{M(2n)t} &= \bar{T}_{2n} H_0 \frac{ik}{4\pi} \sin\phi_{2n}^t \int_C \frac{e^{ik\rho(\cos\phi\sin w\pm\sin\phi\cos w)}}{(k\cos\phi_{2n}^t - k\sin w)k\cos w} k\cos w\, dw \\
&= \bar{T}_{2n} H_0 \frac{i}{4\pi} \int_C \sin\phi_{2n}^t \cos\phi_{2n}^t - \sin w e^{ik\rho(\sin(w\pm\phi)}\, dw. \qquad (4.242)
\end{aligned}
$$

Then, the contribution of the $(2n)$-th transmitted wave is the summation of the radiations from the currents $\boldsymbol{J}_{(2n)t}$, $\boldsymbol{M}_{(2n)t}$

$$
\begin{aligned}
H_z^{(2n)t} &= H_z^{J(2n)t} + H_z^{M(2n)t} \\
&= \bar{T}_{2n} H_0 \frac{i}{4\pi} \int_C \frac{\sin\phi_{2n}^t \pm \cos w}{\cos\phi_{2n}^t - \sin w} e^{ik\rho(\sin(w\pm\phi)}\, dw \\
&= \bar{T}_{2n} H_0 \frac{\sin\phi_{2n}^t + \sin\phi}{\cos\phi_{2n}^t - \cos\phi} C(k\rho) \\
&\quad + \bar{T}_{2n} H_0 e^{ikx\cos\phi_{2n}^t + iky\sin\phi_{2n}^t} U(\pi-\phi_0-\phi)U(\phi). \qquad (4.243)
\end{aligned}
$$

Then, the total scattering field is defined as in Eq. (4.159)

$$H_z^s = H_z^{0r} + H_z^{-i} + \sum_1^N H_z^{(n)t} \tag{4.244}$$

with N is the number of internal reflections.

4.2.2 Scattering by a Dielectric Rectangular cylinder

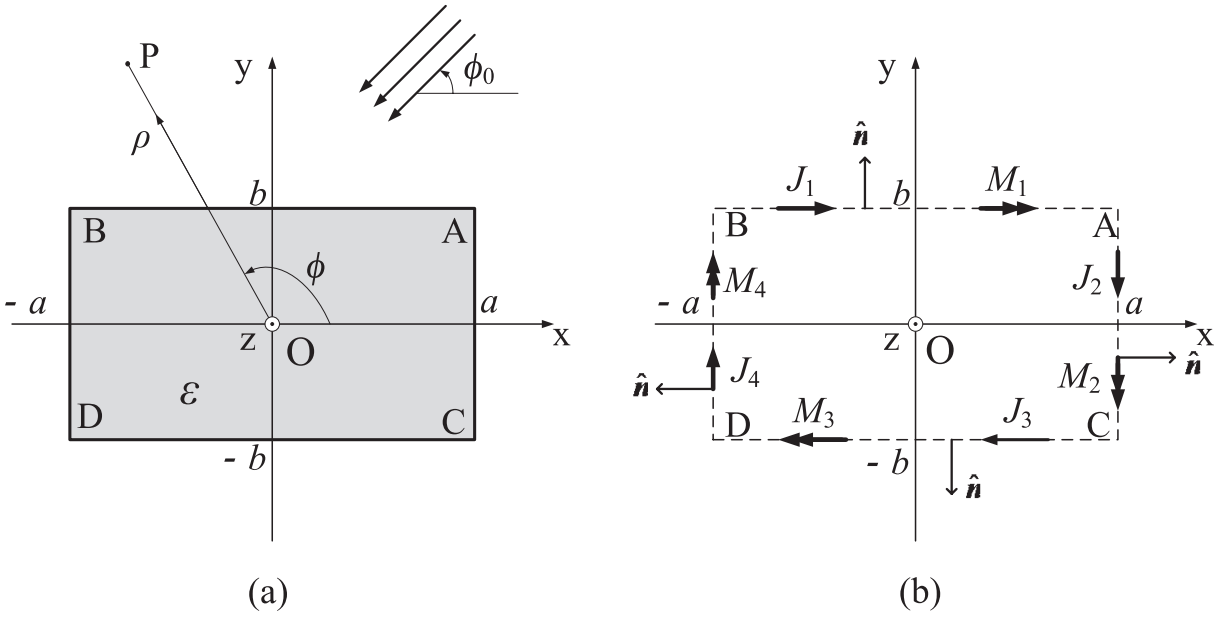

Figure 4.7: Scattering by a rectangular cylinder. (a) An incident plane wave. (b) Radiation from equivalent current sources $\boldsymbol{J}$, $\boldsymbol{M}$ on the cylinder surface.

Let us consider that a transverse plane wave impinges upon a dielectric rectangular cylinder whose dimensions are $2a \times 2b$, and its relative dielectric constant is ε_r, as shown in Fig. 4.7(a).

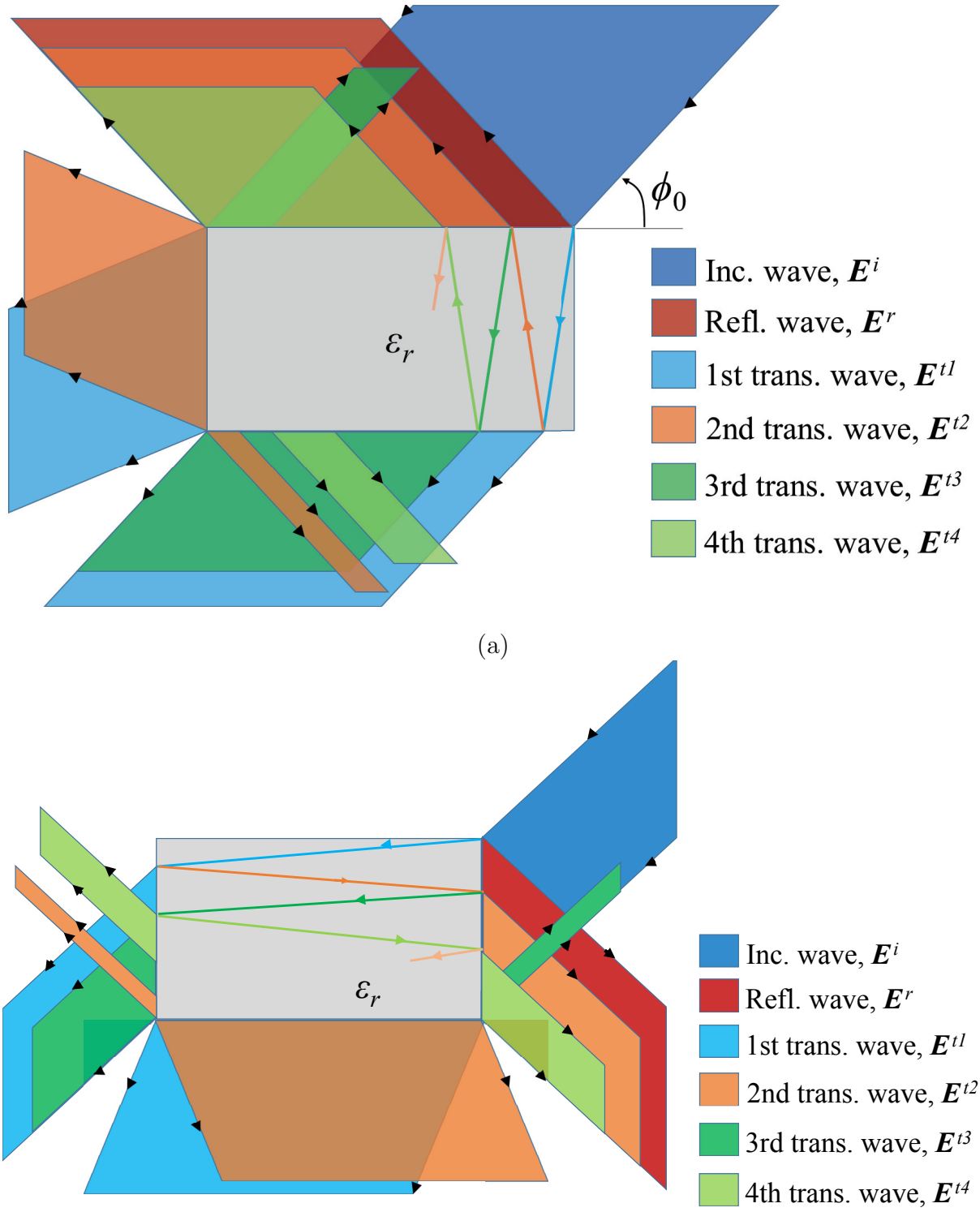

Figure 4.8: Scattering waves with multiply bouncing effect inside the dielectric rectangular cylinder. (a) Only incident wave on the upper surface. (b) Only incident wave on the side surface.

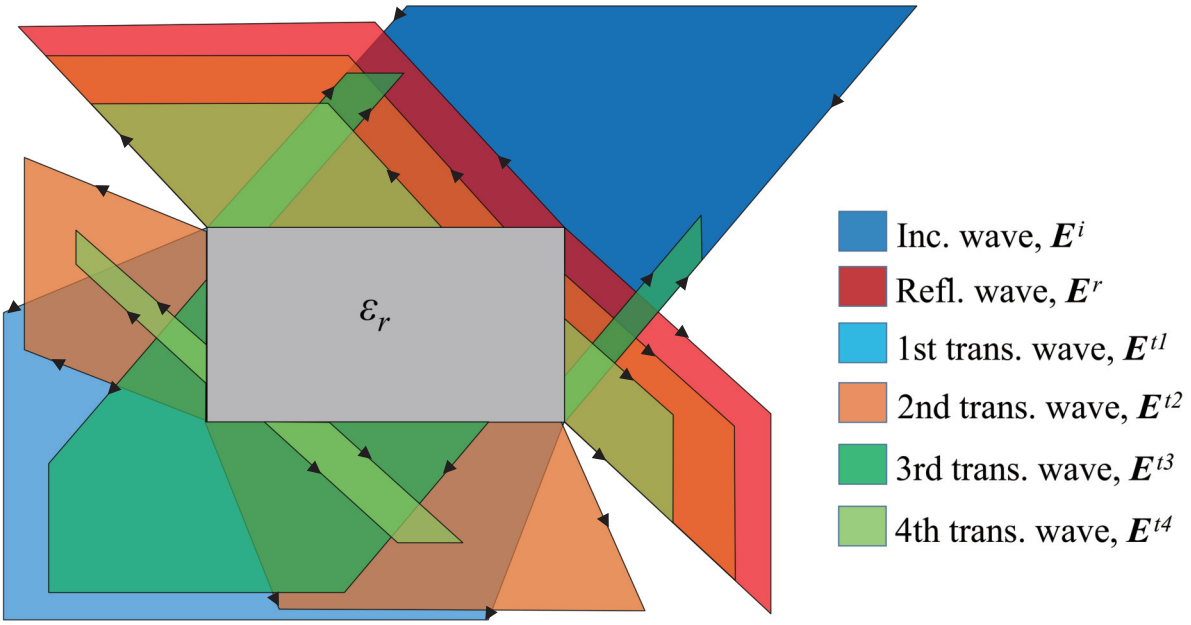

Figure 4.9: Scattering waves with multiply bouncing effect inside the dielectric rectangular cylinder. Incident wave on the upper and side surfaces.

E polarization

An E polarization incident plane wave can be written as

$$\boldsymbol{E}^i = E_0 e^{-ik(x\cos\phi_0 + y\sin\phi_0)}\hat{\boldsymbol{z}}, \tag{4.245}$$

$$\boldsymbol{H}^i = E_0\sqrt{\frac{\varepsilon_0}{\mu_0}}e^{-ik(x\cos\phi_0 + y\sin\phi_0)}(-\sin\phi_0\hat{\boldsymbol{x}} + \cos\phi_0\hat{\boldsymbol{y}}). \tag{4.246}$$

Then, the reflected waves at the illuminated surfaces are expressed for surface AB as

$$\boldsymbol{E}^{rAB} = \Gamma_{AB}E_0 e^{-ik(x\cos\phi_0 + (2b-y)\sin\phi_0)}\hat{\boldsymbol{z}}, \tag{4.247}$$

$$\boldsymbol{H}^{rAB} = \Gamma_{AB}E_0\sqrt{\frac{\varepsilon_0}{\mu_0}}e^{-ik(x\cos\phi_0 + (2b-y)\sin\phi_0)}(\sin\phi_0\hat{\boldsymbol{x}} + \cos\phi_0\hat{\boldsymbol{y}}), \tag{4.248}$$

and for surface AC as

$$\boldsymbol{E}^{rAC} = \Gamma_{AC}E_0 e^{-ik((2a-x)\cos\phi_0 + y\sin\phi_0)}\hat{\boldsymbol{z}}, \tag{4.249}$$

$$\boldsymbol{H}^{rAC} = \Gamma_{AC}E_0\sqrt{\frac{\varepsilon_0}{\mu_0}}e^{-ik((2a-x)\cos\phi_0 + y\sin\phi_0)}(-\sin\phi_0\hat{\boldsymbol{x}} - \cos\phi_0\hat{\boldsymbol{y}}), \tag{4.250}$$

where Γ_{AB} and Γ_{AC} are the reflection coefficient at the surfaces AB and AC, and are given by:

$$\Gamma_{AB} = \frac{\sin\phi_0 - \sqrt{\varepsilon_r - \cos^2\phi_0}}{\sin\phi_0 + \sqrt{\varepsilon_r - \cos^2\phi_0}}, \tag{4.251}$$

$$\Gamma_{AC} = \frac{\cos\phi_0 - \sqrt{\varepsilon_r - \sin^2\phi_0}}{\cos\phi_0 + \sqrt{\varepsilon_r - \sin^2\phi_0}}. \tag{4.252}$$

The contribution from the transmitted waves $\boldsymbol{E}^t$, $\boldsymbol{H}^t$ should be treated carefully, since they propagate with multiple internal bouncing in the dielectric body, then they depart from the body to all direction, as shown in Fig. 4.9. Then, the total scattering field becomes

$$E_z^s = E_z^0 + \big(\text{cont. from } (\boldsymbol{E}^t,\, \boldsymbol{H}^t)\big), \tag{4.253}$$

$$E_z^0 = E_z^{AB} + E_z^{AC} + E_z^{CD} + E_z^{BD}. \tag{4.254}$$

The primary scattering fields $E_z^{AB}, E_z^{AC}, E_z^{CD}, E_z^{BD}$ in Eq. (4.254) are derived from the reflected waves on surfaces AB, AC and the minus incident waves on surfaces CD, BD. The radiation integrals due to the equivalent currents can be derived by saddle point method as the same as the conducting case.

Considering four surfaces of the dielectric rectangular cylinder, the equivalent currents $\boldsymbol{J}_1 \sim \boldsymbol{J}_4$ and $\boldsymbol{M}_1 \sim \boldsymbol{M}_4$ in Fig. 4.7(b) excited from the reflected and minus incident waves can be obtained from Eqs. (2.12) and (2.13) as

$$\boldsymbol{J}_1 = \hat{\boldsymbol{y}} \times \boldsymbol{H}^{rAB}\Big|_{y=b} = \Gamma_{AB} E_0 \sqrt{\frac{\varepsilon_0}{\mu_0}} \sin\phi_0 \; e^{-ikx\cos\phi_0 - ikb\sin\phi_0}\hat{\boldsymbol{z}}, \tag{4.255}$$

$$\boldsymbol{M}_1 = \boldsymbol{E}^{rAB} \times \hat{\boldsymbol{y}}\Big|_{y=b} = \Gamma_{AB} E_0 e^{-ikx\cos\phi_0 - ikb\sin\phi_0}\hat{\boldsymbol{x}}, \tag{4.256}$$

$$\boldsymbol{J}_2 = \hat{\boldsymbol{x}} \times \boldsymbol{H}^{rAC}\Big|_{x=a} = \Gamma_{AC} E_0 \sqrt{\frac{\varepsilon_0}{\mu_0}} \cos\phi_0 \; e^{-ika\cos\phi_0 - iky\sin\phi_0}\hat{\boldsymbol{z}}, \tag{4.257}$$

$$\boldsymbol{M}_2 = \boldsymbol{E}^{rAC} \times \hat{\boldsymbol{x}}\Big|_{x=a} = -\Gamma_{AC} E_0 e^{-ika\cos\phi_0 - iky\sin\phi_0}\hat{\boldsymbol{y}}, \tag{4.258}$$

$$\boldsymbol{J}_3 = (-\hat{\boldsymbol{y}}) \times (-\boldsymbol{H}^i)\Big|_{y=-b} = E_0 \sqrt{\frac{\varepsilon_0}{\mu_0}} \sin\phi_0 e^{-ikx\cos\phi_0 + ikb\sin\phi_0}\hat{\boldsymbol{z}}, \tag{4.259}$$

$$\boldsymbol{M}_3 = (-\boldsymbol{E}^i) \times (-\hat{\boldsymbol{y}})\Big|_{y=-b} = -E_0 e^{-ikx\cos\phi_0 + ikb\sin\phi_0}\hat{\boldsymbol{x}}, \tag{4.260}$$

$$\boldsymbol{J}_4 = (-\hat{\boldsymbol{x}}) \times (-\boldsymbol{H}^i)\Big|_{x=-a} = -E_0 \sqrt{\frac{\varepsilon_0}{\mu_0}} \cos\phi_0 \; e^{ika\cos\phi_0 - iky\sin\phi_0}\hat{\boldsymbol{z}}, \tag{4.261}$$

$$\boldsymbol{M}_4 = (-\boldsymbol{E}^i) \times (-\hat{\boldsymbol{x}})\Big|_{x=-a} = E_0 e^{ika\cos\phi_0 - iky\sin\phi_0}\hat{\boldsymbol{y}}. \tag{4.262}$$

The radiation fields due to the above currents can be derived by integrating along the cylinder surface S using the Green's function as [22]

$$E_z^{J1} = -\int_{-a}^{a}\left[\Gamma_{AB}E_0\frac{k}{4\pi}\sin\phi_0 e^{-ik(x\cos\phi_0+b\sin\phi_0)}\int_{-\infty}^{\infty}\frac{e^{i\xi(x-x')+i\sqrt{k^2-\xi^2}|y-b|}}{\sqrt{k^2-\xi^2}}\,d\xi\right]dx'$$

$$= -\Gamma_{AB}E_0\frac{ik}{4\pi}\sin\phi_0 e^{-ikb\sin\phi_0}e^{-ika\cos\phi_0}\int_{-\infty}^{\infty}\frac{e^{i\xi(x-a)\pm i\sqrt{k^2-\xi^2}(y-b)}}{(k\cos\phi_0+\xi)\sqrt{k^2-\xi^2}}\,d\xi$$

$$+\Gamma_{AB}E_0\frac{ik}{4\pi}\sin\phi_0 e^{-ikb\sin\phi_0}e^{ika\cos\phi_0}\int_{-\infty}^{\infty}\frac{e^{i\xi(x+a)\pm i\sqrt{k^2-\xi^2}(y-b)}}{(k\cos\phi_0+\xi)\sqrt{k^2-\xi^2}}\,d\xi,(y\gtrless b),\quad(4.263)$$

$$E_z^{M1} = \mp\int_{-a}^{a}\left[\Gamma_{AB}E_0\frac{1}{4\pi}e^{-ik(x\cos\phi_0+b\sin\phi_0)}\int_{-\infty}^{\infty}e^{i\xi(x-x')+i\sqrt{k^2-\xi^2}|y-b|}\,d\xi\right]dx'$$

$$= \mp\Gamma_{AB}E_0\frac{i}{4\pi}e^{-ikb\sin\phi_0}e^{-ika\cos\phi_0}\int_{-\infty}^{\infty}\frac{e^{i\xi(x-a)\pm i\sqrt{k^2-\xi^2}(y-b)}}{k\cos\phi_0+\xi}\,d\xi$$

$$\pm\Gamma_{AB}E_0\frac{i}{4\pi}e^{-ikb\sin\phi_0}e^{ika\cos\phi_0}\int_{-\infty}^{\infty}\frac{e^{i\xi(x+a)\pm i\sqrt{k^2-\xi^2}(y-b)}}{k\cos\phi_0+\xi}\,d\xi,(y\gtrless b),\quad(4.264)$$

$$E_z^{J2} = -\int_{-b}^{b}\left[\Gamma_{AC}E_0\frac{k}{4\pi}\cos\phi_0 e^{-ik(a\cos\phi_0+y\sin\phi_0)}\int_{-\infty}^{\infty}\frac{e^{i\xi(x-a)+i\sqrt{k^2-\xi^2}|y-y'|}}{\sqrt{k^2-\xi^2}}\,d\xi\right]dy'$$

$$= -\Gamma_{AC}E_0\frac{ik}{4\pi}\cos\phi_0 e^{-ika\cos\phi_0}e^{-ikb\cos\phi_0}\int_{-\infty}^{\infty}\frac{e^{i\xi(x-a)\pm i\sqrt{k^2-\xi^2}(y-b)}}{(k\cos\phi_0+\sqrt{k^2-\xi^2})\sqrt{k^2-\xi^2}}\,d\xi$$

$$+\Gamma_{AC}E_0\frac{ik}{4\pi}\cos\phi_0 e^{-ika\cos\phi_0}e^{ikb\cos\phi_0}\int_{-\infty}^{\infty}\frac{e^{i\xi(x-a)\pm i\sqrt{k^2-\xi^2}(y+b)}}{(k\cos\phi_0+\sqrt{k^2-\xi^2})\sqrt{k^2-\xi^2}}\,d\xi,$$
$$(y\gtrless y'),\quad(4.265)$$

$$E_z^{M2} = -\int_{-b}^{b}\left[\Gamma_{AC}E_0\frac{1}{4\pi}e^{-ik(a\cos\phi_0+y\sin\phi_0)}\int_{-\infty}^{\infty}\frac{\xi e^{i\xi(x-a)+i\sqrt{k^2-\xi^2}|y-y'|}}{\sqrt{k^2-\xi^2}}\,d\xi\right]dy'$$

$$= -\Gamma_{AC}E_0\frac{i}{4\pi}e^{-ika\cos\phi_0}e^{-ikb\cos\phi_0}\int_{-\infty}^{\infty}\frac{\xi e^{i\xi(x-a)\pm i\sqrt{k^2-\xi^2}(y-b)}}{(k\cos\phi_0+\sqrt{k^2-\xi^2})\sqrt{k^2-\xi^2}}\,d\xi$$

$$+\Gamma_{AC}E_0\frac{ik}{4\pi}e^{-ika\cos\phi_0}e^{ikb\cos\phi_0}\int_{-\infty}^{\infty}\frac{\xi e^{i\xi(x-a)\pm i\sqrt{k^2-\xi^2}(y+b)}}{(k\cos\phi_0+\sqrt{k^2-\xi^2})\sqrt{k^2-\xi^2}}\,d\xi,$$
$$(y\gtrless y'),\quad(4.266)$$

$$E_z^{J3} = -\int_{-a}^{a}\left[E_0\frac{k}{4\pi}\sin\phi_0 e^{-ik(x\cos\phi_0+b\sin\phi_0)}\int_{-\infty}^{\infty}\frac{e^{i\xi(x-x')+i\sqrt{k^2-\xi^2}|y+b|}}{\sqrt{k^2-\xi^2}}\,d\xi\right]dx'$$

$$= -E_0\frac{ik}{4\pi}\sin\phi_0 e^{ikb\sin\phi_0}e^{-ika\cos\phi_0}\int_{-\infty}^{\infty}\frac{e^{i\xi(x-a)\pm i\sqrt{k^2-\xi^2}(y+b)}}{(k\cos\phi_0+\xi)\sqrt{k^2-\xi^2}}\,d\xi$$

$$+E_0\frac{ik}{4\pi}\sin\phi_0 e^{ikb\sin\phi_0}e^{ika\cos\phi_0}\int_{-\infty}^{\infty}\frac{e^{i\xi(x+a)\pm i\sqrt{k^2-\xi^2}(y+b)}}{(k\cos\phi_0+\xi)\sqrt{k^2-\xi^2}}\,d\xi,(y\gtrless -b),\quad(4.267)$$

$$E_z^{M3} = \pm \int_{-a}^{a} \left[H_0 \frac{1}{4\pi} e^{-ik(x\cos\phi_0 + b\sin\phi_0)} \int_{-\infty}^{\infty} e^{i\xi(x-x') + i\sqrt{k^2-\xi^2}|y-b|}\, d\xi \right] dx'$$

$$= \pm E_0 \frac{i}{4\pi} e^{ikb\sin\phi_0} e^{-ika\cos\phi_0} \int_{-\infty}^{\infty} \frac{e^{i\xi(x-a) \pm i\sqrt{k^2-\xi^2}(y+b)}}{k\cos\phi_0 + \xi}\, d\xi$$

$$\mp E_0 \frac{i}{4\pi} e^{ikb\sin\phi_0} e^{ika\cos\phi_0} \int_{-\infty}^{\infty} \frac{e^{i\xi(x+a) \pm i\sqrt{k^2-\xi^2}(y+b)}}{k\cos\phi_0 + \xi}\, d\xi, (y \gtrless -b), \tag{4.268}$$

$$E_z^{J4} = \int_{-b}^{b} \left[E_0 \frac{k}{4\pi} \cos\phi_0 e^{-ik(a\cos\phi_0 + y\sin\phi_0)} \int_{-\infty}^{\infty} \frac{e^{i\xi(x-a) + i\sqrt{k^2-\xi^2}|y-y'|}}{\sqrt{k^2-\xi^2}}\, d\xi \right] dy'$$

$$= -E_0 \frac{ik}{4\pi} \cos\phi_0 e^{-ika\cos\phi_0} e^{-ikb\cos\phi_0} \int_{-\infty}^{\infty} \frac{e^{i\xi(x-a) \pm i\sqrt{k^2-\xi^2}(y-b)}}{(k\cos\phi_0 + \sqrt{k^2-\xi^2})\sqrt{k^2-\xi^2}}\, d\xi$$

$$+ E_0 \frac{ik}{4\pi} \cos\phi_0 e^{-ika\cos\phi_0} e^{ikb\cos\phi_0} \int_{-\infty}^{\infty} \frac{e^{i\xi(x-a) \pm i\sqrt{k^2-\xi^2}(y+b)}}{(k\cos\phi_0 + \sqrt{k^2-\xi^2})\sqrt{k^2-\xi^2}}\, d\xi,$$

$$(y \gtrless y'), \tag{4.269}$$

$$E_z^{M4} = \int_{-b}^{b} \left[E_0 \frac{1}{4\pi} e^{-ik(a\cos\phi_0 + y\sin\phi_0)} \int_{-\infty}^{\infty} \frac{\xi e^{i\xi(x-a) + i\sqrt{k^2-\xi^2}|y-y'|}}{\sqrt{k^2-\xi^2}}\, d\xi \right] dy'$$

$$= E_0 \frac{i}{4\pi} e^{-ika\cos\phi_0} e^{-ikb\cos\phi_0} \int_{-\infty}^{\infty} \frac{\xi e^{i\xi(x-a) \pm i\sqrt{k^2-\xi^2}(y-b)}}{(k\cos\phi_0 + \sqrt{k^2-\xi^2})\sqrt{k^2-\xi^2}}\, d\xi$$

$$- E_0 \frac{ik}{4\pi} e^{-ika\cos\phi_0} e^{ikb\cos\phi_0} \int_{-\infty}^{\infty} \frac{\xi e^{i\xi(x-a) \pm i\sqrt{k^2-\xi^2}(y+b)}}{(k\cos\phi_0 + \sqrt{k^2-\xi^2})\sqrt{k^2-\xi^2}}\, d\xi,$$

$$(y \gtrless y'). \tag{4.270}$$

While the above integral cannot evaluate analytically,the saddle point technique may be used for the high frequency asymptotic evaluation for a large k [22] as in section [cond.cyl]. Then, the radiation fields from the equivalent currents $\boldsymbol{J}_1 \sim \boldsymbol{M}_4$ becomes

$$E_z^{J1} = i2\Gamma_{AB} E_0 e^{-ikb(\sin\phi + \sin\phi_0)} \sin[ka(\cos\phi_0 + \cos\phi)] \frac{\sin\phi_0}{\cos\phi_0 + \cos\phi} C(k\rho), \tag{4.271}$$

$$E_z^{M1} = i2\Gamma_{AB} E_0 e^{-ikb(\sin\phi + \sin\phi_0)} \sin[ka(\cos\phi_0 + \cos\phi)] \frac{\sin\phi}{\cos\phi_0 + \cos\phi} C(k\rho), \tag{4.272}$$

$$E_z^{J2} = i2\Gamma_{AC} E_0 e^{-ika(\cos\phi + \cos\phi_0)} \sin[kb(\sin\phi_0 + \sin\phi)] \frac{\cos\phi_0}{\sin\phi_0 + \sin\phi} C(k\rho), \tag{4.273}$$

$$E_z^{M2} = i2\Gamma_{AC} E_0 e^{-ika(\cos\phi + \cos\phi_0)} \sin[kb(\sin\phi_0 + \sin\phi)] \frac{\cos\phi}{\sin\phi_0 + \sin\phi} C(k\rho), \tag{4.274}$$

$$E_z^{J3} = i2E_0 e^{ikb(\sin\phi + \sin\phi_0)} \sin[ka(\cos\phi_0 + \cos\phi)] \frac{\sin\phi_0}{\cos\phi_0 + \cos\phi} C(k\rho), \tag{4.275}$$

$$E_z^{M3} = -i2E_0 e^{ikb(\sin\phi + \sin\phi_0)} \sin[ka(\cos\phi_0 + \cos\phi)] \frac{\sin\phi}{\cos\phi_0 + \cos\phi} C(k\rho), \tag{4.276}$$

$$E_z^{J4} = i2E_0 e^{ika(\cos\phi + \cos\phi_0)} \sin[kb(\sin\phi_0 + \sin\phi)] \frac{\cos\phi_0}{\sin\phi_0 + \sin\phi} C(k\rho), \tag{4.277}$$

$$E_z^{M4} = -i2E_0 e^{ika(\cos\phi + \cos\phi_0)} \sin[kb(\sin\phi_0 + \sin\phi)] \frac{\cos\phi}{\sin\phi_0 + \sin\phi} C(k\rho). \tag{4.278}$$

Then, the corresponding electric far fields of four surfaces AB, AC, CD, BD are given by:

$$
\begin{aligned}
E_z^{AB} &= E_z^{J1} + E_z^{M1} \\
&= i2\Gamma_{AB}\frac{\sin\phi_0 + \sin\phi}{\cos\phi_0 + \cos\phi}\sin[ka(\cos\phi_0 + \cos\phi)]e^{jkb(\sin\phi+\sin\phi_0)}C(k\rho), \quad (4.279) \\
E_z^{AC} &= E_z^{J2} + E_z^{M2} \\
&= i2\Gamma_{AC}\frac{\cos\phi_0 + \cos\phi}{\sin\phi_0 + \sin\phi}\sin[kb(\sin\phi_0 + \sin\phi)]e^{jka(\cos\phi+\cos\phi_0)}C(k\rho), \quad (4.280) \\
E_z^{CD} &= E_z^{J3} + E_z^{M3} \\
&= i2\frac{\sin\phi_0 - \sin\phi}{\cos\phi_0 + \cos\phi}\sin[ka(\cos\phi_0 + \cos\phi)]e^{-jkb(\sin\phi+\sin\phi_0)}C(k\rho), \quad (4.281) \\
E_z^{BD} &= E_z^{J4} + E_z^{M4} \\
&= i2\frac{\cos\phi_0 - \cos\phi}{\sin\phi_0 + \sin\phi}\sin[kb(\sin\phi_0 + \sin\phi)]e^{-jka(\cos\phi+\cos\phi_0)}C(k\rho). \quad (4.282)
\end{aligned}
$$

When the incident plane wave impinges on the illuminated surfaces of a dielectric cylinder, it excites the reflected wave at the illuminated surfaces and transmitted waves inside the cylinder. In addition, the originally transmitted wave excites the internal reflected and transmitted waves due to the multiple bouncing effects and they radiate again from the body. Because of the finite dimension, one may also notice that the internal bouncing waves eventually experience the reflection at the side interfaces, and depart from the scattering body as seen in Fig. 4.9. Then, the scattering field E_z^{tn} due to the multiply bouncing effect can be calculated as the summation of the radiations from the equivalent sources due to these n-th transmitted waves. One notes that these equivalent currents flow a part of the surface, in accord to the incident angle, so that the integration range varies.

The intensity of these internal reflected waves depends on the dielectric constant and the dimension of scattering objects, and becomes weak when the number of internal reflections increases. This bouncing process continues until all the incident energy dissipates or leaks out. Accordingly, one needs to add these contributions E_z^{tn}.

The effect of the multiple internal bouncing may be considered by using a collective form, which is derived from the corresponding reflection/transmission coefficient for dielectric slab geometry. For example, the reflection coefficient Γ_{AB}, Γ_{AC} in Eqs. (4.251),

(4.252) at the surfaces AB, AC may be modified by [39]

$$\Gamma_{ABm} = \frac{\Gamma_{AB}(1 - e^{i4kb\sqrt{\varepsilon_r - \cos^2\phi_0}})}{1 - \Gamma_{AB}^2(\phi_0)e^{i4kb\sqrt{\varepsilon_r - \cos^2\phi_0}}}, \tag{4.283}$$

$$\Gamma_{ACm} = \frac{\Gamma_{AC}(1 - e^{i4ka\sqrt{\varepsilon_r - \sin^2\phi_0}})}{1 - \Gamma_{AC}^2(\phi_0)e^{i4ka\sqrt{\varepsilon_r - \sin^2\phi_0}}}. \tag{4.284}$$

However, the above collective coefficients Γ_{ABm}, Γ_{ABm} is valid only around the normal incident direction or for the case which the reflected surfaces are infinitely long. For the oblique incident direction, the expressions of these contributions E_z^{tn} become more complex than the primary one, then these formulations are omitted here.

H polarization

A H polarization incident plane wave can be written as

$$\boldsymbol{H}^i = H_0 e^{-ik(x\cos\phi_0 + y\sin\phi_0)}\hat{\boldsymbol{z}}, \tag{4.285}$$

$$\boldsymbol{E}^i = H_0\sqrt{\frac{\mu_0}{\varepsilon_0}}e^{-ik(x\cos\phi_0 + y\sin\phi_0)}(\sin\phi_0\hat{\boldsymbol{x}} - \cos\phi_0\hat{\boldsymbol{y}}). \tag{4.286}$$

Then, the reflected waves at the illuminated surfaces are expressed for surface AB as

$$\boldsymbol{H}^{rAB} = \bar{\Gamma}_{AB}H_0 e^{-ik(x\cos\phi_0 + (2b-y)\sin\phi_0)}\hat{\boldsymbol{z}}, \tag{4.287}$$

$$\boldsymbol{E}^{rAB} = \bar{\Gamma}_{AB}H_0\sqrt{\frac{\mu_0}{\varepsilon_0}}e^{-ik(x\cos\phi_0 + (2b-y)\sin\phi_0)}(-\sin\phi_0\hat{\boldsymbol{x}} - \cos\phi_0\hat{\boldsymbol{y}}), \tag{4.288}$$

and for surface AC as

$$\boldsymbol{E}^{rAC} = \bar{\Gamma}_{AC}E_0 e^{-ik((2a-x)\cos\phi_0 + y\sin\phi_0)}\hat{\boldsymbol{z}}, \tag{4.289}$$

$$\boldsymbol{H}^{rAC} = \bar{\Gamma}_{AC}H_0\sqrt{\frac{\mu_0}{\varepsilon_0}}e^{-ik((2a-x)\cos\phi_0 + y\sin\phi_0)}(\sin\phi_0\hat{\boldsymbol{x}} + \cos\phi_0\hat{\boldsymbol{y}}), \tag{4.290}$$

where $\bar{\Gamma}_{AB}$ and $\bar{\Gamma}_{AC}$ are the reflection coefficient at the surfaces AB and AC, and are given by:

$$\bar{\Gamma}_{AB} = -\frac{\varepsilon_r\sin\phi_0 - \sqrt{\varepsilon_r - \cos^2\phi_0}}{\varepsilon_r\sin\phi_0 + \sqrt{\varepsilon_r - \cos^2\phi_0}}, \tag{4.291}$$

$$\bar{\Gamma}_{AC} = -\frac{\varepsilon_r\cos\phi_0 - \sqrt{\varepsilon_r - \sin^2\phi_0}}{\varepsilon_r\cos\phi_0 + \sqrt{\varepsilon_r - \sin^2\phi_0}}. \tag{4.292}$$

The contribution from the transmitted waves $\boldsymbol{E}^t$, $\boldsymbol{H}^t$ should be treated carefully, since they propagate with multiple internal bouncing in the dielectric body, then they depart

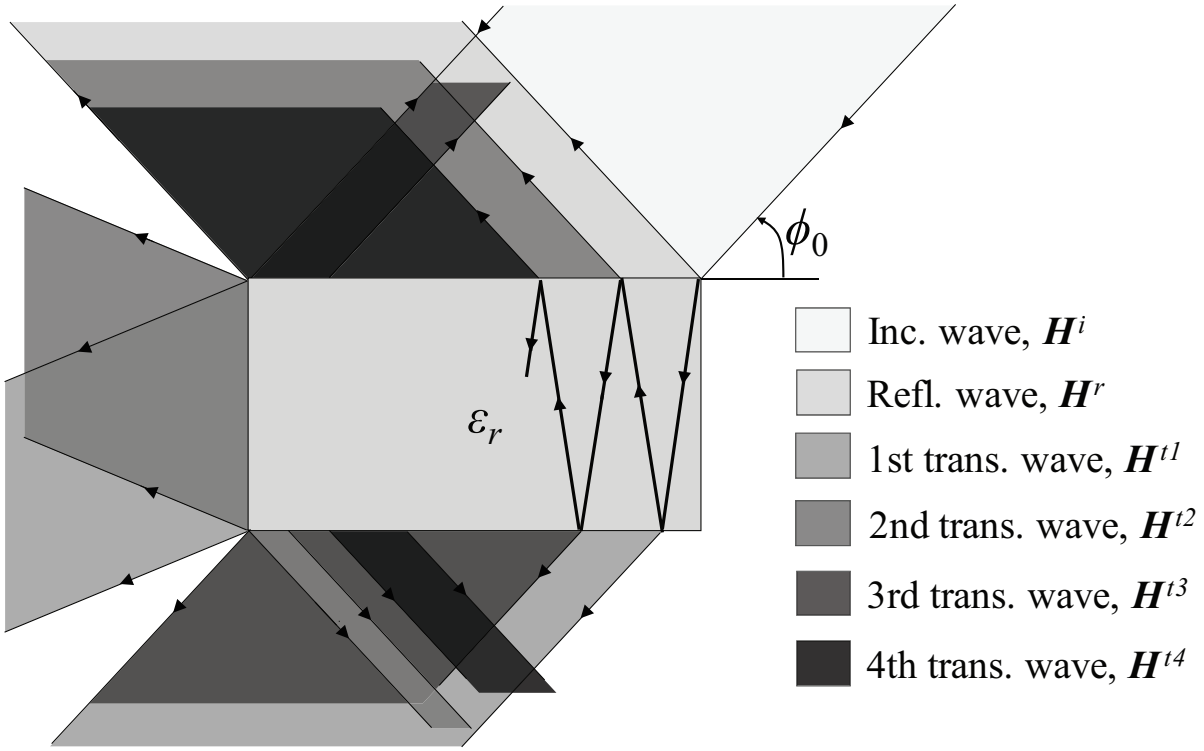

Figure 4.10: Scattering waves with multiply bouncing effect inside the dielectric rectangular cylinder. Incident wave on the upper surface is only shown here.

from the body to all direction, as shown in Fig. 4.9. Then, the total scattering field becomes

$$H_z^s = H_z^0 + \big(\text{cont. from } (\boldsymbol{E}^t, \boldsymbol{H}^t)\big), \tag{4.293}$$

$$H_z^0 = H_z^{AB} + H_z^{AC} + H_z^{CD} + H_z^{BD}. \tag{4.294}$$

The primary scattering fields $H_z^{AB}, H_z^{AC}, H_z^{CD}, H_z^{BD}$ in Eq. (4.294) are derived from the reflected waves on surfaces AB, AC and the minus incident waves on surfaces CD, BD. The radiation integrals due to the equivalent currents can be derived by saddle point method as the same as the conducting case.

Considering four surfaces of the dielectric rectangular cylinder, the equivalent currents $\boldsymbol{J}_1 \sim \boldsymbol{J}_4$ and $\boldsymbol{M}_1 \sim \boldsymbol{M}_4$ in Fig. 4.7(b) excited from the reflected and minus incident

waves can be obtained from Eqs. (2.12) and (2.13) without effect of transmitted waves as

$$\boldsymbol{J}_1 = \hat{\boldsymbol{y}} \times \boldsymbol{H}^{rAB}\Big|_{y=b} = \bar{\Gamma}_{AB} H_0 e^{-ik(x\cos\phi_0 + b\sin\phi_0)}\hat{\boldsymbol{x}}, \tag{4.295}$$

$$\boldsymbol{M}_1 = \boldsymbol{E}^{rAB} \times \hat{\boldsymbol{y}}\Big|_{y=b} = -\bar{\Gamma}_{AB} H_0 \sqrt{\frac{\mu_0}{\varepsilon_0}} \sin\phi_0 e^{-ik(x\cos\phi_0 + b\sin\phi_0)}\hat{\boldsymbol{z}}, \tag{4.296}$$

$$\boldsymbol{J}_2 = \hat{\boldsymbol{x}} \times \boldsymbol{H}^{rAC}\Big|_{x=a} = -\bar{\Gamma}_{AC} H_0 e^{-ik(a\cos\phi_0 + y\sin\phi_0)}\hat{\boldsymbol{y}}, \tag{4.297}$$

$$\boldsymbol{M}_2 = \boldsymbol{E}^{rAC} \times \hat{\boldsymbol{x}}\Big|_{x=a} = -\bar{\Gamma}_{AC} H_0 \sqrt{\frac{\mu_0}{\varepsilon_0}} \cos\phi_0 e^{-ik(a\cos\phi_0 + y\sin\phi_0)}\hat{\boldsymbol{z}}, \tag{4.298}$$

$$\boldsymbol{J}_3 = -\hat{\boldsymbol{y}} \times (-\boldsymbol{H}^{i})\Big|_{y=-b} = H_0 e^{-ik(x\cos\phi_0 + b\sin\phi_0)}\hat{\boldsymbol{x}}, \tag{4.299}$$

$$\boldsymbol{M}_3 = (-\boldsymbol{E}^{i}) \times (-\hat{\boldsymbol{y}})\Big|_{y=-b} = H_0 \sqrt{\frac{\mu_0}{\varepsilon_0}} \sin\phi_0 e^{-ik(x\cos\phi_0 + b\sin\phi_0)}\hat{\boldsymbol{z}}, \tag{4.300}$$

$$\boldsymbol{J}_4 = (-\hat{\boldsymbol{x}}) \times (-\boldsymbol{H}^{i})\Big|_{x=-a} = -H_0 e^{-ik(-a\cos\phi_0 + y\sin\phi_0)}\hat{\boldsymbol{y}}, \tag{4.301}$$

$$\boldsymbol{M}_4 = (-\boldsymbol{E}^{i}) \times (-\hat{\boldsymbol{x}})\Big|_{x=-a} = H_0 \sqrt{\frac{\mu_0}{\varepsilon_0}} \cos\phi_0 e^{-ik(-a\cos\phi_0 + y\sin\phi_0)}\hat{\boldsymbol{z}}. \tag{4.302}$$

The radiation fields due to the above currents can be derived by integrating along the cylinder surface S using the Green's function as [22]

$$\begin{aligned} H_z^{J1} &= \int_S \frac{i}{4} J_1 \frac{\partial}{\partial y'} \mathrm{H}_0^{(1)}(k\sqrt{(x-x')^2 + (y-y')^2})\Big|_{y'=b} dS, \\ &= \pm\bar{\Gamma}_{AB} H_0 \frac{i}{4\pi} e^{-ikb\sin\phi_0} e^{-ika\cos\phi_0} \int_{-\infty}^{\infty} \frac{e^{i\xi(x-a)\pm i\sqrt{k^2-\xi^2}(y-b)}}{k\cos\phi_0 + \xi}\, d\xi \\ &\quad \mp \bar{\Gamma}_{AB} H_0 \frac{i}{4\pi} e^{-ikb\sin\phi_0} e^{ika\cos\phi_0} \int_{-\infty}^{\infty} \frac{e^{i\xi(x+a)\pm i\sqrt{k^2-\xi^2}(y-b)}}{k\cos\phi_0 + \xi}\, d\xi, (y \gtrless b), \end{aligned} \tag{4.303}$$

$$\begin{aligned} H_z^{M1} &= -\int_S \frac{i}{4} J_2 \frac{\partial}{\partial x'} \mathrm{H}_0^{(1)}(k\sqrt{(x-x')^2 + (y-y')^2})\Big|_{x'=a} dS \\ &= \bar{\Gamma}_{AB} H_0 \frac{ik}{4\pi} \sin\phi_0 e^{-ikb\sin\phi_0} e^{-ika\cos\phi_0} \int_{-\infty}^{\infty} \frac{e^{i\xi(x-a)\pm i\sqrt{k^2-\xi^2}(y-b)}}{(k\cos\phi_0 + \xi)\sqrt{k^2-\xi^2}}\, d\xi \\ &\quad - \bar{\Gamma}_{AB} H_0 \frac{ik}{4\pi} \sin\phi_0 e^{-ikb\sin\phi_0} e^{ika\cos\phi_0} \int_{-\infty}^{\infty} \frac{e^{i\xi(x+a)\pm i\sqrt{k^2-\xi^2}(y-b)}}{(k\cos\phi_0 + \xi)\sqrt{k^2-\xi^2}}\, d\xi, \\ &\qquad\qquad (y \gtrless b), \end{aligned} \tag{4.304}$$

$$\begin{aligned} H_z^{J2} &= -\int_S \frac{i}{4} J_2 \frac{\partial}{\partial x'} \mathrm{H}_0^{(1)}(k\sqrt{(x-x')^2 + (y-y')^2})\Big|_{x'=a} dS, \\ &= \bar{\Gamma}_{AC} H_0 \frac{i}{4\pi} e^{-ika\cos\phi_0} e^{-ikb\cos\phi_0} \int_{-\infty}^{\infty} \frac{\xi e^{i\xi(x-a)\pm i\sqrt{k^2-\xi^2}(y-b)}}{(k\cos\phi_0 + \sqrt{k^2-\xi^2})\sqrt{k^2-\xi^2}}\, d\xi \\ &\quad - \bar{\Gamma}_{AC} H_0 \frac{ik}{4\pi} e^{-ika\cos\phi_0} e^{ikb\cos\phi_0} \int_{-\infty}^{\infty} \frac{\xi e^{i\xi(x-a)\pm i\sqrt{k^2-\xi^2}(y+b)}}{(k\cos\phi_0 + \sqrt{k^2-\xi^2})\sqrt{k^2-\xi^2}}\, d\xi, \\ &\qquad\qquad (y \gtrless y'), \end{aligned} \tag{4.305}$$

$$H_z^{M2} = -\int_S \frac{\omega\mu_0}{4} M_2 \mathrm{H}_0^{(1)}(k\sqrt{(x-x')^2+(y-y')^2})\Big|_{x'=a} dS,$$
$$= \bar{\Gamma}_{AC} H_0 \frac{ik}{4\pi} \cos\phi_0 e^{-ika\cos\phi_0} e^{-ikb\cos\phi_0} \int_{-\infty}^{\infty} \frac{e^{i\xi(x-a)\pm i\sqrt{k^2-\xi^2}(y-b)}}{(k\cos\phi_0+\sqrt{k^2-\xi^2})\sqrt{k^2-\xi^2}}\, d\xi$$
$$- \bar{\Gamma}_{AC} H_0 \frac{ik}{4\pi} \cos\phi_0 e^{-ika\cos\phi_0} e^{ikb\cos\phi_0} \int_{-\infty}^{\infty} \frac{e^{i\xi(x-a)\pm i\sqrt{k^2-\xi^2}(y+b)}}{(k\cos\phi_0+\sqrt{k^2-\xi^2})\sqrt{k^2-\xi^2}}\, d\xi, \quad (y \gtrless y'), \tag{4.306}$$

$$H_z^{J3} = \int_S \frac{i}{4} J_3 \frac{\partial}{\partial y'} \mathrm{H}_0^{(1)}(k\sqrt{(x-x')^2+(y-y')^2})\Big|_{y'=-b} dS,$$
$$= \pm H_0 \frac{i}{4\pi} e^{ikb\sin\phi_0} e^{-ika\cos\phi_0} \int_{-\infty}^{\infty} \frac{e^{i\xi(x-a)\pm i\sqrt{k^2-\xi^2}(y+b)}}{k\cos\phi_0+\xi}\, d\xi$$
$$\mp H_0 \frac{i}{4\pi} e^{ikb\sin\phi_0} e^{ika\cos\phi_0} \int_{-\infty}^{\infty} \frac{e^{i\xi(x+a)\pm i\sqrt{k^2-\xi^2}(y+b)}}{k\cos\phi_0+\xi}\, d\xi, (y \gtrless -b), \tag{4.307}$$

$$H_z^{M3} = -\int_S \frac{\omega\mu_0}{4} M_3 \mathrm{H}_0^{(1)}(k\sqrt{(x-x')^2+(y-y')^2})\Big|_{y'=-b} dS,$$
$$= -H_0 \frac{ik}{4\pi} \sin\phi_0 e^{ikb\sin\phi_0} e^{-ika\cos\phi_0} \int_{-\infty}^{\infty} \frac{e^{i\xi(x-a)\pm i\sqrt{k^2-\xi^2}(y+b)}}{(k\cos\phi_0+\xi)\sqrt{k^2-\xi^2}}\, d\xi$$
$$+ H_0 \frac{ik}{4\pi} \sin\phi_0 e^{ikb\sin\phi_0} e^{ika\cos\phi_0} \int_{-\infty}^{\infty} \frac{e^{i\xi(x+a)\pm i\sqrt{k^2-\xi^2}(y+b)}}{(k\cos\phi_0+\xi)\sqrt{k^2-\xi^2}}\, d\xi, (y \gtrless -b), \tag{4.308}$$

$$H_z^{J4} = -\int_S \frac{i}{4} J_4 \frac{\partial}{\partial x'} \mathrm{H}_0^{(1)}(k\sqrt{(x-x')^2+(y-y')^2})\Big|_{x'=-a} dS,$$
$$= H_0 \frac{i}{4\pi} e^{-ika\cos\phi_0} e^{-ikb\cos\phi_0} \int_{-\infty}^{\infty} \frac{\xi e^{i\xi(x-a)\pm i\sqrt{k^2-\xi^2}(y-b)}}{(k\cos\phi_0+\sqrt{k^2-\xi^2})\sqrt{k^2-\xi^2}}\, d\xi$$
$$- H_0 \frac{ik}{4\pi} e^{-ika\cos\phi_0} e^{ikb\cos\phi_0} \int_{-\infty}^{\infty} \frac{\xi e^{i\xi(x-a)\pm i\sqrt{k^2-\xi^2}(y+b)}}{(k\cos\phi_0+\sqrt{k^2-\xi^2})\sqrt{k^2-\xi^2}}\, d\xi, \quad (y \gtrless y'), \tag{4.309}$$

$$H_z^{M4} = -\int_S \frac{\omega\mu_0}{4} M_4 \mathrm{H}_0^{(1)}(k\sqrt{(x-x')^2+(y-y')^2})\Big|_{x'=-a} dS$$
$$= -H_0 \frac{ik}{4\pi} \cos\phi_0 e^{-ika\cos\phi_0} e^{-ikb\cos\phi_0} \int_{-\infty}^{\infty} \frac{e^{i\xi(x-a)\pm i\sqrt{k^2-\xi^2}(y-b)}}{(k\cos\phi_0+\sqrt{k^2-\xi^2})\sqrt{k^2-\xi^2}}\, d\xi$$
$$+ H_0 \frac{ik}{4\pi} \cos\phi_0 e^{-ika\cos\phi_0} e^{ikb\cos\phi_0} \int_{-\infty}^{\infty} \frac{e^{i\xi(x-a)\pm i\sqrt{k^2-\xi^2}(y+b)}}{(k\cos\phi_0+\sqrt{k^2-\xi^2})\sqrt{k^2-\xi^2}}\, d\xi, \quad (y \gtrless y'). \tag{4.310}$$

While the above integral cannot evaluate analytically,the saddle point technique may be used for the high frequency asymptotic evaluation for a large k [22] as in section [cond.cyl].

Then, the radiation fields from the equivalent currents $\boldsymbol{J}_1 \sim \boldsymbol{M}_4$ becomes

$$H_z^{J1} = -i2\bar{\Gamma}_{AB} H_0 e^{-ikb(\sin\phi+\sin\phi_0)} \sin[ka(\cos\phi_0+\cos\phi)] \frac{\sin\phi_0}{\cos\phi_0+\cos\phi} C(k\rho), \quad (4.311)$$

$$H_z^{M1} = -i2\bar{\Gamma}_{AB} H_0 e^{-ikb(\sin\phi+\sin\phi_0)} \sin[ka(\cos\phi_0+\cos\phi)] \frac{\sin\phi}{\cos\phi_0+\cos\phi} C(k\rho), \quad (4.312)$$

$$H_z^{J2} = -i2\bar{\Gamma}_{AC} H_0 e^{-ika(\cos\phi+\cos\phi_0)} \sin[kb(\sin\phi_0+\sin\phi)] \frac{\cos\phi_0}{\sin\phi_0+\sin\phi} C(k\rho), \quad (4.313)$$

$$H_z^{M2} = -i2\bar{\Gamma}_{AC} H_0 e^{-ika(\cos\phi+\cos\phi_0)} \sin[kb(\sin\phi_0+\sin\phi)] \frac{\cos\phi}{\sin\phi_0+\sin\phi} C(k\rho), \quad (4.314)$$

$$H_z^{J3} = -i2 H_0 e^{ikb(\sin\phi+\sin\phi_0)} \sin[ka(\cos\phi_0+\cos\phi)] \frac{\sin\phi_0}{\cos\phi_0+\cos\phi} C(k\rho), \quad (4.315)$$

$$H_z^{M3} = i2 H_0 e^{ikb(\sin\phi+\sin\phi_0)} \sin[ka(\cos\phi_0+\cos\phi)] \frac{\sin\phi}{\cos\phi_0+\cos\phi} C(k\rho), \quad (4.316)$$

$$H_z^{J4} = -i2 H_0 e^{ika(\cos\phi+\cos\phi_0)} \sin[kb(\sin\phi_0+\sin\phi)] \frac{\cos\phi_0}{\sin\phi_0+\sin\phi} C(k\rho), \quad (4.317)$$

$$H_z^{M4} = i2 H_0 e^{ika(\cos\phi+\cos\phi_0)} \sin[kb(\sin\phi_0+\sin\phi)] \frac{\cos\phi}{\sin\phi_0+\sin\phi} C(k\rho). \quad (4.318)$$

Then, the corresponding electric far fields of four surfaces AB, AC, CD, BD are given by:

$$\begin{aligned} H_z^{AB} &= H_z^{J1} + H_z^{M1} \\ &= -i2\bar{\Gamma}_{AB} \frac{\sin\phi_0+\sin\phi}{\cos\phi_0+\cos\phi} \sin[ka(\cos\phi_0+\cos\phi)] e^{-ikb(\sin\phi+\sin\phi_0)} C(k\rho), \quad (4.319) \\ H_z^{AC} &= H_z^{J2} + H_z^{M2} \\ &= -i2\bar{\Gamma}_{AC} \frac{\cos\phi_0+\cos\phi}{\sin\phi_0+\sin\phi} \sin[kb(\sin\phi_0+\sin\phi)] e^{-ika(\cos\phi+\cos\phi_0)} C(k\rho), \quad (4.320) \\ H_z^{CD} &= H_z^{J3} + H_z^{M3} \\ &= -i2 \frac{\sin\phi_0-\sin\phi}{\cos\phi_0+\cos\phi} \sin[ka(\cos\phi_0+\cos\phi)] e^{ikb(\sin\phi+\sin\phi_0)} C(k\rho), \quad (4.321) \\ H_z^{BD} &= H_z^{J4} + H_z^{M4} \\ &= -i2 \frac{\cos\phi_0-\cos\phi}{\sin\phi_0+\sin\phi} \sin[kb(\sin\phi_0+\sin\phi)] e^{ika(\cos\phi+\cos\phi_0)} C(k\rho). \quad (4.322) \end{aligned}$$

The effect of the multiple internal bouncing may be considered by using a collective form, which is derived from the corresponding reflection/transmission coefficient for dielectric slab geometry. For example, the reflection coefficient Γ_{AB}, Γ_{AC} in Eqs. (4.251), (4.252) at the surfaces AB, AC may be modified by [39]

$$\bar{\Gamma}_{ABm} = \frac{\bar{\Gamma}_{AB}(1 - e^{i4kb\sqrt{\varepsilon_r - \cos^2\phi_0}})}{1 - \bar{\Gamma}_{AB}^2(\phi_0) e^{i4kb\sqrt{\varepsilon_r - \cos^2\phi_0}}}, \quad (4.323)$$

$$\bar{\Gamma}_{ACm} = \frac{\bar{\Gamma}_{AC}(1 - e^{i4ka\sqrt{\varepsilon_r - \sin^2\phi_0}})}{1 - \bar{\Gamma}_{AC}^2(\phi_0) e^{i4ka\sqrt{\varepsilon_r - \sin^2\phi_0}}}. \quad (4.324)$$

The expressions of these contributions H_z^{tn} are more complex than the primary one, then these formulations are omitted here.

Numerical Results

Let us now discuss the effect of higher order transmitted waves E_z^{tn}, H_z^{tn} in Figs. 4.11. Here, the incident angle $\phi_0 = 45^o$, the relative permittivity $\varepsilon_r = 6$ and $ka = kb = 15$ are chosen as an example. Since this example is lossless dielectric case, so that one can expect relatively strong contribution from internal transmitted waves. In Fig. 4.11, the contributions of each transmitted wave are plotted separately. It can be seen that the primary contributions E_z^0 for E polarization incident wave and H_z^0 for H polarization incident wave yield a maximum peak at the forward direction (ϕ =–135^o), and two secondary peaks at the specular reflection directions (ϕ =135^o, –45^o) from the reflected waves. While two polarizations have the same contributions at the forward direction, the contributions for E incidence case have much larger than those for H incidence case at the specular reflection directions due to the larger reflection coefficient.

The effect of the first transmitted waves E_z^{t1}, H_z^{t1} are strong at the transmission direction, and their values are smaller than the primary contributions but do contribute to the total field. The second transmitted waves E_z^{t2}, H_z^{t2} contribute at the specular reflection directions as shown in Fig. 4.9. The third transmitted waves E_z^{t3}, H_z^{t3} affect at the backscattering direction ($\phi = 45^o$), and the fourth waves E_z^{t4}, H_z^{t4} contribute a little at the forward scattering direction. While the fifth transmitted waves E_z^{t5}, H_z^{t5} have small contributions at the backscattering direction, the sixth waves E_z^{t6}, H_z^{t6} contribute weakly to the total field and its value is mostly 40 dB below the primary contribution. Due to the smaller transmitted coefficient, the values of the transmitted waves E_z^{tn} are smaller than those of H_z^{tn}. Therefore, the effects of the contributions of the transmitted waves H_z^{tn} to the total scattering field are stronger than those of E_z^{tn}.

The partial summations of these contributions are shown in Fig. 4.12. It is easy to find that the summation result converges by the sixth transmitted wave, so that we can omit the effect of the subsequent transmitted waves. Also, due to the stronger bouncing effects, the results for the H polarization case are more oscillative than those for E polarization case. This discussion is true even for the lossy dielectric cases, since all transmitted waves experience additional decay as they pass through the cylinder.

Let us now discuss the accuracy of our formulation by comparing the numerical results with those obtained from the HFSS simulation. Figures 4.13–4.15 show the far-field scattering patterns from the dielectric rectangular cylinders for the nearly conducting case $\varepsilon_r = 6 + 1000i$. One can easily observe that our results for nearly conducting case coincide with those derived by the PEC case. Because of the high loss in the dielectric cylinders, one needs only the primary contributions and those from the transmitted waves can be omitted. These results calculated using the collective form are included in all figures as EPO(c). This also matches with the PEC results. Additionally, one may observed that the results for E and H polarizations have almost the same main reflection and forward direction lobes, and a difference arises at the boundary direction owing to the difference in the boundary condition.

The far-field scattering patterns from the dielectric rectangular cylinders for high lossy case $\varepsilon_r = 6 + 1i$ are shown in Figs. 4.16–4.18. As the loss of the dielectric material decreases, the lobes in the specular reflection directions become smaller than PEC cases due to the smaller reflection coefficient while the lobe at forward scattering direction is still same as one by PEC case. Also because of high dielectric loss, the effect of multiple bouncing is weak. Then, the contributions of the high order transmitted waves are small. Therefore, we still only need the contributions from the primary ones and the results by the collective approximation are still valid. Additionally, one may observed that the results for E and H polarizations have almost the same main forward direction lobes, but a difference arises at the reflection direction lobes due to the different reflection coefficient.

Figures 4.19–4.21 show the far-field scattering patterns from the dielectric rectangular cylinders for almost lossless case $\varepsilon_r = 6 + 0.1i$. Also because of the slight dielectric loss, the effect of multiple bouncing becomes stronger. Then, the lobes becomes more oscillatory due to the interference between the multiply bouncing transmitted waves. Also, the results by the collective approximation are not valid, except the normal incident case, due to the fact that the effects of the multiply bouncing transmitted waves are pretty strong and their phases should be taken into the calculation. The E polarization scattering field patterns have a same beam-like radiation with the H polarization cases at the forward direction because of the strong contribution of the minus incident wave, but some differences arise at the specular reflection directions. Here, the results of E polarization cases are somewhat stronger and less oscillatory than that of H polarization

cases due to the stronger reflection coefficient.

The normal incidence ($\phi_0 = 90^o$) is shown Figs. 4.13, 4.16 and 4.19. A symmetric pattern can be seen with respect to the vertical (y) axis due to the symmetry of the problem. As the incident wave penetrates into the dielectric cylinder, the reflected wave with multiply internal bouncing interfere with the primary surface-reflected wave to lower the backscattering lobe. However, the level of the forward scattering lobe does not change too much. One also observes that the main scattering lobes in the forward and the specular reflection directions coincide the HFSS simulation results, while some differences can be noticed at the minor lobes.

A different incidence ($\phi_0 = 45^o$) is selected in Figs. 4.14, 4.17 and 4.20. Again a symmetric pattern with respect to the incident angle ($\phi_0 = 45^o$) can be seen. As the loss of the dielectric material decreases, the lobes in the specular reflection directions become smaller and more oscillatory. A different side ratio, $ka = 15$ and $kb = 10$ are shown in Figs. 4.15, 4.18 and 4.21. Same observations can be found, except that the symmetric pattern does not exist for this cylinder. Additionally, the beam-like radiations are smaller than those in $ka = kb = 15$ cases. The beam width is inverse proportional to the length of the transmission/reflection surfaces; namely, the wider the surface is, the sharper the beam is. All of these results are good agreement with those by HFSS simulation.

Figures 4.22–4.24 show the far-field scattering patterns from the dielectric rectangular cylinders for lossless case $\varepsilon_r = 6$. While the same observation with the almost lossless case $\varepsilon_r = 6 + 0.1i$ can be seen, the analytical results have some differences with those by HFSS simulation. Since the results by the HFSS simulation are obtained by the 3D to 2D conversion, these results may also contain some error due to this conversion. Accordingly, we need further comparison with other reference solution.

The case of the smaller size of the rectangular cylinder $ka = kb = 8$ are selected in Figs. 4.25, 4.26. While the analytical results have a good agreement with HFSS simulation results at the forward and specular reflection directions, some differences arise at other directions. It is not clear so far for these differences. It may be from the HFSS simulation or the size limit of the approximation. Then we may need some evaluations to verify the accuracy of the approximation method for the smaller size rectangular cylinder.

We may need some evaluations to verify the accuracy of the approximation method

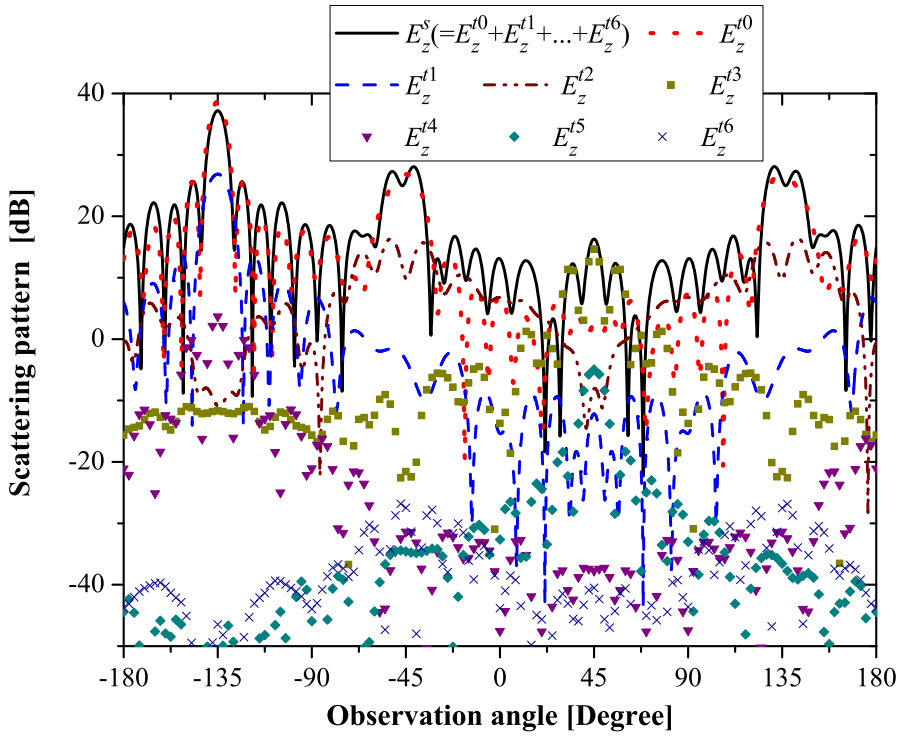

(a)

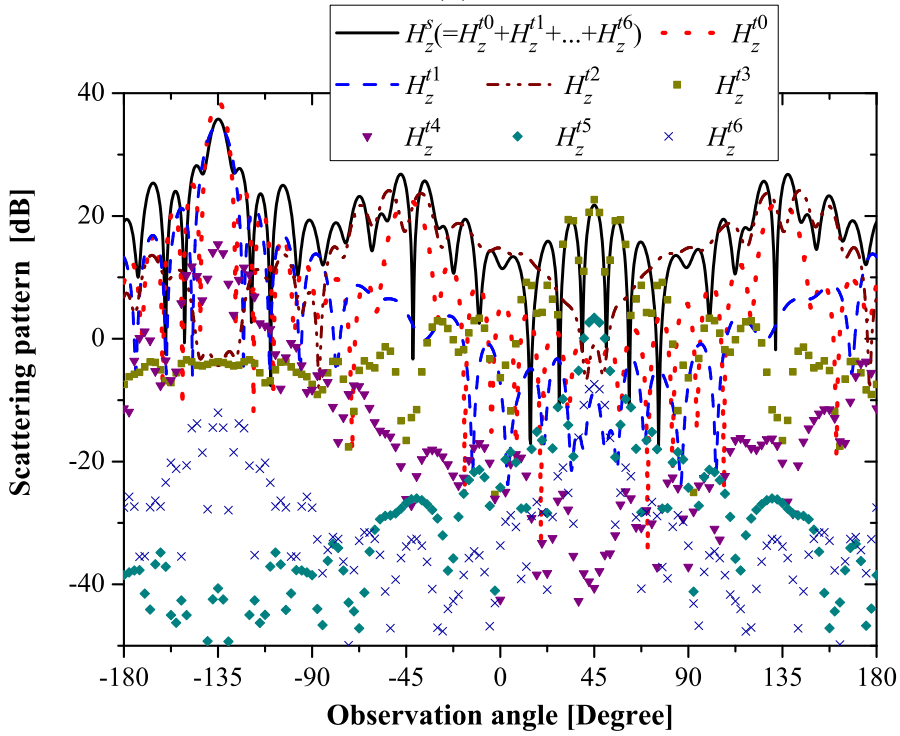

(b)

Figure 4.11: Contribution of each internal multiple bouncing waves from a dielectric cylinder. $ka = kb = 15$, $\phi_0 = 45^o$, $\varepsilon_r = 6$. (a) E polarization incident wave. (b) H polarization incident wave.

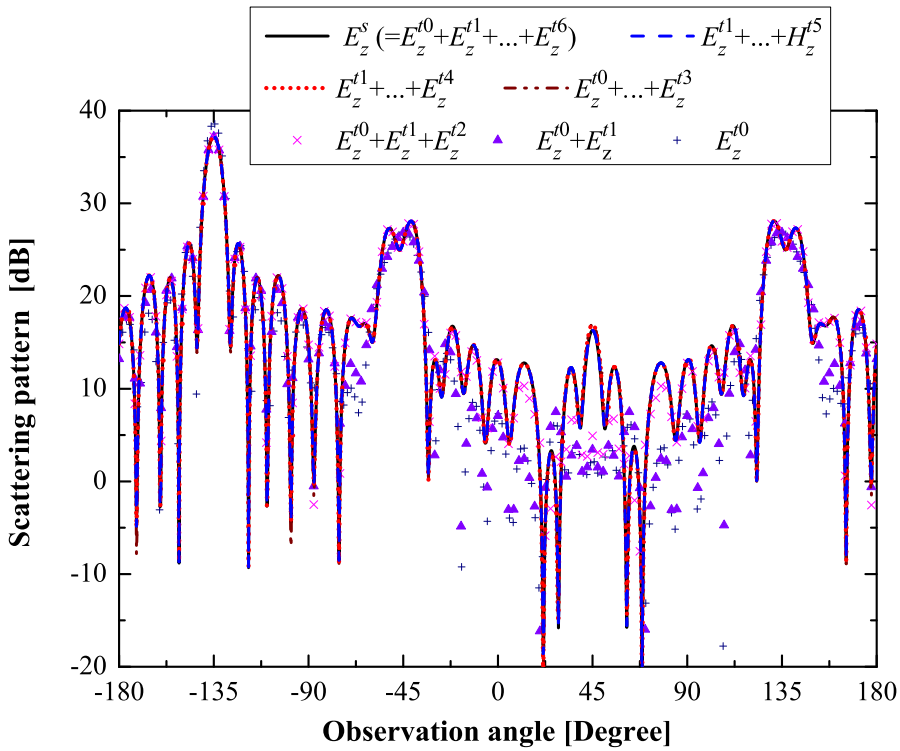

(a)

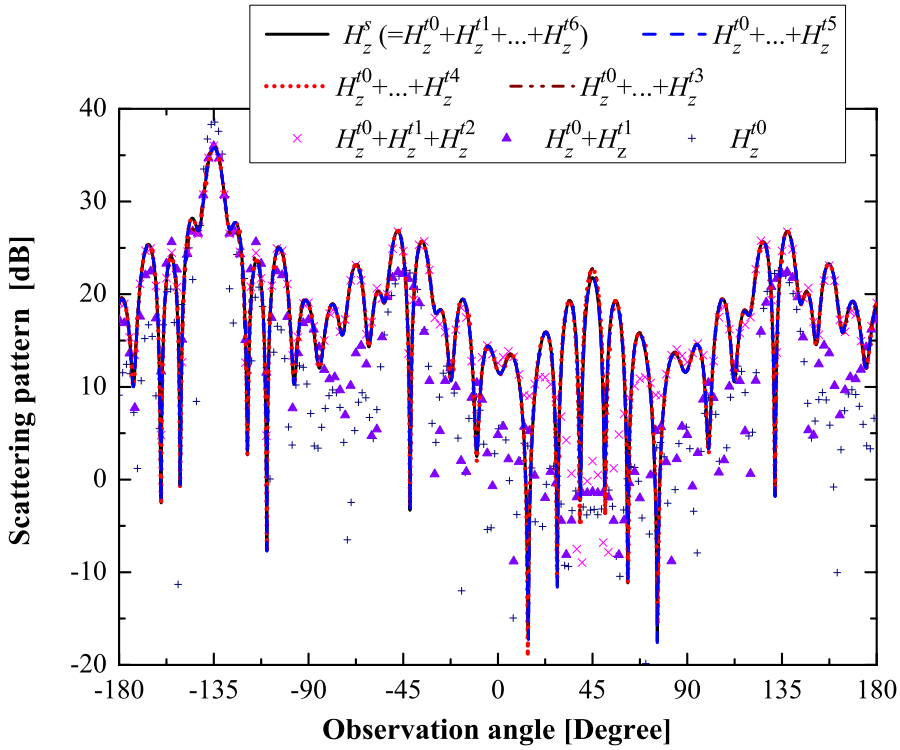

(b)

Figure 4.12: Summation of the contributions of internal multiple bouncing waves from a dielectric cylinder. $ka = kb = 15$, $\phi_0 = 45°$, $\varepsilon_r = 6$. (a) E polarization incident wave. (b) H polarization incident wave.

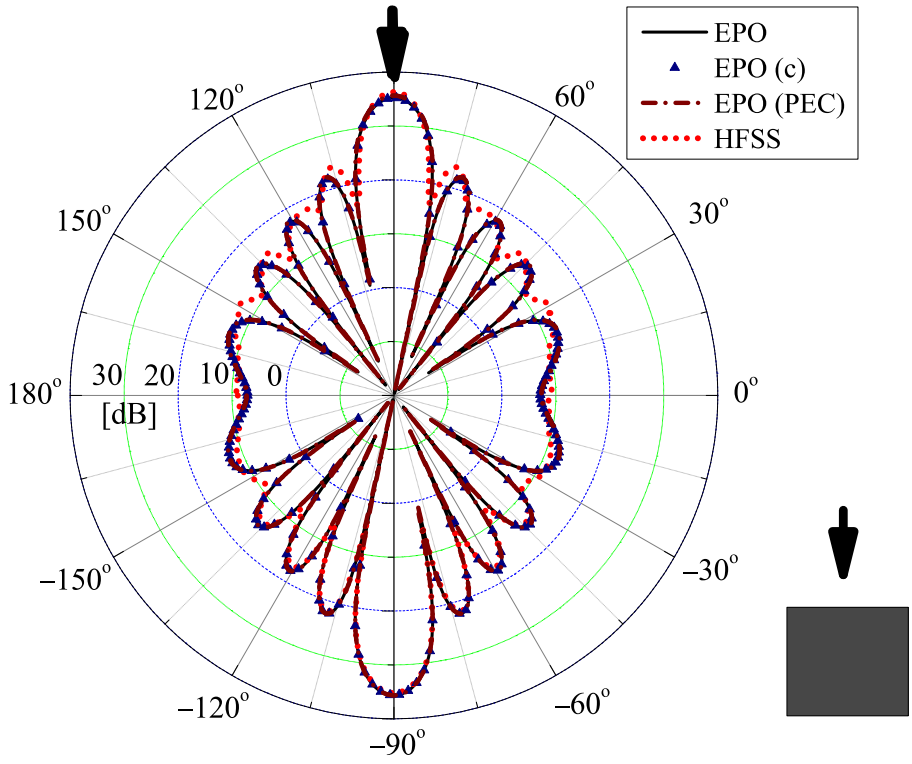

(a)

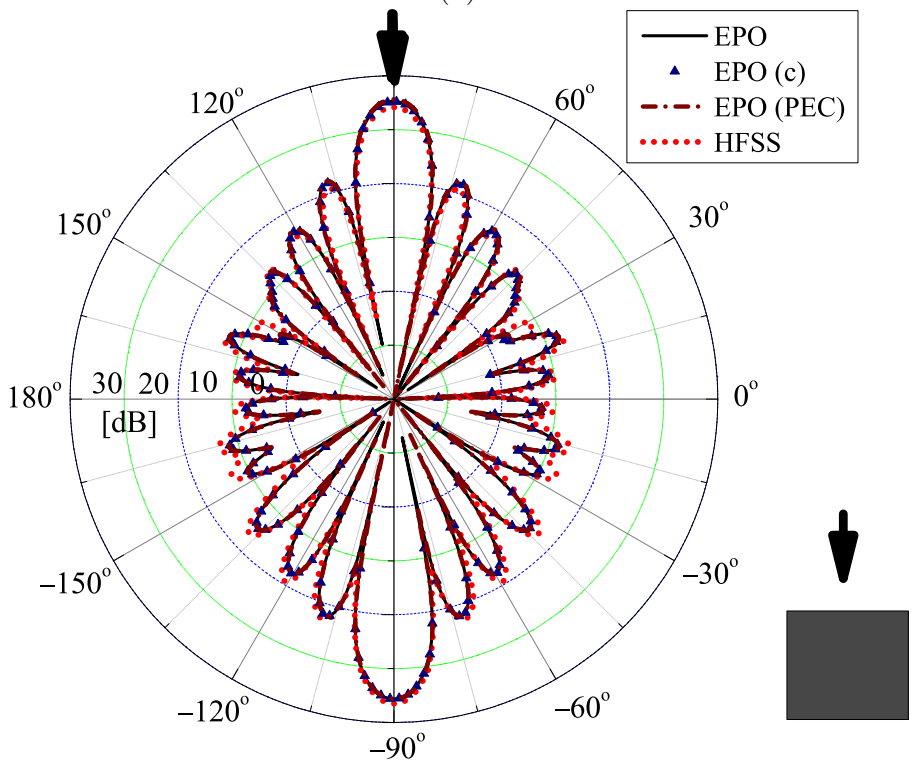

(b)

Figure 4.13: Radiation pattern of a dielectric rectangular cylinder. $ka = kb = 15$, $\phi_0 = 90^o$. $\varepsilon_r = 6 + 1000i$. (a) E polarization incident wave. (b) H polarization incident wave.

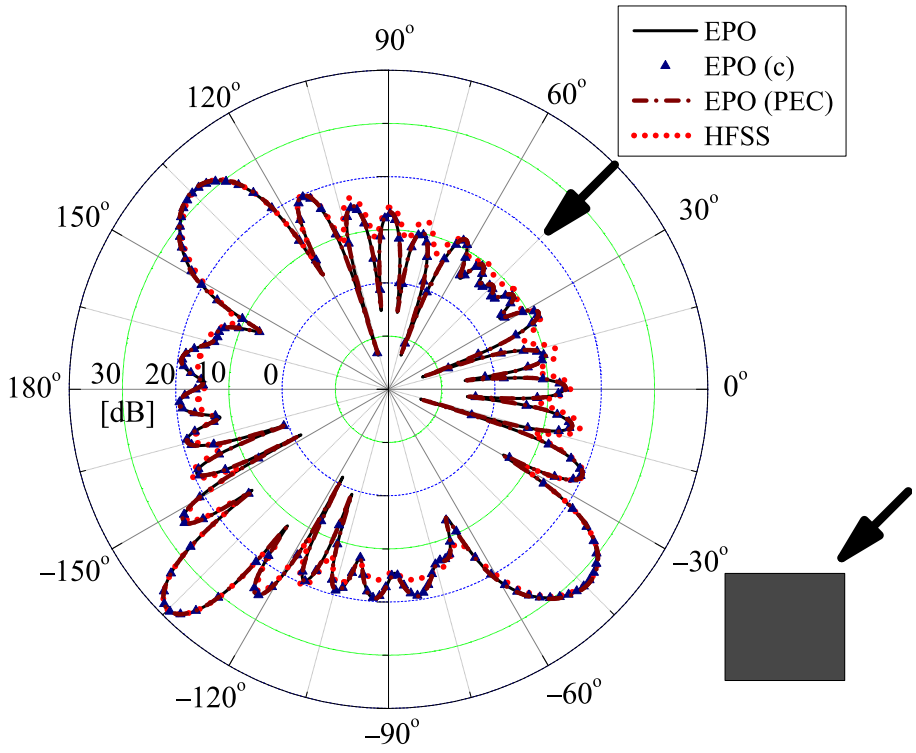

(a)

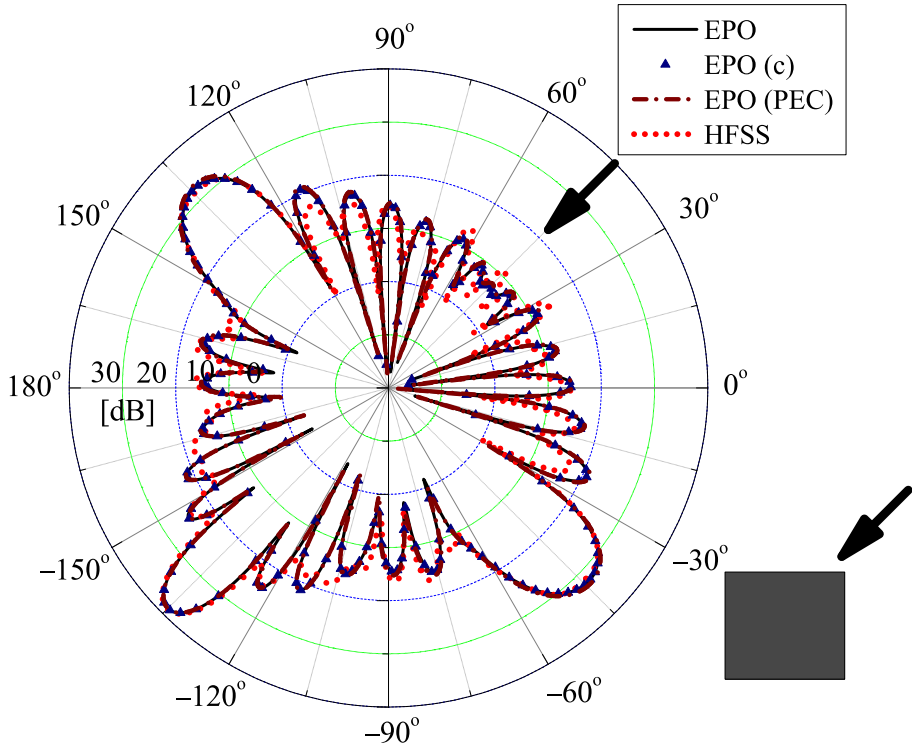

(b)

Figure 4.14: Radiation pattern of a dielectric rectangular cylinder. $ka = kb = 15$, $\phi_0 = 45^o$. $\varepsilon_r = 6 + 1000i$. (a) E polarization incident wave. (b) H polarization incident wave.

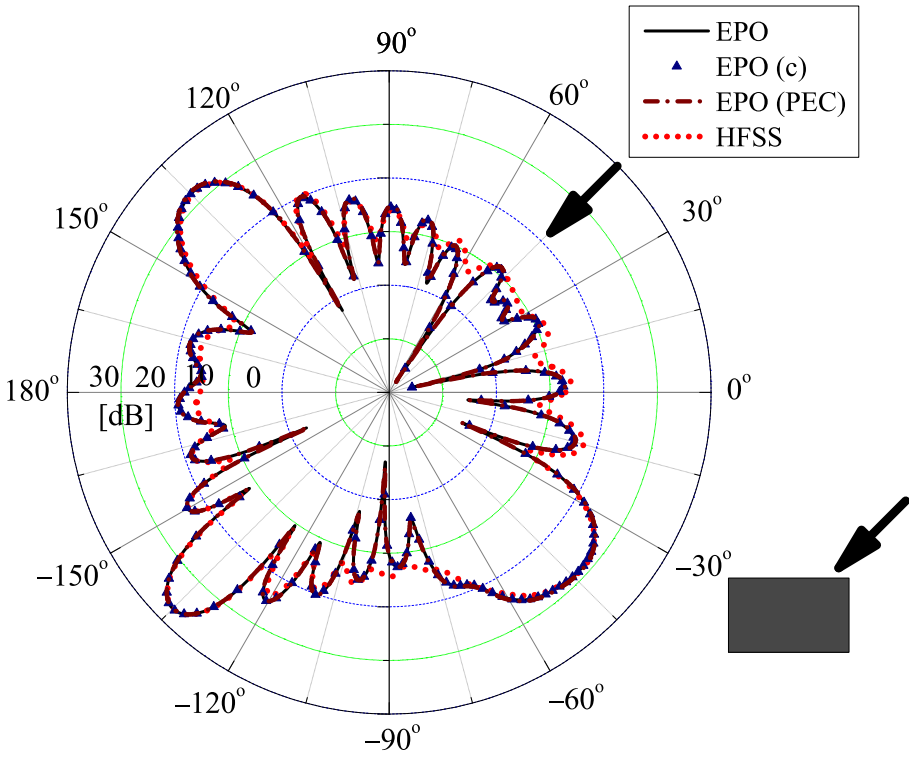

(a)

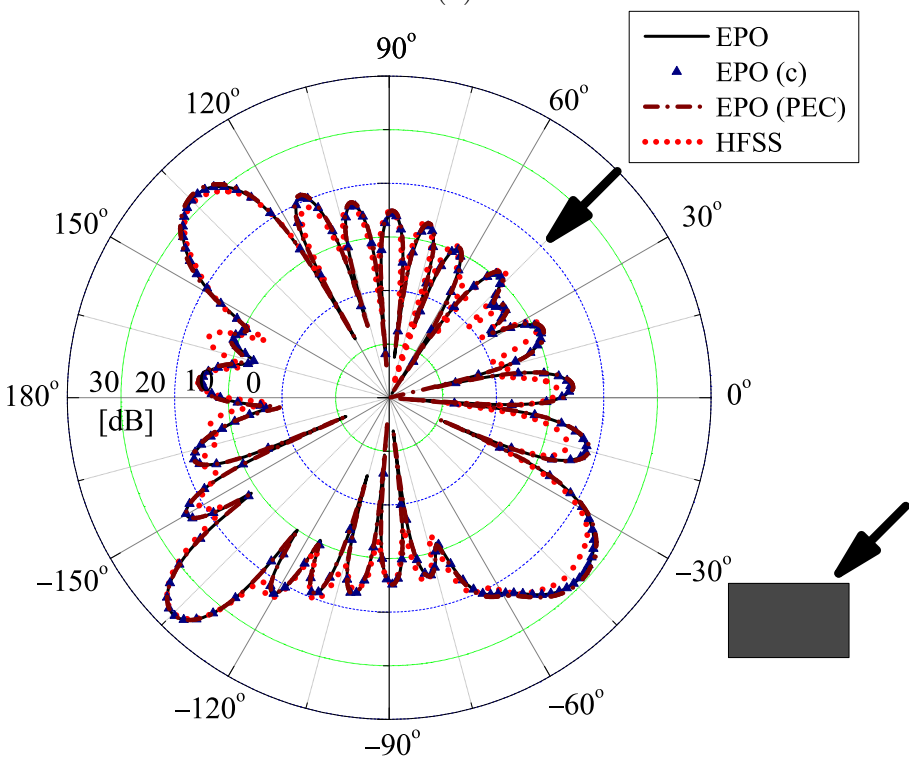

(b)

Figure 4.15: Radiation pattern of a dielectric rectangular cylinder. $ka = 15$, $kb = 10$, $\phi_0 = 45^{\circ}$. $\varepsilon_r = 6 + 1000i$. (a) E polarization incident wave. (b) H polarization incident wave.

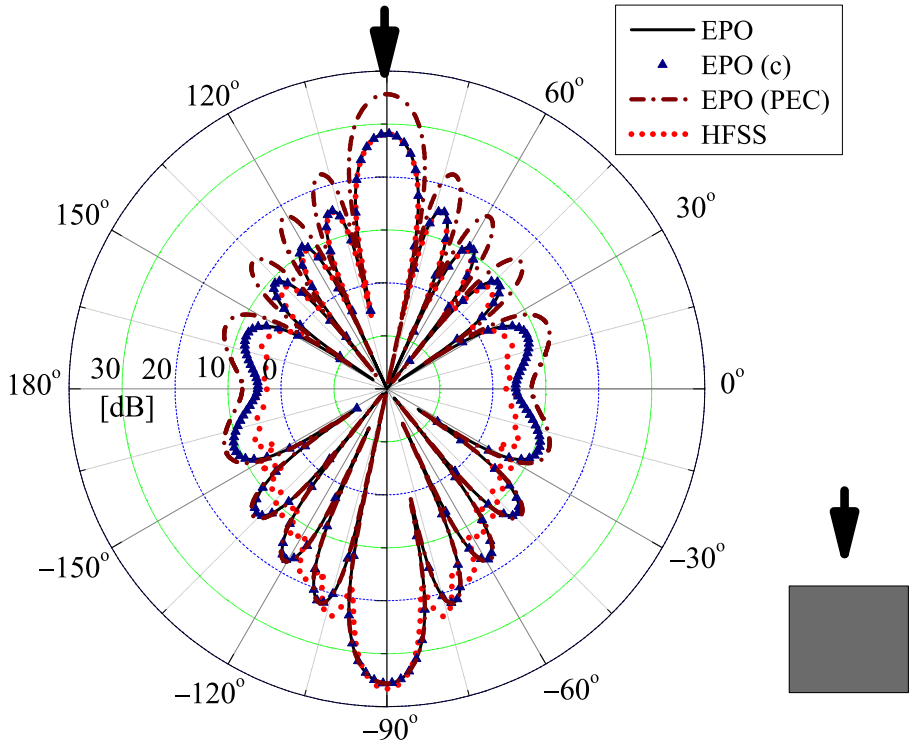

(a)

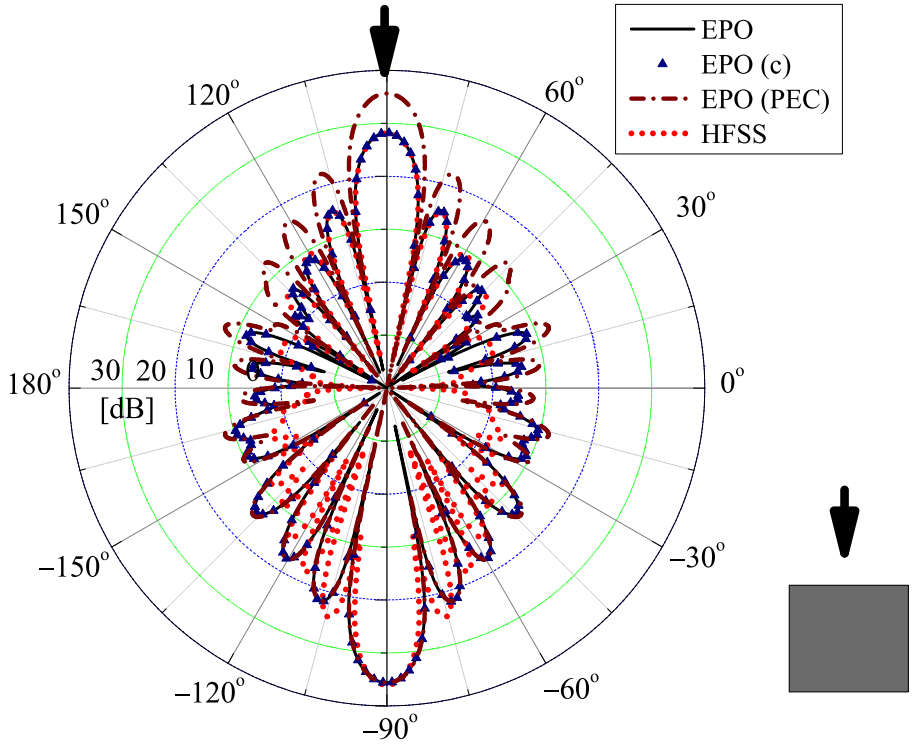

(b)

Figure 4.16: Radiation pattern of a dielectric rectangular cylinder. $ka = kb = 15$, $\phi_0 = 90^o$. $\varepsilon_r = 6 + 1i$. (a) E polarization incident wave. (b) H polarization incident wave.

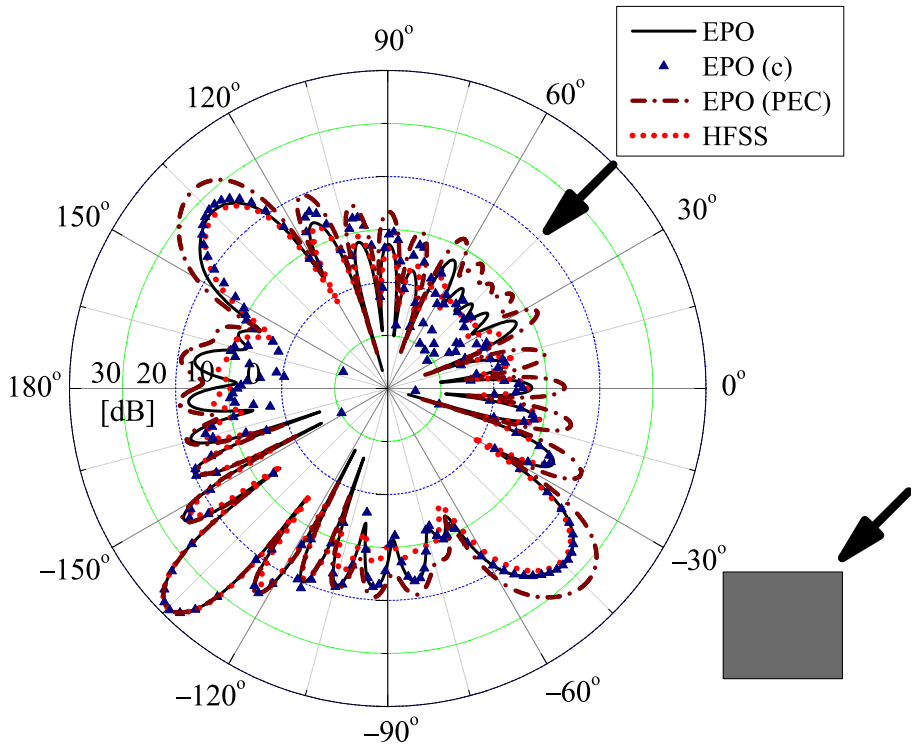

(a)

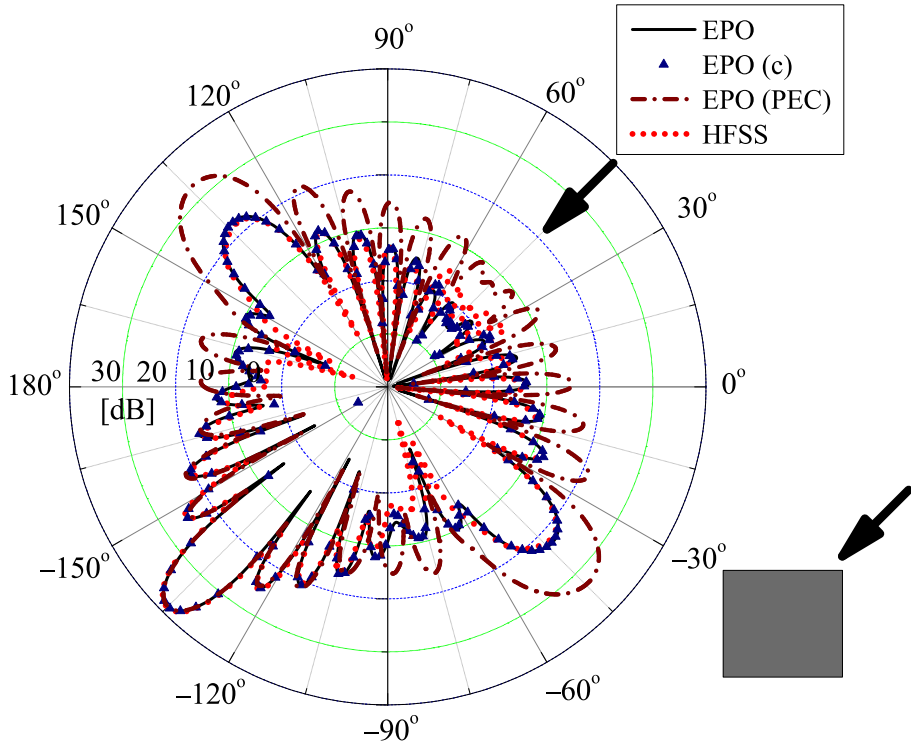

(b)

Figure 4.17: Radiation pattern of a dielectric rectangular cylinder. $ka = kb = 15$, $\phi_0 = 45^o$. $\varepsilon_r = 6 + 1i$. (a) E polarization incident wave. (b) H polarization incident wave.

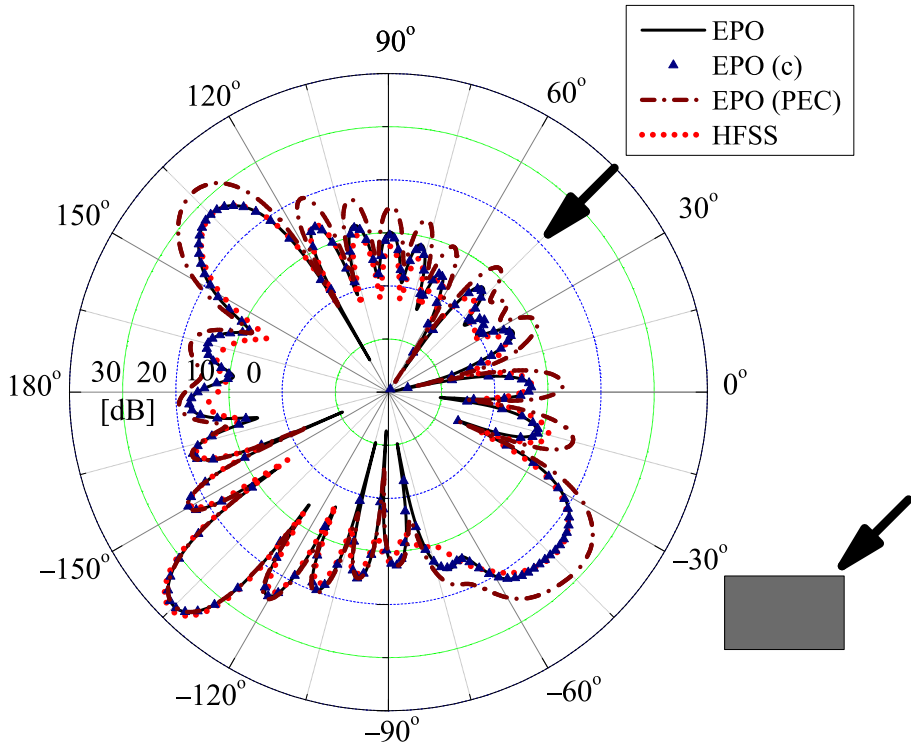

(a)

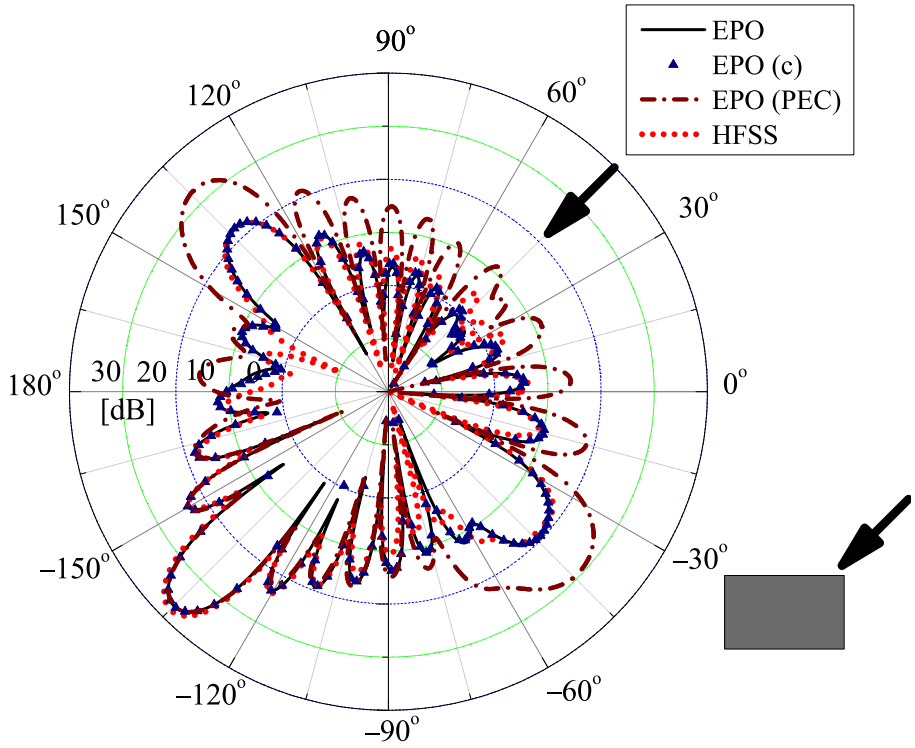

(b)

Figure 4.18: Radiation pattern of a dielectric rectangular cylinder. $ka = 15$, $kb = 10$, $\phi_0 = 45^{\circ}$. $\varepsilon_r = 6 + 1i$. (a) E polarization incident wave. (b) H polarization incident wave.

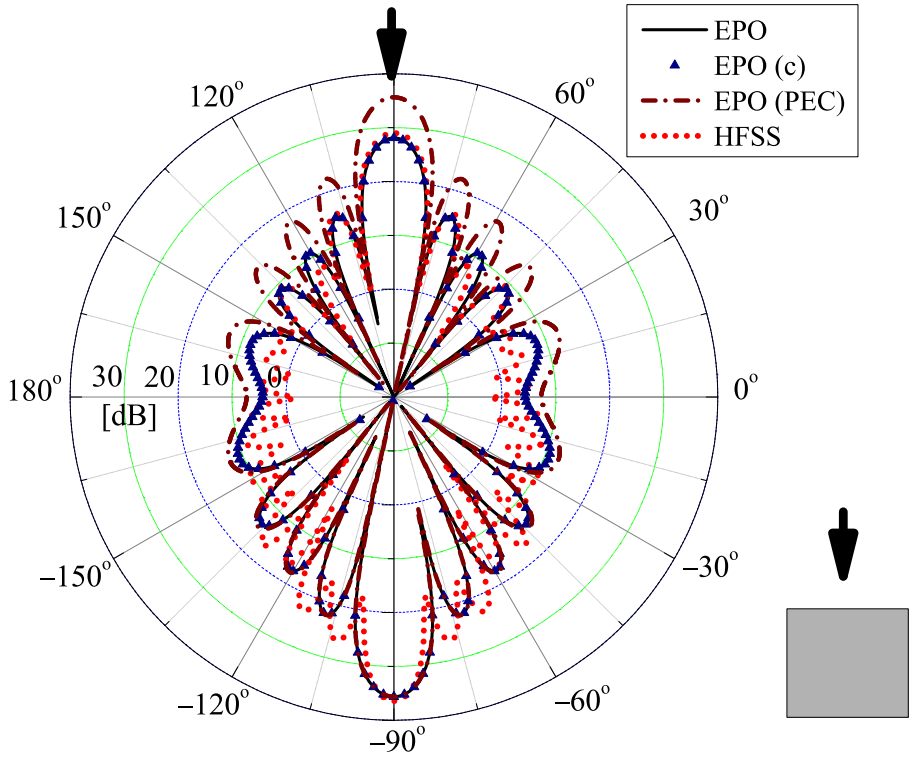

(a)

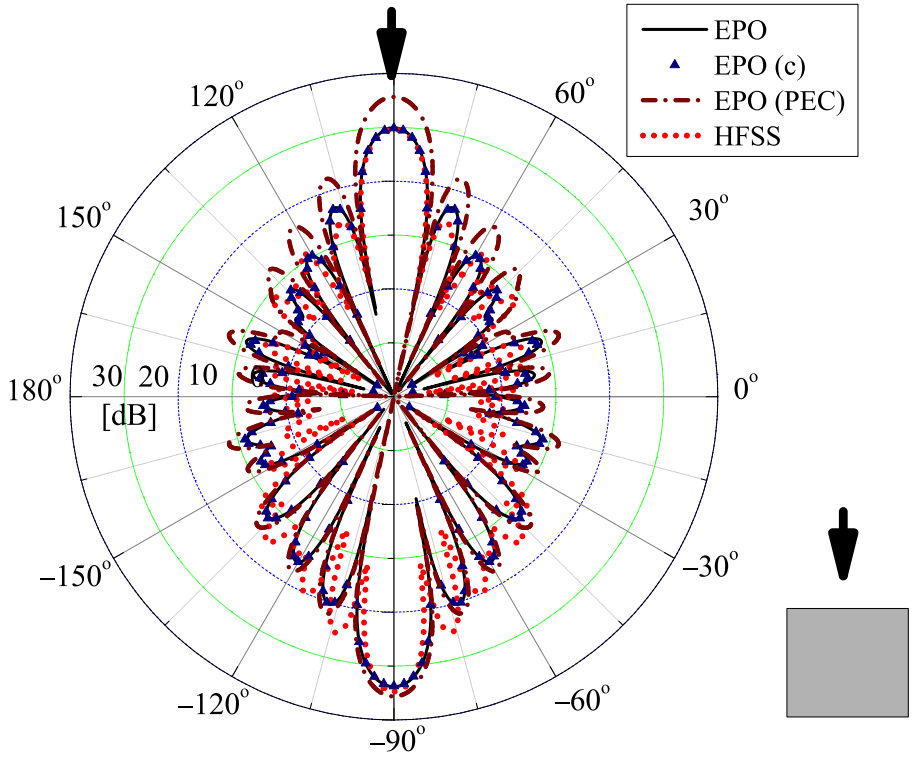

(b)

Figure 4.19: Radiation pattern of a dielectric rectangular cylinder. $ka = kb = 15$, $\phi_0 = 90^o$. $\varepsilon_r = 6 + 0.1i$. (a) E polarization incident wave. (b) H polarization incident wave.

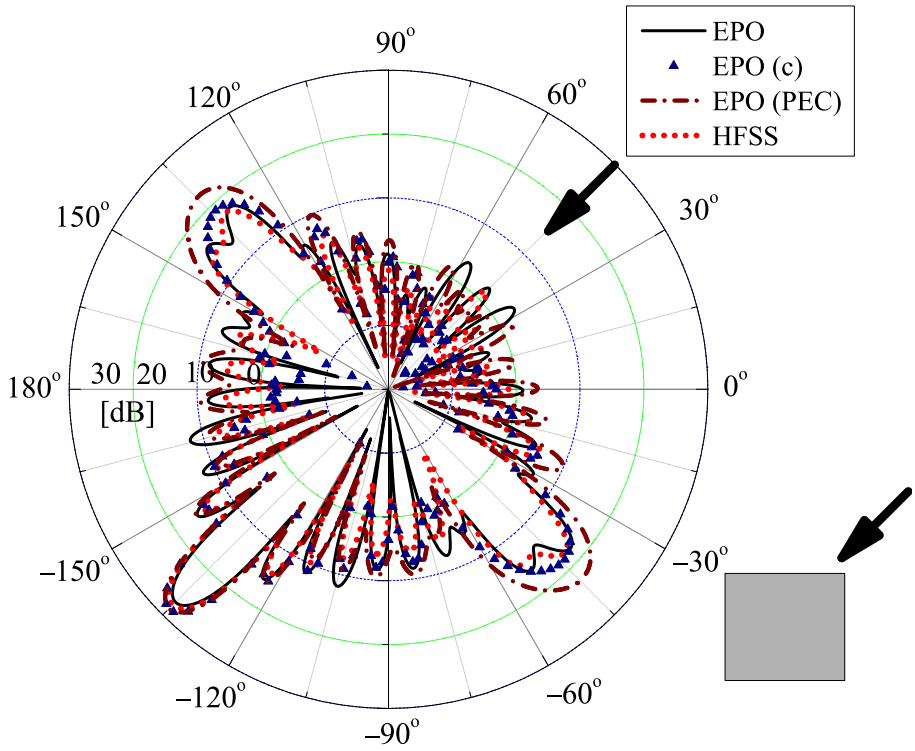

(a)

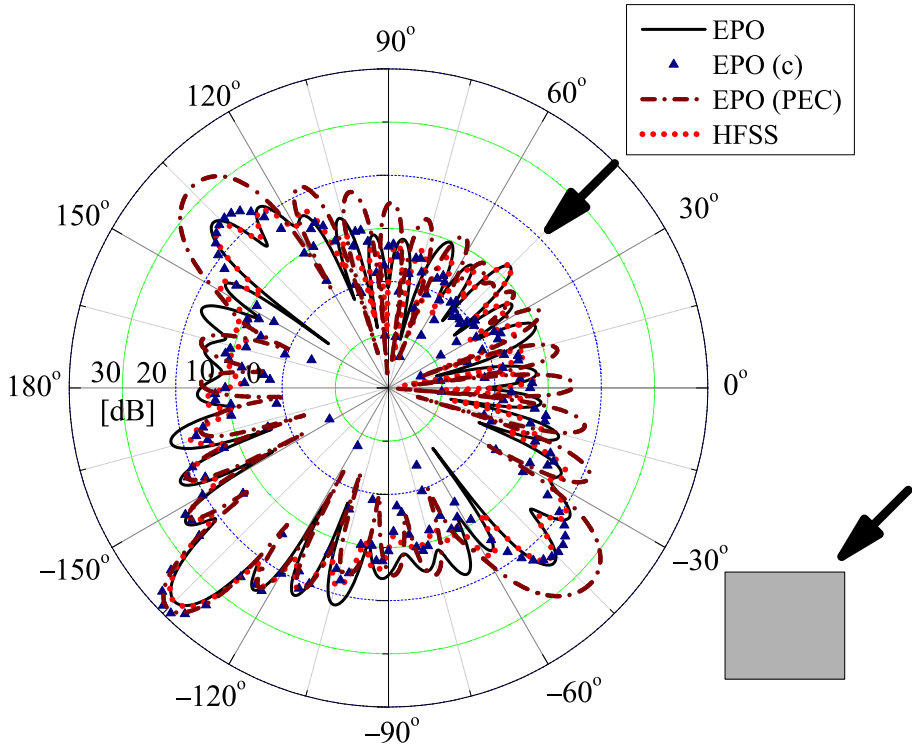

(b)

Figure 4.20: Radiation pattern of a dielectric rectangular cylinder. $ka = kb = 15$, $\phi_0 = 45^o$. $\varepsilon_r = 6 + 0.1i$. (a) E polarization incident wave. (b) H polarization incident wave.

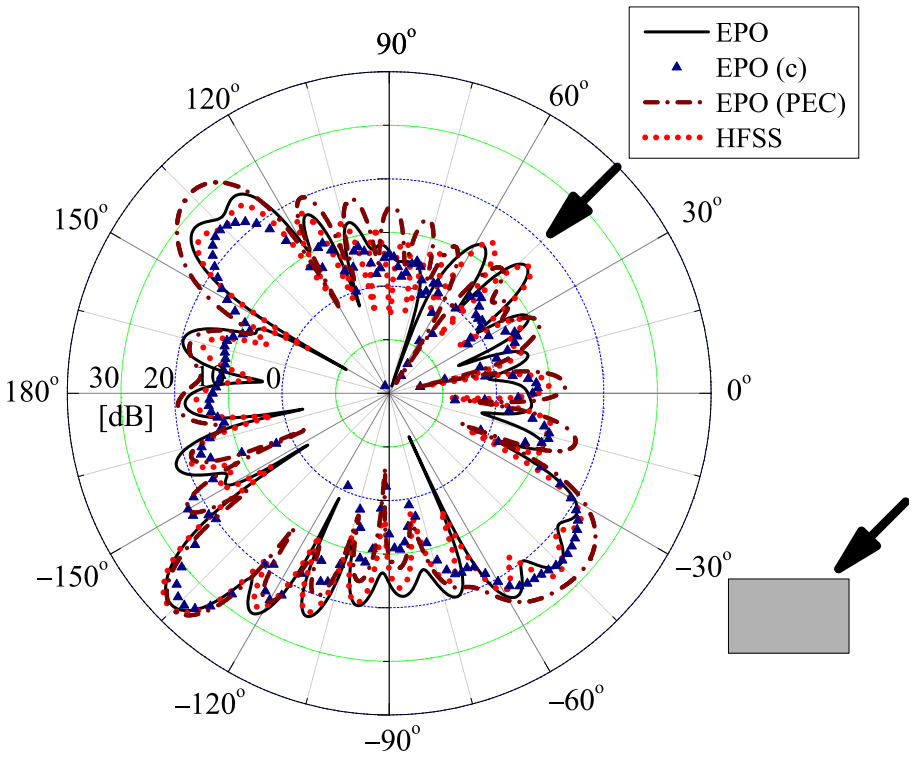

(a)

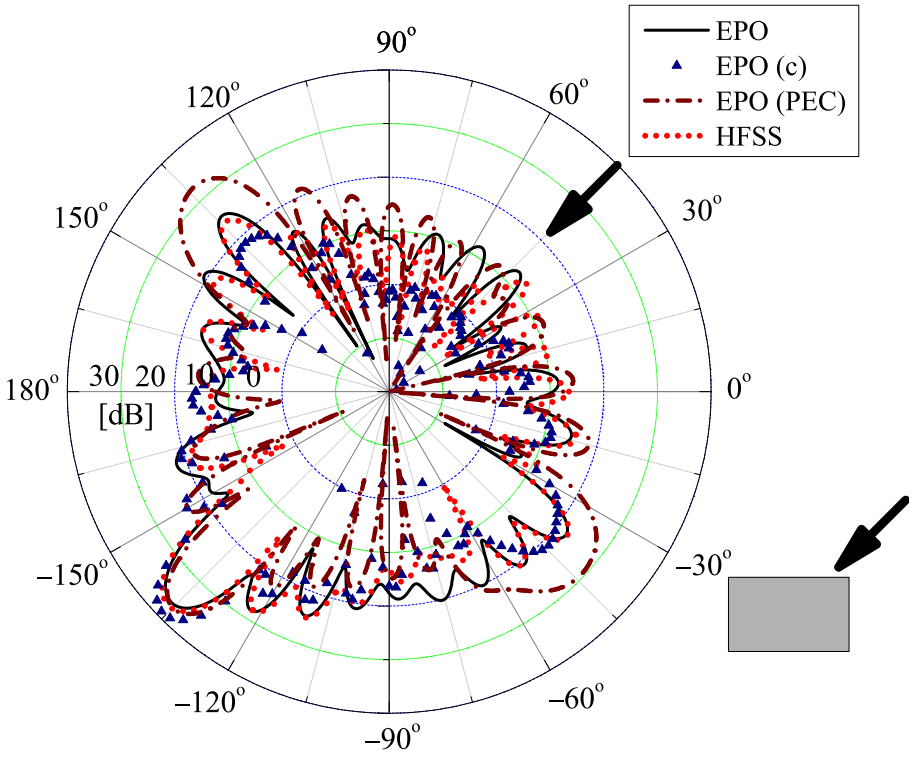

(b)

Figure 4.21: Radiation pattern of a dielectric rectangular cylinder. $ka = 15$, $kb = 10$, $\phi_0 = 45^{\circ}$. $\varepsilon_r = 6 + 0.1i$. (a) E polarization incident wave. (b) H polarization incident wave.

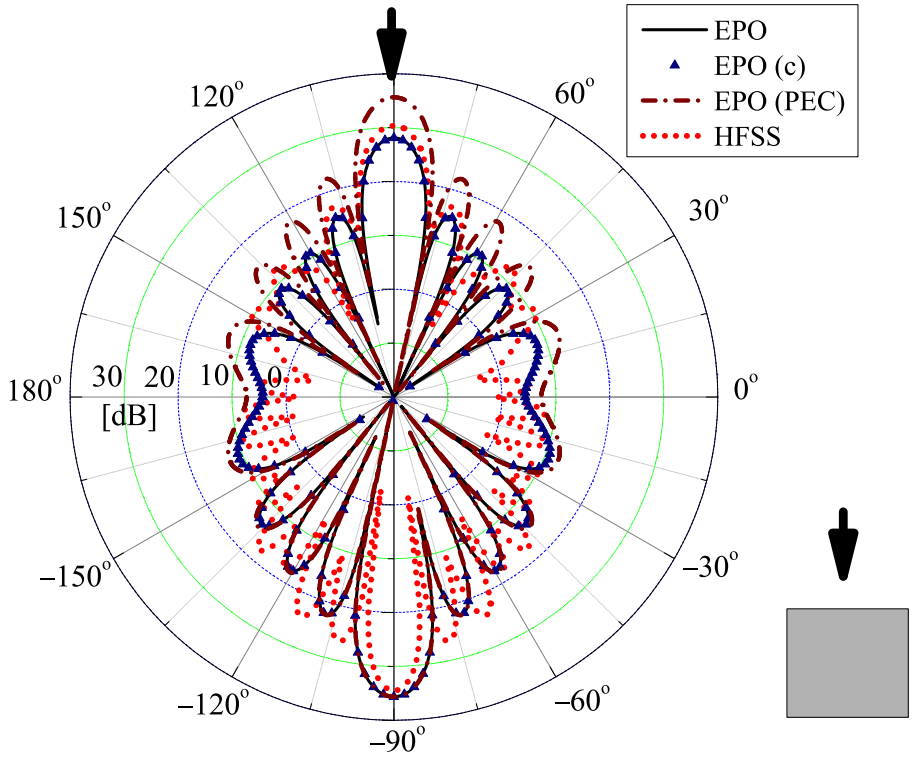

(a)

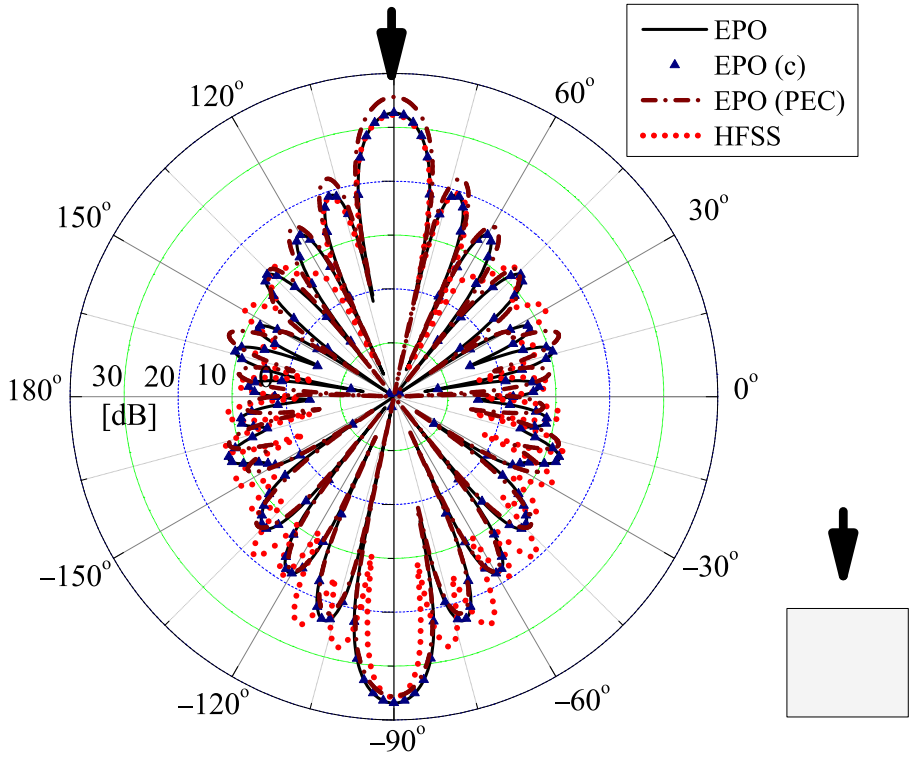

(a)

Figure 4.22: Radiation pattern of a dielectric rectangular cylinder. $ka = kb = 15$, $\phi_0 = 90^o$. $\varepsilon_r = 6$. (a) E polarization incident wave. (b) H polarization incident wave.

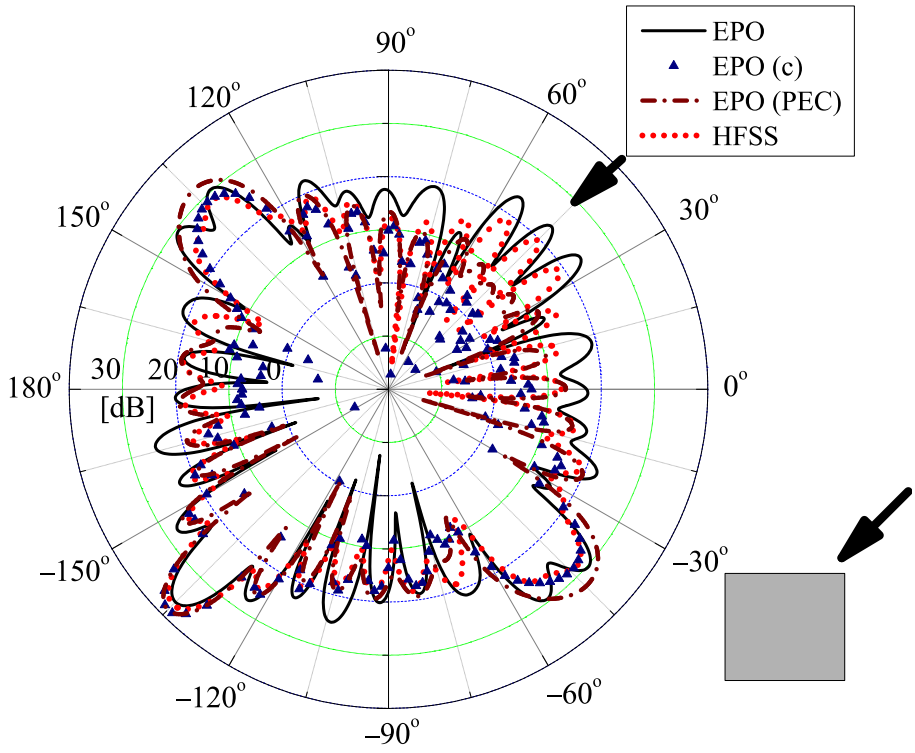

(a)

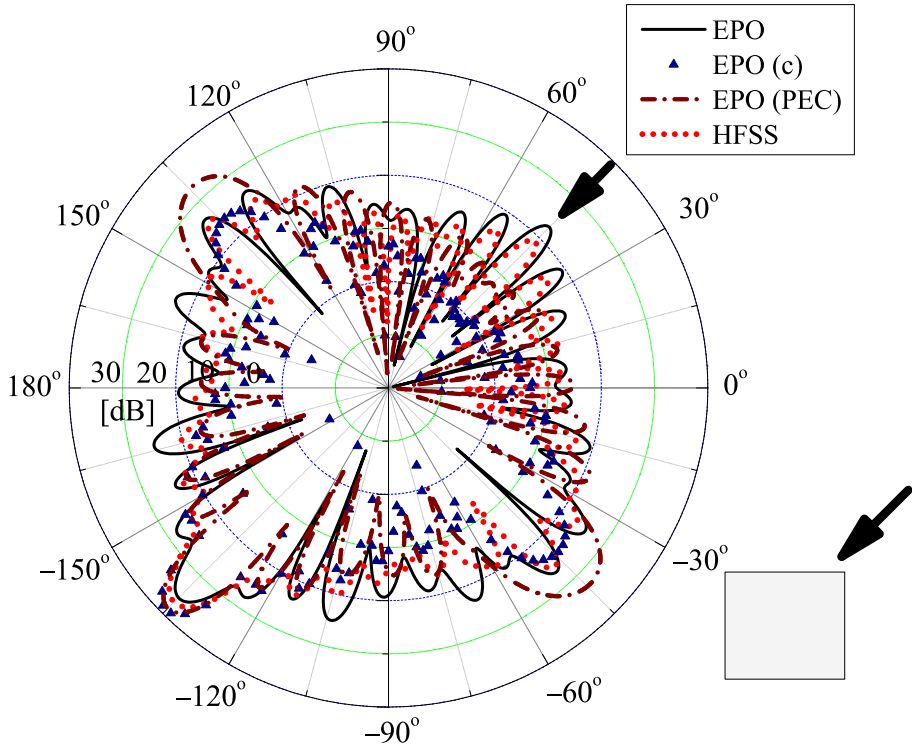

(b)

Figure 4.23: Radiation pattern of a dielectric rectangular cylinder. $ka = kb = 15$, $\phi_0 = 45^o$. $\varepsilon_r = 6$. (a) E polarization incident wave. (b) H polarization incident wave.

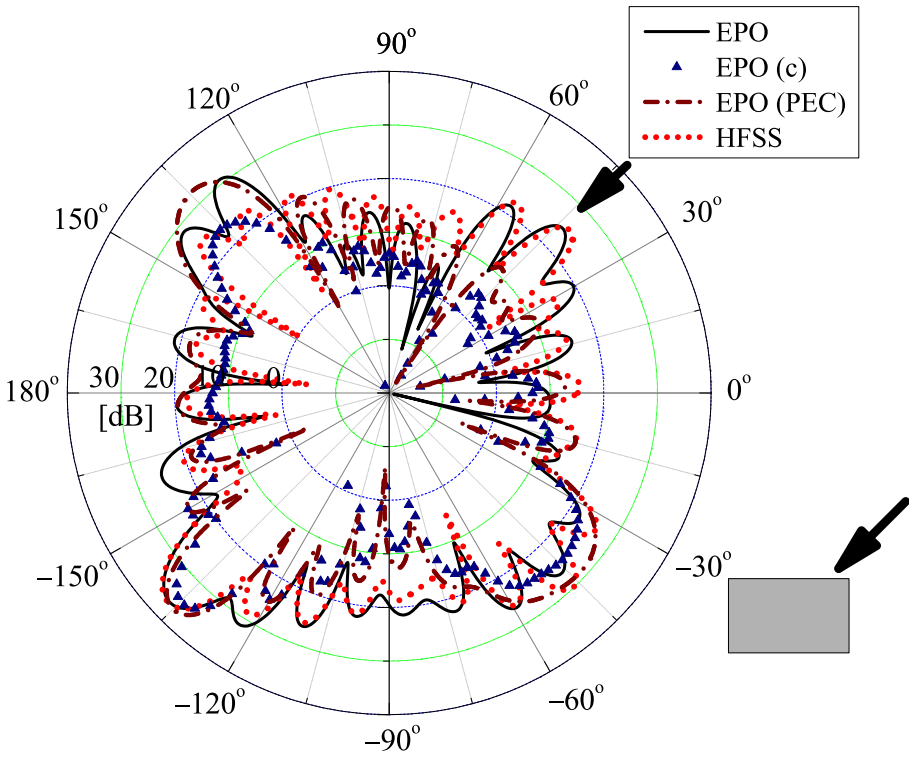

(a)

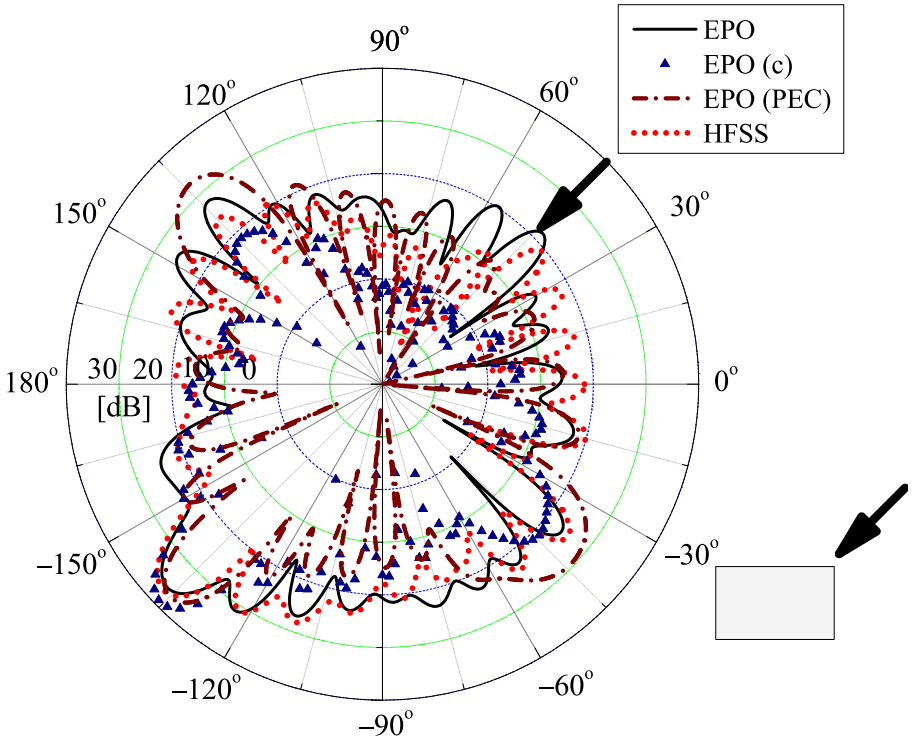

(b)

Figure 4.24: Radiation pattern of a dielectric rectangular cylinder. $ka = 15$, $kb = 10$, $\phi_0 = 45^o$. $\varepsilon_r = 6$. (a) E polarization incident wave. (b) H polarization incident wave.

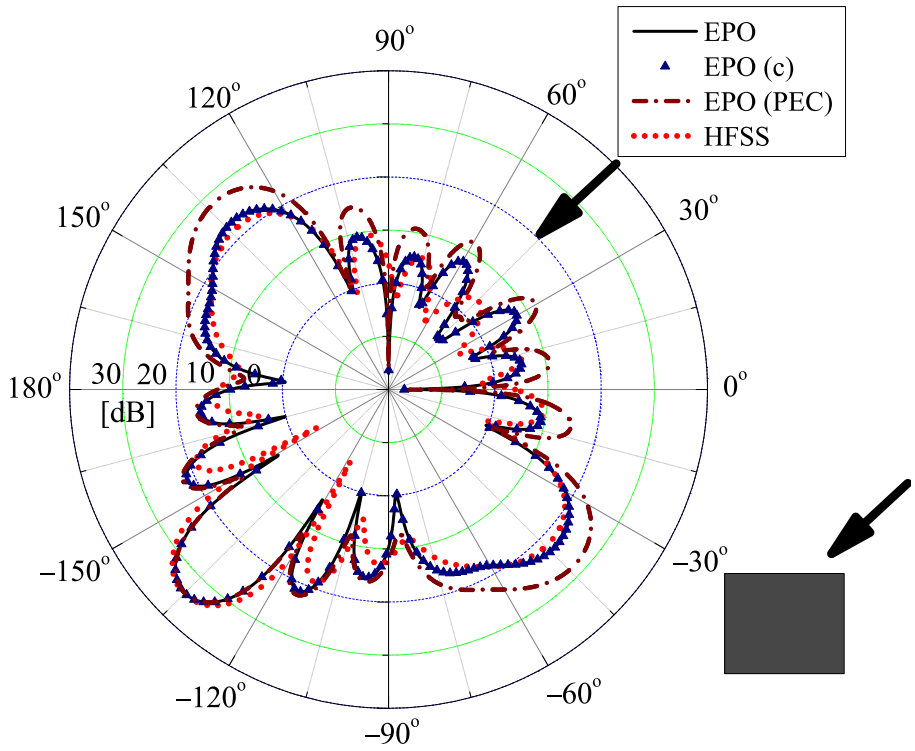

(a)

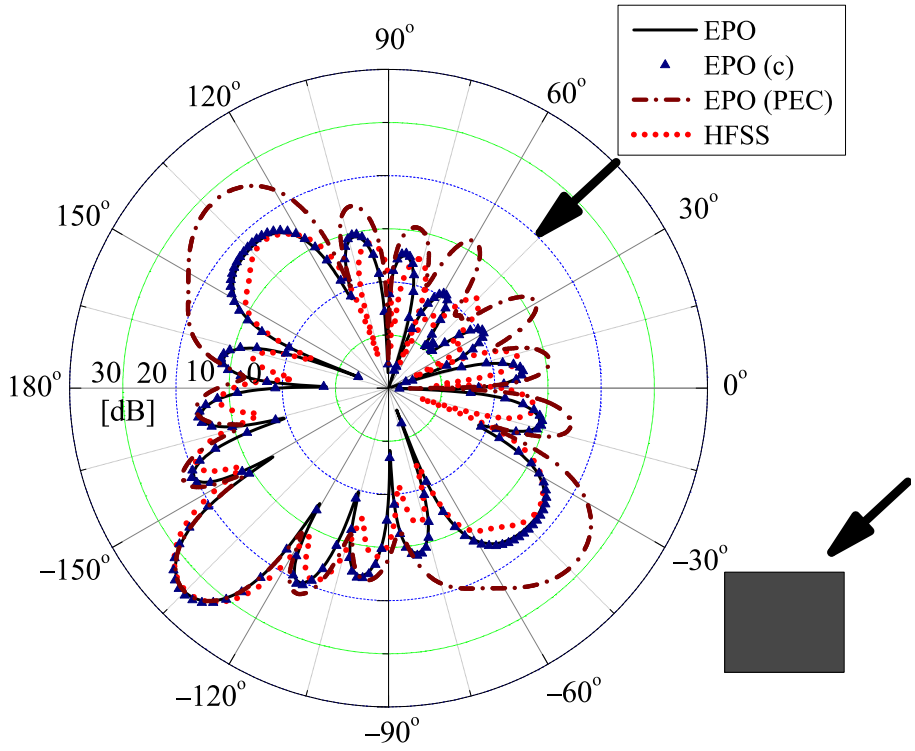

(a)

Figure 4.25: Radiation pattern of a dielectric rectangular cylinder. $ka = kb = 8$, $\phi_0 = 45^o$. $\varepsilon_r = 6{+}1i$. (a) E polarization incident wave. (b) H polarization incident wave.

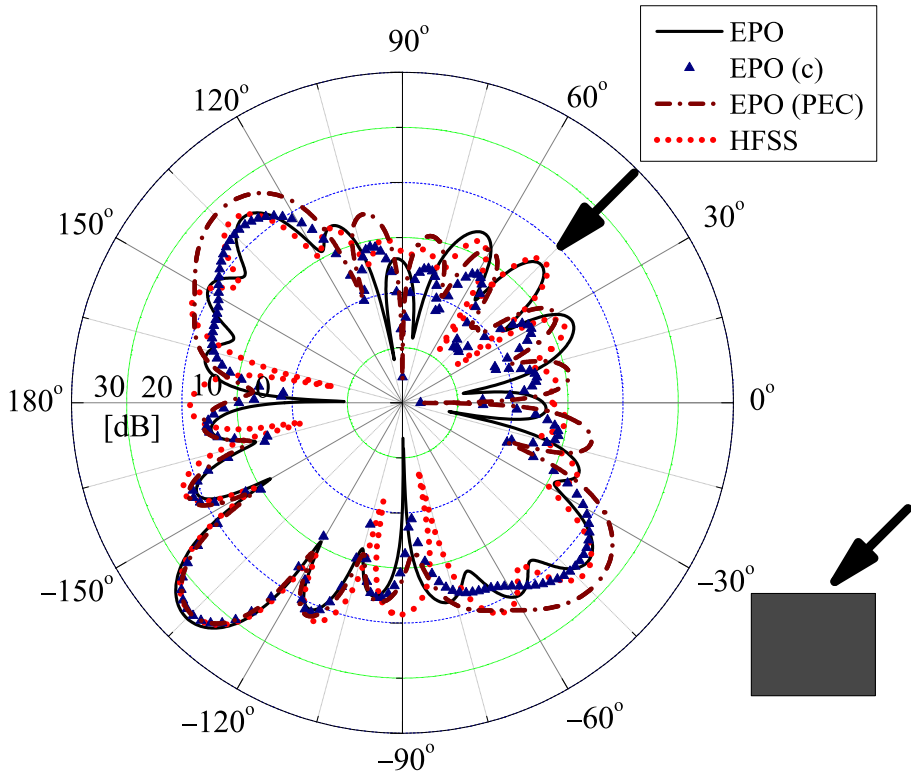

(a)

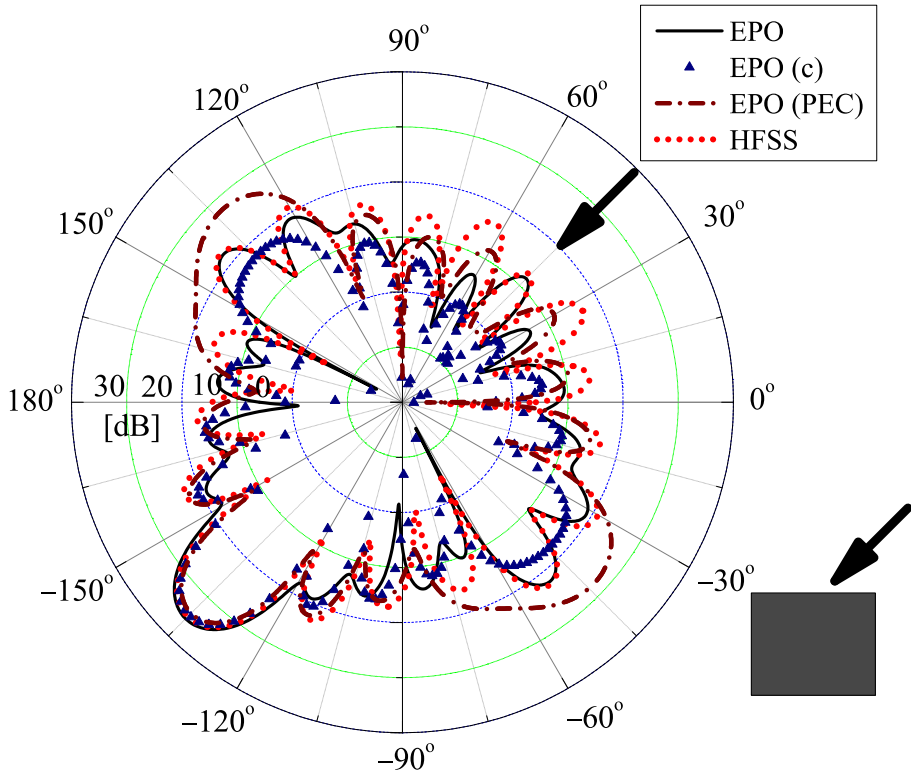

(a)

Figure 4.26: Radiation pattern of a dielectric rectangular cylinder. $ka = kb = 8$, $\phi_0 = 45^o$. $\varepsilon_r = 6{+}0.1i$. (a) E polarization incident wave. (b) H polarization incident wave.

Chapter 5

Conclusion

A new high frequency approximation method to analyze the electromagnetic scattering by edged objects has been proposed. This method is based on the assumption that scattering far field is generated by the equivalent electric and magnetic currents calculated from reflected/transmitted GO waves.

Firstly, the scattering fields from the conducting wedge and rectangular cylinder illuminated by a transverse incident plane wave are formulated by using the physical optics approximation in Chapter 3. Here, the scattering fields are approximated by the radiation fields from the physical optics currents induced by the magnetic incident waves. While the result by the con ducting wedge includes the edge diffracted field and the GO field which gives a reflected field in the illuminated region or a field to cancel the incident field in the shadow region, the one by conducting rectangular cylinder only include the diffracted field and no GO components are necessary.

In chapter 4, the scattering fields by a conducting wedge and rectangular cylinder are approximated by using surface equivalence theorem and the results are compared with those obtained from the physical optic approximation. According to the surface equivalence theorem, the corresponding equivalent electric and magnetic currents $\boldsymbol{J}_s$, $\boldsymbol{M}_s$ on the illuminated surfaces may be obtained from the GO reflected fields $\boldsymbol{E}^r$, $\boldsymbol{H}^r$ s, and those on the shadow surfaces are obtained from the incident GO fields $-\boldsymbol{E}^i$, $-\boldsymbol{H}^i$. The total scattering fields given by summing up the contributions derived from these currents are found to match with the those obtained by the PO approximation, excepted the GO component from the conducting wedge due to the assumption of the surface equivalent theorem. Therefore, from our derivation, one may include that the results by surface

equivalence theorem are found to match with those obtained by the PO approximation in Chapter 3, which utilizes the induced electric currents on the illuminated physical surfaces. One may also expect that the field formulation as a radiation integral due to these equivalent sources has the similar accuracy as PO formulation.

For the dielectric objects, due to the multiple bouncing effect, the equivalent currents $\boldsymbol{J}_s$, $\boldsymbol{M}_s$ on the illuminated surfaces may be obtained from the GO reflected/transmitted fields $\boldsymbol{E}^r + \boldsymbol{E}^t$, $\boldsymbol{H}^r + \boldsymbol{H}^t$, and those on the shadow surface are obtained from the incident/transmitted GO fields $-\boldsymbol{E}^i + \boldsymbol{E}^t$, $-\boldsymbol{H}^i + \boldsymbol{H}^t$. While the expressions of the equivalent currents $\boldsymbol{J}_s$, $\boldsymbol{M}_s$ and the radiation field formulations due to the multiply bouncing transmitted waves are derived for the dielectric wedge, those for the dielectric rectangular cylinder are omitted, except the main results. Also some numerical results for the dielectric rectangular cylinder are calculated to compare with those by HFSS simulation. From our numerical results, it is found that the summation result by the lossless dielectric rectangular cylinder converges by a limited transmitted wave, so that we can omit the effect of the subsequent transmitted waves. For the nearly conducting case, one can observe that our results coincide with those derived by the PEC case, then one needs only the primary contributions due to the weak bouncing effect. As the loss of the dielectric material decreases, the lobes in the specular reflection directions become smaller and more oscillatory due to the stronger interference between the multiply bouncing transmitted waves. Also the good agreements between our method and HFSS simulation have been observed in the forward and specular reflection directions to verify the accuracy of our method. It is also easy to extend our calculation to three dimensional scattering problems and applicable for the scattering estimation from more general edged objects.

Acknowledgment

I truly appreciate that MEXT and Chuo University have provided me the great opportunity to study in Japan. And I would like to express my reverence to Prof. Hiroshi Shirai for his guidance, inspiration and academic advice during my doctoral course. I have duly noticed and appreciated his kindnesses and patience over these years. He has set a standard of professional and ethical excellence to emulate. His continued guidance and support led me to the right way.

I also want to thank Prof. Keiji Goto from the National Defense Academy, Prof. Kazuya Kobayashi and Prof. Chao Jinhui from Chuo University for their advices and comments that leaded to important improvements in this thesis and my research.

I would like to express my deepest gratitude to my family and Shirai Lab's members, especially dad, mom, Dr. Nguyen Ngoc An, Dr. Fujita Keisuke, Mr. Tei Si Sai, Dr. Chu Ba Hien, and Mr. Nguyen Nam Khanh. The encouragement from them is the main source of motivation and resilience for me to overcome tough times, to finish the research and to write this thesis.

Appendix A

$$
\begin{aligned}
A = {} & e^{-ikb(\sin\phi+\sin\phi_0)}\sin[ka(\cos\phi_0+\cos\phi)]\frac{\sin\phi_0}{\cos\phi_0+\cos\phi} \\
& +e^{-ikb(\sin\phi+\sin\phi_0)}\sin[ka(\cos\phi_0+\cos\phi)]\frac{\sin\phi}{\cos\phi_0+\cos\phi} \\
& +e^{-ika(\cos\phi+\cos\phi_0)}\sin[kb(\sin\phi_0+\sin\phi)]\frac{\cos\phi_0}{\sin\phi_0+\sin\phi} \\
& +e^{-ika(\cos\phi+\cos\phi_0)}\sin[kb(\sin\phi_0+\sin\phi)]\frac{\cos\phi}{\sin\phi_0+\sin\phi} \\
& +e^{ikb(\sin\phi+\sin\phi_0)}\sin[ka(\cos\phi_0+\cos\phi)]\frac{\sin\phi_0}{\cos\phi_0+\cos\phi} \\
& -e^{ikb(\sin\phi+\sin\phi_0)}\sin[ka(\cos\phi_0+\cos\phi)]\frac{\sin\phi}{\cos\phi_0+\cos\phi} \\
& +e^{ika(\cos\phi+\cos\phi_0)}\sin[kb(\sin\phi_0+\sin\phi)]\frac{\cos\phi_0}{\sin\phi_0+\sin\phi} \\
& -e^{ika(\cos\phi+\cos\phi_0)}\sin[kb(\sin\phi_0+\sin\phi)]\frac{\cos\phi}{\sin\phi_0+\sin\phi} \\
= {} & \{\cos[kb(\sin\phi+\sin\phi_0)]-i\sin[kb(\sin\phi+\sin\phi_0)]\}\sin[ka(\cos\phi_0+\cos\phi)] \\
& \cdot\frac{(\sin\phi+\sin\phi_0)(\sin\phi+\sin\phi_0)}{(\cos\phi_0+\cos\phi)(\sin\phi+\sin\phi_0)} \\
& +\{\cos[ka(\cos\phi_0+\cos\phi)]-i\sin[ka(\cos\phi_0+\cos\phi)]\}\sin[kb(\sin\phi_0+\sin\phi)] \\
& \cdot\frac{(\cos\phi_0+\cos\phi)(\cos\phi_0+\cos\phi)}{(\cos\phi_0+\cos\phi)(\sin\phi+\sin\phi_0)} \\
& +\{\cos[kb(\sin\phi+\sin\phi_0)]+i\sin[kb(\sin\phi+\sin\phi_0)]\}\sin[ka(\cos\phi_0+\cos\phi)] \\
& \cdot\frac{(\sin\phi_0-\sin\phi)(\sin\phi+\sin\phi_0)}{(\cos\phi_0+\cos\phi)(\sin\phi+\sin\phi_0)} \\
& +\{\cos[ka(\cos\phi_0+\cos\phi)]+i\sin[ka(\cos\phi_0+\cos\phi)]\}\sin[kb(\sin\phi_0+\sin\phi)] \\
& \cdot\frac{(\cos\phi_0-\cos\phi)(\cos\phi_0+\cos\phi)}{(\cos\phi_0+\cos\phi)(\sin\phi+\sin\phi_0)}
\end{aligned}
$$

$$
\begin{aligned}
&\big\{ \cos[kb(\sin\phi+\sin\phi_0)]\sin[ka(\cos\phi_0+\cos\phi)][(\sin\phi+\sin\phi_0)^2+\sin^2\phi_0-\sin^2\phi] \\
&\quad - i\sin[kb(\sin\phi+\sin\phi_0)]\sin[ka(\cos\phi_0+\cos\phi)][(\sin\phi+\sin\phi_0)^2-\sin^2\phi_0+\sin^2\phi] \\
&\quad + \cos[ka(\cos\phi_0+\cos\phi)]\sin[kb(\sin\phi_0+\sin\phi)][(\cos\phi_0+\cos\phi)^2+\cos^2\phi_0-\cos^2\phi] \\
&= \frac{-i\sin[ka(\cos\phi_0+\cos\phi)]\sin[kb(\sin\phi_0+\sin\phi)][(\cos\phi_0+\cos\phi)^2-\cos^2\phi_0+\cos^2\phi]\big\}}{(\cos\phi_0+\cos\phi)(\sin\phi+\sin\phi_0)} \\
&\quad \big\{ \cos[kb(\sin\phi+\sin\phi_0)]\sin[ka(\cos\phi_0+\cos\phi)][2\sin\phi\sin\phi_0+2\sin^2\phi_0] \\
&\qquad - i\sin[kb(\sin\phi+\sin\phi_0)]\sin[ka(\cos\phi_0+\cos\phi)][2\sin\phi\sin\phi_0+2\sin^2\phi] \\
&\quad + \cos[ka(\cos\phi_0+\cos\phi)]\sin[kb(\sin\phi_0+\sin\phi)][2\cos\phi_0\cos\phi+2\cos^2\phi_0] \\
&= \frac{-i\sin[ka(\cos\phi_0+\cos\phi)]\sin[kb(\sin\phi_0+\sin\phi)][2\cos\phi_0\cos\phi+2\cos^2\phi]\big\}}{(\cos\phi_0+\cos\phi)(\sin\phi+\sin\phi_0)} \\
&\quad \big\{\{\cos[kb(\sin\phi+\sin\phi_0)]-i\sin[kb(\sin\phi+\sin\phi_0)]\} \\
&\qquad \cdot\sin[ka(\cos\phi_0+\cos\phi)]2\sin\phi_0(\sin\phi_0+\sin\phi) \\
&\quad + \{\cos[ka(\cos\phi_0+\cos\phi)]-i\sin[ka(\cos\phi_0+\cos\phi)]\} \\
&= \frac{\cdot\sin[kb(\sin\phi_0+\sin\phi)]2\cos\phi_0(\cos\phi+\cos\phi_0)\big\}}{(\cos\phi_0+\cos\phi)(\sin\phi+\sin\phi_0)} \\
&\quad = e^{-ikb(\sin\phi+\sin\phi_0)}\sin[ka(\cos\phi_0+\cos\phi)]\frac{2\sin\phi_0}{\cos\phi_0+\cos\phi} \\
&\qquad + e^{-ika(\cos\phi+\cos\phi_0)}\sin[kb(\sin\phi_0+\sin\phi)]\frac{2\cos\phi_0}{\sin\phi_0+\sin\phi}. \qquad \text{(A.1)}
\end{aligned}
$$

$$
\begin{aligned}
B = {} & e^{-ikb(\sin\phi+\sin\phi_0)}\sin[ka(\cos\phi_0+\cos\phi)]\frac{\sin\phi_0}{\cos\phi_0+\cos\phi} \\
& + e^{-ikb(\sin\phi+\sin\phi_0)}\sin[ka(\cos\phi_0+\cos\phi)]\frac{\sin\phi}{\cos\phi_0+\cos\phi} \\
& + e^{-ika(\cos\phi+\cos\phi_0)}\sin[kb(\sin\phi_0+\sin\phi)]\frac{\cos\phi_0}{\sin\phi_0+\sin\phi} \\
& + e^{-ika(\cos\phi+\cos\phi_0)}\sin[kb(\sin\phi_0+\sin\phi)]\frac{\cos\phi}{\sin\phi_0+\sin\phi} \\
& - e^{ikb(\sin\phi+\sin\phi_0)}\sin[ka(\cos\phi_0+\cos\phi)]\frac{\sin\phi_0}{\cos\phi_0+\cos\phi} \\
& + e^{ikb(\sin\phi+\sin\phi_0)}\sin[ka(\cos\phi_0+\cos\phi)]\frac{\sin\phi}{\cos\phi_0+\cos\phi} \\
& - e^{ika(\cos\phi+\cos\phi_0)}\sin[kb(\sin\phi_0+\sin\phi)]\frac{\cos\phi_0}{\sin\phi_0+\sin\phi} \\
& + e^{ika(\cos\phi+\cos\phi_0)}\sin[kb(\sin\phi_0+\sin\phi)]\frac{\cos\phi}{\sin\phi_0+\sin\phi}
\end{aligned}
$$

$$
\begin{aligned}
&= \{\cos[kb(\sin\phi+\sin\phi_0)] - i\sin[kb(\sin\phi+\sin\phi_0)]\}\sin[ka(\cos\phi_0+\cos\phi)] \\
&\qquad \cdot \frac{(\sin\phi+\sin\phi_0)(\sin\phi+\sin\phi_0)}{(\cos\phi_0+\cos\phi)(\sin\phi+\sin\phi_0)} \\
&\quad + \{\cos[ka(\cos\phi_0+\cos\phi)] - i\sin[ka(\cos\phi_0+\cos\phi)]\}\sin[kb(\sin\phi_0+\sin\phi)] \\
&\qquad \cdot \frac{(\cos\phi_0+\cos\phi)(\cos\phi_0+\cos\phi)}{(\cos\phi_0+\cos\phi)(\sin\phi+\sin\phi_0)} \\
&\quad + \{\cos[kb(\sin\phi+\sin\phi_0)] + i\sin[kb(\sin\phi+\sin\phi_0)]\}\sin[ka(\cos\phi_0+\cos\phi)] \\
&\qquad \cdot \frac{(\sin\phi-\sin\phi_0)(\sin\phi+\sin\phi_0)}{(\cos\phi_0+\cos\phi)(\sin\phi+\sin\phi_0)} \\
&\quad + \{\cos[ka(\cos\phi_0+\cos\phi)] + i\sin[ka(\cos\phi_0+\cos\phi)]\}\sin[kb(\sin\phi_0+\sin\phi)] \\
&\qquad \cdot \frac{(\cos\phi-\cos\phi_0)(\cos\phi_0+\cos\phi)}{(\cos\phi_0+\cos\phi)(\sin\phi+\sin\phi_0)} \\
&\quad \Big\{ \cos[kb(\sin\phi+\sin\phi_0)]\sin[ka(\cos\phi_0+\cos\phi)][(\sin\phi+\sin\phi_0)^2 - \sin^2\phi_0 + \sin^2\phi] \\
&\qquad - i\sin[kb(\sin\phi+\sin\phi_0)]\sin[ka(\cos\phi_0+\cos\phi)][(\sin\phi+\sin\phi_0)^2 + \sin^2\phi_0 - \sin^2\phi] \\
&\qquad + \cos[ka(\cos\phi_0+\cos\phi)]\sin[kb(\sin\phi_0+\sin\phi)][(\cos\phi_0+\cos\phi)^2 - \cos^2\phi_0 + \cos^2\phi] \\
&= \frac{-i\sin[ka(\cos\phi_0+\cos\phi)]\sin[kb(\sin\phi_0+\sin\phi)][(\cos\phi_0+\cos\phi)^2 + \cos^2\phi_0 - \cos^2\phi]\Big\}}{(\cos\phi_0+\cos\phi)(\sin\phi+\sin\phi_0)} \\
&\quad \Big\{ \cos[kb(\sin\phi+\sin\phi_0)]\sin[ka(\cos\phi_0+\cos\phi)][2\sin\phi\sin\phi_0 + 2\sin^2\phi] \\
&\qquad - i\sin[kb(\sin\phi+\sin\phi_0)]\sin[ka(\cos\phi_0+\cos\phi)][2\sin\phi\sin\phi_0 + 2\sin^2\phi_0] \\
&\qquad + \cos[ka(\cos\phi_0+\cos\phi)]\sin[kb(\sin\phi_0+\sin\phi)][2\cos\phi_0\cos\phi + 2\cos^2\phi] \\
&= \frac{-i\sin[ka(\cos\phi_0+\cos\phi)]\sin[kb(\sin\phi_0+\sin\phi)][2\cos\phi_0\cos\phi + 2\cos^2\phi_0]\Big\}}{(\cos\phi_0+\cos\phi)(\sin\phi+\sin\phi_0)} \\
&\quad \Big\{\{\cos[kb(\sin\phi+\sin\phi_0)] - i\sin[kb(\sin\phi+\sin\phi_0)]\} \\
&\qquad \cdot \sin[ka(\cos\phi_0+\cos\phi)]2\sin\phi(\sin\phi_0+\sin\phi) \\
&\qquad + \{\cos[ka(\cos\phi_0+\cos\phi)] - i\sin[ka(\cos\phi_0+\cos\phi)]\} \\
&= \frac{\cdot \sin[kb(\sin\phi_0+\sin\phi)]2\cos\phi(\cos\phi+\cos\phi_0)\Big\}}{(\cos\phi_0+\cos\phi)(\sin\phi+\sin\phi_0)} \\
&= e^{-ikb(\sin\phi+\sin\phi_0)}\sin[ka(\cos\phi_0+\cos\phi)]\frac{2\sin\phi}{\cos\phi_0+\cos\phi} \\
&\qquad + e^{-ika(\cos\phi+\cos\phi_0)}\sin[kb(\sin\phi_0+\sin\phi)]\frac{2\cos\phi}{\sin\phi_0+\sin\phi}. \qquad \text{(A.2)}
\end{aligned}
$$

References

[1] L. A. Weinstein, *The Theory of Diffraction and the Factorization Method (Generalized Wiener–Hopf Technique)*, Golem Press, 1969.

[2] R. Mittra and S. W. Lee, *Analytical Techniques in the Theory of Guided Waves*, The Macmillan Co., 1971.

[3] B. V. Budaev, *Diffraction by Wedges*, Longman Scientific & Technical, 1995

[4] V. M. Babich, M. A. Lyalinov and V. G. Grikurov, *Sommerfeld–Malyuzhinets Technique in Diffraction Theory*, Alpha Science International, 2007

[5] V. Daniele and R. Zich, *The Wiener–Hopf Method in Electromagnetics*, SciTech Publishing, 2014

[6] M.A. Morgan, *Finite Element and Finite Difference Methods in Electromagnetic Scattering*, Elsevier, New York 1989.

[7] D. L. Colton and R. Kress, *Inverse Acoustic and Electromagnetic Scattering Theory*, Springer–Verlag, 1992

[8] S. Bilbao, *Wave and Scattering: Methods for Numerical Simulation*, John Wiley & Sons, 2004.

[9] L. Tsang, J. A. Kong and K. H. Ding, *Scattering of Electromagnetic Waves: Numerical Simulations*, John Wiley & Sons, 2014

[10] A. V. Osipov and S. A. Tretyakov, *Modern Electromagnetic Scattering Theory with Applications*, John Wiley & Sons, 2017

[11] M. Tomita and K. Yasuura, "Numerical analysis of plane wave scattering from dielectric cylinders," *IEICE Trans. Commun.,* vol. J62–B, no. 2, pp. 132–139, 1979. (in Japanese).

[12] T. Yamasaki, T. Hinata and T. Hosono, "Scattering of plane wave electromagnetic waves by a conducting rectangular cylinder –Point matching method considering edged condition–," *IEICE Trans. Electron.,* vol. J72–C–I, no. 11, pp. 703–710, 1989. (in Japanese).

[13] W. Kishida, R. Ozaki and T. Yamasaki, "Scattering of electromagnetic wave by a dielectric rectangular cylinder with conducting strip," *Technical Report on Electromagnetic Theory*, IEEJ, EMT-17-60, pp. 37–40, 2017. (in Japanese).

[14] M. Kline and I. W.Kay, *Electromagnetic Theory and Geometrical Optics*, John Wiley & Sons, 1965

[15] A. D. Wheelon, *Electromagnetic Scintillation: Volume 1, Geometrical Optics*, Cambridge University Press, 2001.

[16] C. G. Someda, *Electromagnetic Waves*, 2nd ed., CRC Press, 2006.

[17] J. G. V. Bladel, *Electromagnetic Fields*, 2nd ed., John Wiley & Sons, 2007.

[18] J. B. Keller, "Geometrical theory of diffraction," *J. Opt. Soc. Am.*, vol. 52, pp. 116–130, February, 1962.

[19] R. A. Ross, "Radar cross section of rectangular flat plates as a function of aspect angle," *IEEE Transaction on Antennas and Propagation*, vol. AP-14, no. 3, pp. 329–335, May, 1966.

[20] G. L. James, *Geometrical Theory of Diffraction for Electromagnetic Waves*, 3rd ed., Peter Peregrinus, 1986.

[21] V.A Borovikov and B.Y Kinber, *Geometrical Theory of Diffraction*, The Institution of Electrical Engineers, 1994.

[22] H. Shirai, *Geometrical Theory of Diffraction*, Corona Publ. Co., Japan, 2015 (in Japanese).

[23] L. Diaz and T. Milligam, *Antenna Engineering Using Physical Optics*, Artech House, Norwood, MA, USA, 1996.

[24] A. Akhmanov and S. Y. Nikitin, *Physical Optics*, Oxford University Press, 1997.

[25] M. N. Vesperinas, *Scattering and Diffraction in Physical Optics*, World Scientific, 2006.

[26] M. Ando,"Physical optics," in *Analysis Methods for Electromagnetic Wave Problems*, (Chap. 4), E. Yamashita ed., Artech House, Boston, MA, USA, 1990.

[27] M. Ando, "Physical optics," in *Antenna and Engineering Handbook*, IEICE ed., Ohmsha, Tokyo, 2008.

[28] P. Ya. Ufimtsev, *Method of Edge Waves in the Physical Theory of Diffraction*, National Technical Information Service, 1971.

[29] P. Ya. Ufimtsev, *Theory of Edge Diffraction in Electromagnetics*, Tech Science Press, Encino, CA, 2003.

[30] P. Ya. Ufimtsev, *Fundamentals of the Physical Theory of Diffraction*, John Wiley & Sons, 2007.

[31] P. Ya. Ufimtsev, *Theory of Edge Diffraction in Electromagnetics: Origination and Validation of the Physical Theory of Diffraction* Institution of Engineering and Technology, 2009.

[32] S. Y. Kim, J. W. Ra and S. Y. Shin, "Diffraction by an arbitrary-angled dielectric wedge: Part I – Physical optics approximation," *IEEE Trans. on Antennas and Propagation*, vol. 39, no. 9, pp. 1272–1281, 1991.

[33] S. Y. Kim and J. W. Ra, "Diffraction by an arbitrary-angled dielectric wedge: Part II – Correction to physical optics solution," *IEEE Trans. on Antennas and Propagation*, vol. 39, no. 9, pp. 1282–1292, 1991.

[34] S. Y. Kim, "Hidden rays of diffraction," *IEEE Trans. on Antennas and Propagation*, vol. 55, no. 3, pp. 892–906, 2007.

[35] S. Y. Kim, "Electromagnetic scattering from a dielectric wedge and the single hypersingular integral equation," *IEEE Trans. on Antennas and Propagation*, vol. 41, no. 8, pp. 1001–1008, 1993.

[36] J. F. Rouviere, N. Douchin and P. F. Combes, " Improvement of the UTD formulation for diffraction of an electromagnetic wave by a dielectric wedge," *Electronics Letters*, Vol. 33, No. 5, pp 373–375, 1997.

[37] C. A. Balanis, *Advanced Engineering Electromagnetic*, 2nd ed., Wiley, NJ, USA, 2012.

[38] A. N. Nguyen and H. Shirai, "Electromagnetic scattering analysis from rectangular dielectric cuboids –TE polarization–," *IEICE Trans. Electron.,* vol. E99–C, no. 1, pp. 11–17, 2016.

[39] J. A. Stratton, *Electromagnetic Theory*, McGraw-Hill Co., USA, 1941. (reissued from Wiley-IEEE Press, USA, 2007.)

[40] L. B. Felsen and N. Marcuvitz, *Radiation and Scattering of Wave*, IEEE Press, 1994.

[41] H. N. Quang and H. Shirai, "A new interpretation of physical optics approximation from surface equivalence theorem," *IEICE Trans. Electron.*, vol. E101–C, no. 8, pp. 664–670, 2018.

[42] H. N. Quang and H. Shirai, "High frequency electromagnetic scattering analysis by rectangular cylinders -TM Polarization-," *IEICE Trans. Electron.*, vol. E102–C, no. 1,pp. 21–29, 2019.

List of Publications

Journal Papers

[1] K. K. Nguyen, H. N. Quang, P. B. N. Huynh and C. N. Dao, "A Novel Metamaterial MIMO Antenna with High Isolation for WLAN Applications," *International Journal of Antennas and Propagation*, Vol. 2015, 2015.
(https://www.hindawi.com/journals/ijap/2015/851904/).

[2] H. N. Quang and H. Shirai, "A New Interpretation of Physical Optics Approximation from Surface Equivalence Theorem," *IEICE Trans. Electron.*, Vol.E101–C, no. 8, pp. 664–670, Aug. 2018.

[3] H. N. Quang and H. Shirai, "High Frequency Electromagnetic Scattering Analysis by Rectangular Cylinders –TM Polarization–," *IEICE Trans. Electron.*, Vol. 102–C, no. 1, pp. 21–29, Jan. 2019.

International Conference Papers

[1] K. K. Nguyen, H. N. Quang, P. B. N. Huynh, S. Q. Ho and C. N. Dao, "Compact Metamaterial Antennas for WLAN Applications," *Proc. of 2012 International Conference on Advanced Technologies for Communications*, pp. 327–330, Vietnam, 2012.

[2] K. K. Nguyen, H. N. Quang, P. B. N. Huynh and C. N. Dao, "A Compact Printed 4 $\times$ 4 MIMO-UWB Antenna with WLAN Band Rejection," *Proc. of 2013 IEEE Antennas and Propagation Society International Symposium (APS/URSI)*, pp. 2245–2246, USA, 2013.

[3] H. N. Quang and H. Shirai, "A Compact Triple-Band Metamaterial Antenna for WLAN

and WiMAX Applications," *Proc. of 2015 International Conference on Electromagnetics in Advanced Applications*, CDROM, Turin, Italy.

[4] H. N. Quang and H. Shirai, "A Compact D-CRLH Metamaterial Antenna for WLAN and WiMAX Multiband," *Proc. of 2016 International Symposium on Antennas and Propagation (ISAP 2016)*, pp. 32–33, Okinawa, Japan.

[5] H. N. Quang and H. Shirai, "High Frequency Plane Wave Scattering Analysis from Dielectric Cuboids –TM Polarization–," *Proc. of 2017 URSI General Assembly and Scientific Symposium (GASS)*, CDROM, Montreal, Canada.

[6] H. N. Quang and H. Shirai, "High Frequency Wedged Diffraction Analysis via Surface Equivalence Theorem," *Proc. of 2018 IEEE International Symposium on Antennas and Propagation (APS/URSI 2018)*, CDROM, Boston, USA.

[7] H . N. Quang and H. Shirai, "High Frequency Scattering from Conducting Rectangular Cylinder via Surface Equivalence Theorem," *Proc. of 2018 Progress in Electromagnetics Research Symposium (PIERS 2018)*, CDROM, Toyama, Japan.

Domestic Conference Papers

[1] H. N. Quang and H. Shirai, "High Frequency Scattering from Dielectric Rectangular Cylinders –TE Polarization–," *IEICE Technical Report on Electromagnetic Theory (EMT)*, EMT2018–50, pp. 53–58, Tottori, Japan.

Academic Award2

[1] 2nd prize of Best Paper Award in *2018 Progress in Electromagnetics Research Symposium (PIERS 2018)*, Toyama, Japan.

[2] 第 32 回 中央大学 渋谷健一奨励賞 受賞, 2019 年 3 月 14 日.